Expression and functional analysis of murine ryanodine receptor type 3

Thesis

oro.open.ac.uk

Federica Bertocchini

Expression and functional analysis of murine ryanodine receptor type 3

A thesis submitted in partial fulfilment of the requirements of the
Open University
for the degree of Doctor of Philosophy

December 1998

DIBIT

Department of Biological and Technical Research
Istituto Scientifico Ospedale San Raffaele
Milan, Italy

Index

Abbreviations

Ca^{2+}	calcium
ER	endoplasmic reticulum
SR	sarcoplasmic reticulum
$InsP_3$	inositol 1, 4, 5-trisphosphate
$InsP_3Rs$	inositol 1, 4, 5-trisphosphate receptors
RyRs	ryanodine receptors
cADPR	Cyclic adenosine 5'-diphosphoribose
CICR	calcium induced calcium release
e-c coupling	excitation-contraction coupling
DHPR	dihydropyridine receptor
DCCR	directly coupled calcium release
LB	Luria-Bertani
ES cells	embryonic stem cells
DMEM	Dulbecco's Modified Eagle's Medium
EDL	extensor digitorum longus
MHC	myosin heavy chain

The Open University

Library authorisation form
Form SE12 (1996)

Please return this form to the Research Degrees Office, Open University Validation Services, 344-354 Gray's Inn Road, London WC1X 8BP. All students should complete Part 1. Part 2 applies only to PhD students.

Student: _FEDERICA BERTOCCHINI_   PI: _PZ77769_

Sponsoring Establishment: _DIBIT, Scientific Institute H. San Raffaele_

Degree for which the thesis is submitted: _PhD_

Thesis title: _Expression And Functional Analysis of Murine Ryanodine Receptor Type 3_

Part 1   Open University Library Authorisation (to be completed by all students)

I confirm that I am willing for my thesis to be made available to readers by the Open University Library and for it to be photocopied, subject to the discretion of the Librarian.

Signed: _Fed. Bertocch._   Date: _JUNE 10th, 2000_

Part 2   British Library Authorisation   (to be completed by PhD students only)

If you want a copy of your thesis to be available on loan to the British Library Thesis Service as and when it is requested, you must sign a British Library Doctoral Thesis Agreement Form and return it to the Research Degrees Office of the University together with this form. The British Library will publicize the details of your thesis and may request a copy on loan from the University Library. Information on the presentation of the thesis is given in the Agreement form.

The University has decided that your participation in the British Library Thesis Service should be voluntary. Please tick **one** of the boxes below to indicate your intentions.

[X] I am willing for the Open University to loan the British Library a copy of my thesis; a signed British Library Doctoral Thesis Agreement Form is attached.

or

[ ] I do not wish the Open University to loan a copy of my thesis to the British Library.

Signed: _Fed. Bertocch._   Date: _JUNE 10th, 2000_

Abstract

Ryanodine receptors (RyRs) are intracellular homotetrameric Ca^{2+}-release channels constituting a family of three different isoforms, named RyR1, RyR2 and RyR3. RyR1 and RyR2 are highly expressed in skeletal and cardiac muscles respectively, where they localize in the terminal cisternae of the sarcoplasmic reticulum (SR). Although RyR1 and RyR2 have been found to be expressed in several other tissues at much lower level than in striated muscles, their major functional role is related to Ca^{2+}-release from the SR following electrical depolarization of the plasma membrane, a process referred to as excitation-contraction (e-c) coupling and known to regulate striated muscle contraction.

The third isoform, RyR3, is characterized by a wide pattern of expression, without any specific association to a tissue or a cell-type. The finding that RyR3 is also expressed in mammalian skeletal muscles parallels the presence of two distinct isoforms, α- and β-RyR, in non-mammalian vertebrate skeletal muscles, and suggests that two functionally distinct RyRs may be involved in the regulation of skeletal muscle contraction.

The expression of RyR3 was analyzed in murine skeletal muscle from late foetal stages to adult, throughout neonatal phases of development. RyR3 was expressed widely during skeletal muscle post-natal development, disappearing in all muscles analyzed except diaphragm and soleus.

RyR3 knockout mice were generated, and contractile properties of skeletal muscles were analyzed. Skeletal muscle contraction in RyR3$^{-/-}$ mice was impaired during the neonatal phase of development. In skeletal muscles isolated from RyR3$^{-/-}$ mice, the twitch elicited by electrical stimulation was strongly

1

depressed. A significant reduction of the contractile activity was also elicited after stimulation with caffeine, an activator of Ca^{2+}-release through RyRs. In the adults, no differences were detected between wild-type and mutant mice.

These results are the first demonstrations of a physiological role of RyR3 in excitation-contraction coupling mechanisms of skeletal muscle, and support the model of a two-channel system regulating skeletal muscle contraction.

In order to further characterize the RyR3$^{-/-}$ mouse, [^{3}H]ryanodine binding experiments were performed on diaphragm and total hindlimb skeletal muscles from RyR3$^{+/+}$ and RyR3$^{-/-}$ mice. Preliminary results will be presented and discussed.

Introduction

Chapter 1

1.1. Ryanodine Receptors.

1.1.1. Intracellular calcium signalling.

Cellular signalling mechanisms allow the transmission of information from the cell surface membrane to specific targets within the cell. The transmission occurs via intracellular messengers, of which the calcium ion, Ca^{2+}, is one of the most important.

Ca^{2+} is ubiquitously distributed and controls a wide array of cellular processes as diverse as secretion, cell proliferation, contraction, learning and memory (Berridge, 1993; Berridge et al., 1998).

In resting cells, the intracellular Ca^{2+} concentration appears to vary between 10 and 100nM. During stimulation, $[Ca^{2+}]_i$ can rise up to several micromolar values, depending on the cell type.

The versatility of Ca^{2+} signals counts for all the different processes in which it is involved: Ca^{2+} can operate in small cellular compartments, pervade the entire cytoplasm, or penetrate organelles such as mitochondria and the nucleus. In addition, the duration of Ca^{2+} signals spans from microseconds to hours, and it can be in a transient or in a pulsatile manner. As a consequence, the signals achieved by the cell vary in localization, kinetics, amplitude and frequency.

Cells use two sources of Ca^{2+} for generating signals: Ca^{2+} entry from the outside through the plasma membrane and Ca^{2+}-release from intracellular stores such as the endoplasmic reticulum (ER) or sarcoplasmic reticulum (SR), using either inositol 1, 4, 5-trisphosphate receptors (InsP3Rs) or ryanodine receptors (RyRs).

Both Ca^{2+}-release and Ca^{2+}-entry channels, once activated, introduce brief pulses of Ca^{2+} in the cytoplasm, known as "elementary" Ca^{2+} signals, that represent the basic building blocks of Ca^{2+} signaling (Bootman and Berridge, 1995). These elementary events result from the opening of individual or small groups of

5

channels on the internal stores. The openings of individual channels or small groups of channels are fundamental events referred to as "blip" and "puffs", respectively, in the case of the $InsP_3$ receptors or "quark" and "sparks" in the case of the RyRs. The elementary Ca^{2+} signaling units can either activate highly localized cellular processes in the immediate vicinity of the channels, or generate global Ca^{2+} signals as waves and oscillations by recruiting channels throughout the cell (Bootman and Berridge, 1995; Bootman et al., 1997; Berridge et al., 1999).

Many processes are directly controlled by local Ca^{2+} signals, like the release of synaptic and secretory vesicles, or the activation of ion channels. Such elementary signals produce a high localized, specific and rapid effect at relatively low cost to the cell compared to global Ca^{2+} changes.

An example of a Ca^{2+} wave spreading in a regenerative way is represented by the Ca^{2+}-induced Ca^{2+}-release (CICR) mechanism, used by both non-excitable and excitable cells. In this case, an elementary Ca^{2+} signal in one region of the cell provides a pulse of Ca^{2+} that stimulates the neighbouring channels, triggering to global Ca^{2+} signaling (Fig.1.1).

In the specific case of myocytes of cardiac muscle, activated voltage-operating channels recruit clusters of ryanodine receptors that produce a spark (Cheng et al., 1993). The activation of many spark-sites in each myocyte increases the global Ca^{2+} levels in the cardiac cells, triggering the contraction.

The existence of local and global signalling modes is a great advantage for the cells, because Ca^{2+} can be used to control separate processes in the same cell, depending on how it is presented. In smooth muscle cells, Ca^{2+} sparks located near the plasma membrane activates Ca^{2+}-sensitive K^+ channels to give outward currents that cause muscle relaxation by hyperpolarization of the cell membrane (Nelson et al, 1995). On the other hand, a global Ca^{2+} wave generated by coordinated Ca^{2+} sparks triggers muscle contraction. Thus, Ca^{2+} can control
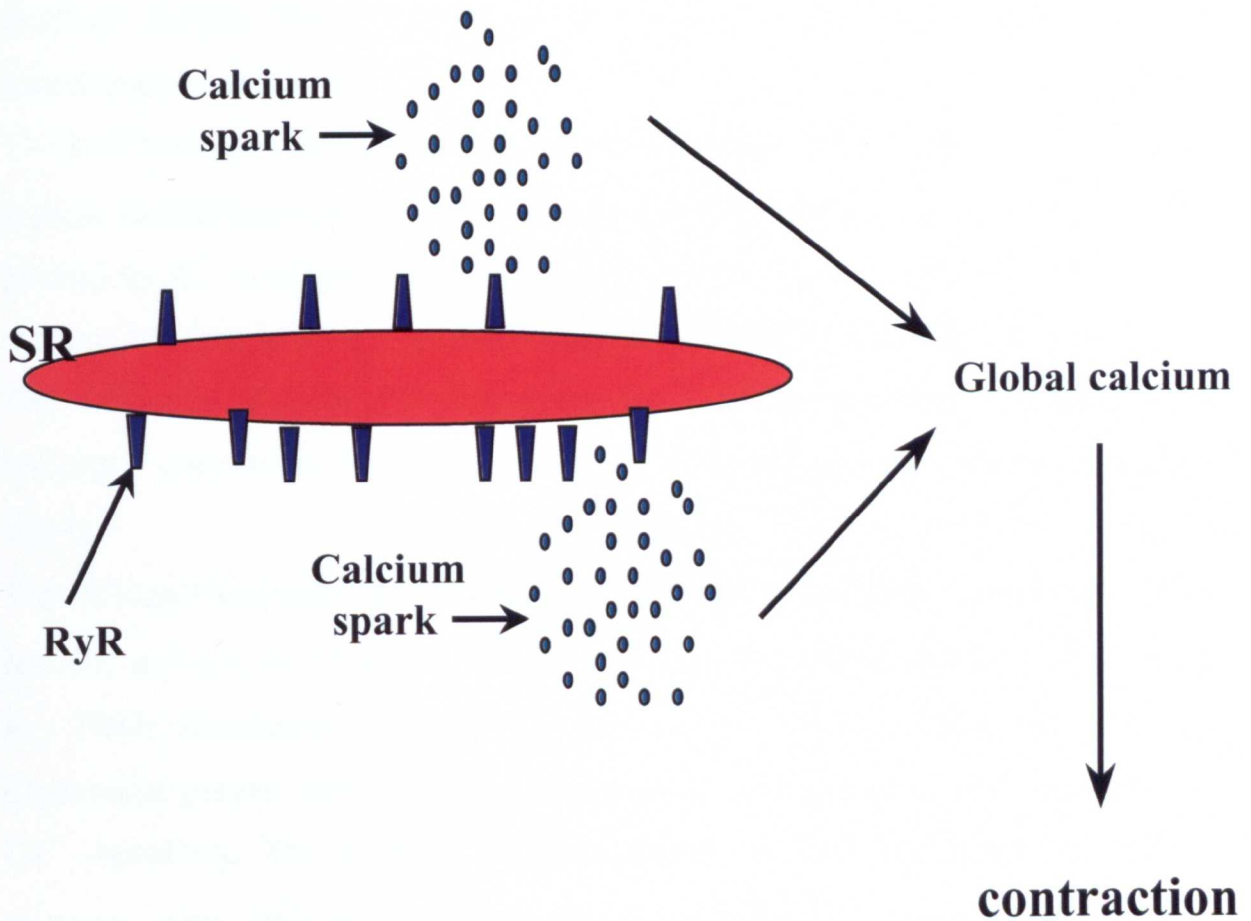
Figure 1.1. Local and global Ca2+ signalling. Groups of ryanodine receptors (RyRs) located on the membrane of the sarcoplasmic reticulum (SR) release localized bursts of of Ca2+ , giving rise to elementary events called "sparks". The sparks contribute to the global calcium signalling, producing contractioon.

both muscle relaxation and contraction, depending on whether it is presented as elementary or global Ca^{2+} signal.

1.1.2. Inositol 1, 4, 5-trisphosphate receptors (InsP3Rs).

The InsP3 and ryanodine receptors constitute the two principal intracellular Ca^{2+} channels that mobilize Ca^{2+} from intracellular stores as a response to external signals. These two types of receptors share similar structural and functional homologies.

The InsP3 receptor has a tetrameric structure with ~300 kD subunits. It contains typical membrane-spanning domains in the C-terminal region, anchoring the protein to the membrane of the intracellular Ca^{2+} store. The large N-terminal domain lies free in the cytoplasm, containing the InsP3 binding site at its end.

The existence of three different genes for InsP3Rs, together with alternative splicings, contributes to the heterogeneity of InsP3 receptor family (Berridge, 1993).

The different isoforms of InsP3Rs are expressed in a tissue- and development-specific manner, and can form homo- and heterotetrameric channels (Newton et al., 1994; Monkawa et al., 1995; Dent et al., 1996). Thus, the complex expression pattern may be responsible for the generation of cell type-specific Ca^{2+} signalling. The relation between the differential expression of InsP3R subtypes and different Ca^{2+} signalling patterns has been studied using genetically engineered B cells, expressing either a single or a combination of InsP3Rs subtypes (Miyakawa et al., 1999). This analysis reveals that different Ca^{2+} signalling patterns are encoded by differential expression of InsP3R subtypes, which differ in their response to intracellular agonists such as InsP3, ATP and Ca^{2+}.

The $InsP_3R$ activity is modulated by Ca^{2+}: first the endogenous ligand $InsP_3$ binds the receptor in the N-terminal domain of a single subunit, determining a conformational change that expose a Ca^{2+} binding site. Ca^{2+} binding provokes a slow inhibition of channel opening (Taylor, 1998).

Furthermore, InsP$_3$Rs are modulated by accessory proteins like ankyrin, calmodulin and FKBP12 (Taylor, 1998).

InsP3, the endogenous ligand, can be released by two different receptor classes, the G protein-coupled receptor class (GPRs), and the receptor tyrosine kinases (RTKs). While GERs activate phospholipase Cβ (PLCβ), RTKs stimulate phospholipase Cγ (PLCγ), converting in both cases phosphatidylinositol (4,5)-bisphosphate into InsP3 and diacylglycerol (DG). InsP3 binds to the tetrameric InsP3 receptor triggering Ca^{2+}-release from the endoplasmic reticulum. (Berridge, 1993; Clapham, 1995).

1.1.3. The ryanodine receptor family.

The RyRs are intracellular Ca^{2+}-release channels originally described in the SR of skeletal and cardiac muscle (Fleischer and Inui, 1989). They were named ryanodine receptors because of their ability to bind the plant alkaloid ryanodine.

The vertebrate RyRs identified to date are homotetramers composed of polypeptide subunits with molecular mass of 500-600 kD, encoded by mRNAs with masses in excess of 15 kb. The ion channel-forming portions of the receptor molecules are constituted by membrane-spanning regions localized in the COOH-terminal of the protein. The RyR channel domains have not been completely defined and has been suggested to consist of either 4 (Takeshima et al., 1989) or 10 (Zorzato et al., 1990) trans-membrane domains (TM). The remaining NH2-terminal parts of the RyR comprise ~80% of the protein mass, and form large cytoplasmic foot-domains that are quaterfoil in arrangement (Wagenknecht and Radermacher, 1995).

Figure 1.2 shows a ryanodine receptor scheme.
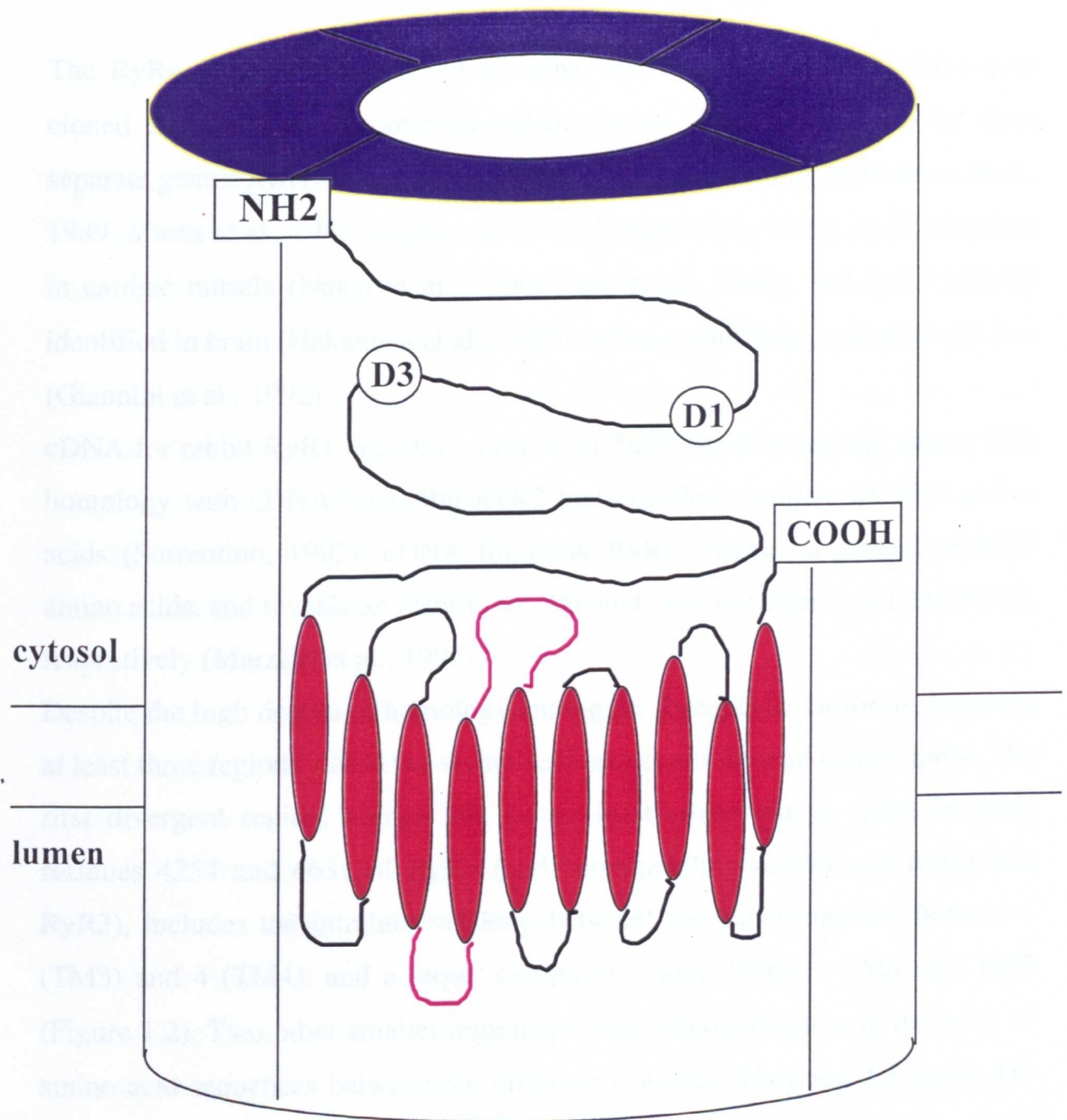
Figure 1.2. Schematic model of ryanodine receptor. Figure represents the tetrameric structure of the channel with the large N-terminal region in the cytosol, ten trans-membrane (according to Zorzato et al., 1990) and the very short C-terminal tail in the cytosol. Divergent regions D1 and D2 are indicated. The divergent region D3 is represented by the pink loops between TM3 and TM4, and between TM4 and TM5.

The RyRs comprise a family of proteins. cDNAs for three RyRs have been cloned and sequenced from mammalian tissues. They are encoded by three separate genes: *RyR1* expressed especially in skeletal muscle (Takeshima et al., 1989; Marks at al., 1989; Otsu et al, 1990; Zorzato et al., 1990), *RyR2* abundant in cardiac muscle (Nakai et al., 1990; Otsu et al., 1990), and *RyR3* initially identified in brain (Hakamata et al., 1992) and in a mink lung epithelial cell line (Giannini et al., 1992).

cDNA for rabbit RyR1 encodes a protein of 5037 amino acids and shares 66% homology with cDNA for rabbit RyR2 that encodes a protein of 4969 amino acids (Sorrentino, 1995). cDNA for mink RyR3 encodes a protein of 4859 amino acids, and reveals an identity of 66% and 70% to rabbit RyR1 and RyR2, respectively (Marziali et al., 1996).

Despite the high degree of homology among the three RyRs isoforms, there are at least three regions where the amino acid sequences diverge significantly. The first divergent region, named D1, is the least conserved: it spans between residues 4254 and 4631 of RyR1 (and corresponding residues of RyR2 and RyR3), includes the intralumenal loop between the transmembrane domain 3 (TM3) and 4 (TM4), and a larger cytoplasmic loop between TM4 and TM5 (Figure 1.2). Two other smaller regions present a diversification at the level of amino acid sequences between the different isoforms. They are the region D2 between residues 1302-1404 of RyR1 and region D3 between residues 1872-1923 of RyR1 and the corresponding regions of RyR2 and RyR3.

1.1.4. Potential regulatory domains

The primary amino acid sequence of RyRs suggests the presence of potential sites of interaction for modulators of channel activity, such as adenine nucleotides, Ca^{2+}, calmodulin and protein kinases.

Several sites for calmodulin-dependent protein kinase (CaM kinase) and cAMP-dependent protein kinase (PKA) have been found in the RyR amino acid sequence, and experimental evidence has shown that CaM kinase preferentially phosphorylates the serine 2809 (Ser^{2809}) in the RyR2 (Witcher et al., 1991). The corresponding site in RyR1 (Ser^{2843}) is phosphorylated by cAMP-, cGMP- and CaM protein kinases (Suko et al., 1993).

Potential binding sites for Ca^{2+}, ATP and calmodulin were predicted in the region between residues 4253-4499 of the rabbit RyR1 (Takeshima et al., 1989; Zorzato et al., 1990). Antibodies against region 4445-4586 influence the channel activity of RyR1, as well as a second antibody against the peptide sequence PEPEPEPEPE, corresponding to amino acids 4489-4499 (Sorrentino, 1995).

Calmodulin binding at several predicted binding sites has also been demonstrated in the rabbit RyR1 (Chen and MacLennan, 1994).

Several potential ATP binding sites are present on each RyR isoform. A region at the C-terminal portion of the molecule seems to contain ATP binding sites, as well as the ryanodine binding site (Sorrentino, 1995).

Another potential regulatory domain has been localized in the region around arginine 615 (Arg^{615}). A single point mutation at nucleotide 1843 (changing C to T) substitutes a Cys for Arg^{615}, and has been identified as the possible cause of malignant hyperthermia in swine and human, an inherited genetic myopathy triggered by some volatile anaesthetics (MacLennan and Phillips, 1992).

1.1.5. Alternative splice variants of RyRs.

Further heterogeneity in the RyR family is achieved by alternative splicing of mRNA. Two alternative splice sites have been found in human and mouse RyR1 mRNA. In the human RyR1 cDNA, two insertions of 5 amino acids after residue 3489 and of 6 amino acids after residue 3864 have been detected (Zhang et al., 1993). In the mouse and rabbit RyR1 cDNA, two similar insertions at the same amino acid position were reported (Futatsugi et al., 1995; Zorzato et al., 1990). Because the 5 and 6 amino acid insertions occur in the region of RyR1 containing putative binding sites for channel modifiers, such as Ca^{2+}, calmodulin, ATP, and the serine residue (Ser^{2843}) that is phosphorylated by the CaM and the cAMP-dependent protein kinase (PKA), it was suggested that these splice events may alter RyR1 function. The possibility that the resulting RyR1 proteins have unique functional roles is supported by the co-expression of the splice variants in the same tissues (skeletal muscle and brain), and the existence of the same variants in human, mouse and rabbit muscles, indicating the conservation in different species (Sutko and Airey, 1996).

An alternative splicing site involving a 24 bp segment encoding amino acids 3716-3723 has been identified in rabbit RyR2 (Nakai et al., 1990), and three alternative splicing sites have been identified in the mink RyR3 cDNA (Marziali et al., 1996). The first two alternative splicing sites consist of insertion of 5 amino acids after residue 3335 and of 6 amino acids after residue 3710. Similar alternative splicing regions have been observed in human, mouse and rabbit (see above). The third splicing site is defined as a mutually exclusive splicing mechanism, in which one out of two exons can be alternatively included in the mature RyR3 mRNA. The region involved in this splicing mechanism spans residues 3495-3527.

Similar to RyR1, alternative splicing sites identified in RyR2 and RyR3 are in a region containing many potential regulatory sites, such as the modulatory region upstream the transmembrane domains. The existence of alternatively spliced variants and, as a possible consequence, of proteins with unique functional properties, may result in further heterogeneity in the Ca^{2+}-release properties of RyRs.

1.1.6. Modulators of RyRs activity

Ryanodine receptors activity can be modulated by several factors, both endogenous and exogenous. Some of these agents have a crucial role in the opening or closing of the channel, while others seem to modulate RyR sensitivity to Ca^{2+}.

Regulation of the RyR channels has been studied in vitro using different techniques: Ca^{2+} fluxes measured in SR vesicles; single channel recordings following the incorporation of SR vesicles or purified channels into planar lipid bilayers; [^{3}H]ryanodine binding studies, using ryanodine as ligand to probe the functional states of the release channel. The following description is a summary of results obtained with these different experimental approaches.

1.1.6a. Ca^{2+}

Ca^{2+} is one of the main regulators of ryanodine receptors, able to activate or inhibit Ca^{2+}-release. In fact, Ca^{2+}-induced Ca^{2+}-release (CICR), the primary activation mechanism for sarcoplasmic reticulum Ca^{2+}-release in cardiac muscle (Fabiato, 1983), seems to be a general property of RyRs (see below). RyR Ca^{2+}-dependence shows a bell-shaped activation curve, with channel opening stimulated by Ca^{2+} in the micromolar range, while Ca^{2+} concentration close to the millimolar range exerts an inhibitory effect (Meissner, 1994; Coronado et al., 1994). These experiments were usually performed on permeabilized muscle fibers, SR vesicles, or purified RyRs incorporated into lipid bilayers

1.1.6b. Mg^{2+} and adenine nucleotides.

Mg^{2+} in the millimolar range produces a strong inhibition of Ca^{2+}-release through RyRs, via a mechanism of competitive antagonism for the Ca^{2+} high-affinity activation sites (Meissner et al., 1994; Murayama et al., 1998).

Several adenine nucleotides, such as, ATP, ADP, AMP, cAMP, AMP-PCP, adenosine, adenine, potentiate Ca^{2+} release through RyRs, counteracting the inhibition by Mg^{2+} (Meissner et al., 1994).

1.1.6c. Ryanodine.

Ryanodine has been shown to exert a concentration-dependent effect on RyR channel activity: at concentrations in the range of 0.01-10μM Ca^{2+} release is stimulated, whereas at higher concentrations release is inhibited (Coronado et al., 1994).

In addition, because ryanodine is a specific ligand for RyRs, analysis of ryanodine binding provides precious information about channel function. Many studies of [^{3}H]ryanodine binding have been performed on skeletal and cardiac sarcoplasmic reticulum, as well as on purified receptors from the same tissues. [^{3}H]ryanodine binding experiments have also been performed on other tissues such as brain, smooth muscle, liver and epithelial cells (Coronado et al., 1994 and references inside). Ryanodine binds preferentially to the open state of the receptors. This is suggested by the fact that ligands known to open the channel and stimulate Ca^{2+} release (micromolar Ca^{2+} or millimolar ATP), stimulate [^{3}H]ryanodine binding. By contrast, ligands known to close the channel and

inhibit Ca^{2+}-release (micromolar ruthenium red and millimolar Mg^{2+}) inhibit [^{3}H]ryanodine binding.

[^{3}H]ryanodine binding is strictly Ca^{2+} dependent: binding to skeletal receptor has a Ca^{2+} threshold of 0.1-1μM, the maximum at 10-100μM and is inhibited at Ca^{2+} concentration >1mM. The bell-shaped Ca^{2+} dependence of [^{3}H]ryanodine binding is similar to that obtained with Ca^{2+} flux experiments.

[^{3}H]ryanodine binding to the cardiac isoform has a Ca^{2+} threshold ~1μM, is optimal in the range 10μM-1mM but is little inhibited at high Ca^{2+} concentrations.

Caffeine in the molar range stimulates [^{3}H]ryanodine binding to the skeletal receptor, and, to a lesser extent, to the cardiac receptor. Adenine nucleotides in millimolar concentration stimulate [^{3}H]ryanodine binding to the skeletal receptor, but have little effect on the cardiac isoform. Increasing pH, temperature and KCl or NaCl stimulates [^{3}H]ryanodine binding to both skeletal and cardiac isoforms.

[^{3}H]ryanodine binding to skeletal receptor, but not to cardiac receptor, is inhibited by Mg^{2+} in the millimolar range, while ruthenium red in nanomolar concentration inhibits the binding to the two isoforms (Coronado et al., 1994 and references therein).

At variance with the large number of studies performed on skeletal and cardiac channels, [^{3}H]ryanodine binding experiments on RyR3 were recently performed on the receptor purified from rabbit and bovine diaphragm (Murayama and Ogawa, 1997; Jeyakumar et al., 1998). The Ca^{2+} dependence experiments show that RyR3 is about 7-fold less sensitive to Ca^{2+} compared to RyR1. RyR3 results more resistant to Mg^{2+} inhibition than RyR1, while binding is strongly inhibited by ruthenium red and procaine. Activators of RyRs such as caffeine and AMP-PCP, a nonhydrolyzable ATP analogue, increase [^{3}H]ryanodine binding to RyR3. Contrasting results have been obtained on

microsomes from mouse parotid acini, containing only RyR3: Mg^{2+}, together with ruthenium red, was shown to strongly inhibit ryanodine binding to RyR3, while ATP and caffeine were much less efficient as activators (DiJulio et al., 1997)

1.1.6d. Caffeine

Caffeine has been used as a pharmacological agent to stimulate RyR opening. The Ca^{2+}-release activity of RyR channels treated with caffeine in the millimolar range displays a bell-shaped dependence as that shown by untreated channels. Caffeine increases the sensitivity of RyRs to Ca^{2+}, prolonging the duration of open channel events (Berridge et al., 1995).

The three isoforms seem to have different sensitivities to caffeine, with the cardiac isoform, RyR2, being the most sensitive, followed by the skeletal muscle isoform, RyR1, and then by RyR3 (Berridge et al., 1995; Takeshima et al., 1995; Chen et al., 1997).

1.1.6e. Cyclic adenosine 5'-diphosphoribose (cADPR).

Ca^{2+}-release through RyRs can be activated by cyclic ADP-ribose (cADPR), a ubiquitous metabolite of nicotinamide adenine dinucleotide (NAD^+) (Galione, 1993). cADPR was first discovered studying Ca^{2+}-release from microsomes derived from the endoplasmic reticulum of sea urchin eggs after addiction of NAD^+ (Dargie et al., 1990). A several minute latency period suggested that

NAD$^+$ was converted into an active metabolite, identified as cADPR. cADPR mobilizes Ca^{2+} by a mechanism completely independent of the IP3 receptors as demonstrated by desensitization studies and by the use of channel antagonists. In fact, after Ca^{2+}-release by cADPR microsomes were desensitized to further release by an additional dose of cADPR, but they remained sensitive to Ca^{2+}-release by IP3. On the contrary, IP3-induced Ca^{2+}-release desensitized microsomes to subsequent release by IP3, but not by cADPR. Secondly, the IP3 antagonist heparin inhibits Ca^{2+}-release by IP3 but has no effect on cADPR-induced Ca^{2+}-release (Galione and Summerhill, 1995). Desensitization studies with known RyR antagonists showed that cADPR releases Ca^{2+} via a ryanodine-sensitive CICR mechanism (Galione et al., 1991). In fact, after Ca^{2+}-release by ryanodine or caffeine cADPR can not elicit further Ca^{2+}-release, while IP3 is still able to induce Ca^{2+}-release. Conversely, after Ca^{2+}-release by cADPR, the stores are insensitive to further release by cADPR, caffeine or ryanodine, while they are still sensitive to IP3. In addition, RyR blockers such as ruthenium red and procaine block cADPR-induced Ca^{2+}-release. The Ca^{2+}-release activity of cADPR is also stimulated by calmodulin (CaM) and Ca^{2+} (Lee, 1995; Galione and Summerhill, 1995). Taken together, these results support the hypothesis that cADPR is an endogenous modulator of CICR through RyRs. In addition to sea urchin eggs, cADPR has been shown to have Ca^{2+} mobilizing activity in many other cells, including mammalian and amphibian cells (Lee, 1995), however, it is not clear yet whether cADPR works as a second messenger for extracellular stimuli. In the standard messenger model, the activation signal (induction of Ca^{2+}-release) would come from a ligand-induced increase in the intracellular concentration of cADPR. The main problem in investigating if cADPR could be a second messenger comes from the technical difficulties in measuring changes in intracellular cADPR concentration. In the alternative modulator model, the activation signal would come from the increase in

intracellular Ca^{2+} concentration without the necessity of an elevation of cADPR concentration.

Although the ability of cADPR to activate Ca^{2+}-release through RyRs is well established, the interaction between cADPR and mammalian RyRs is highly debated (Lee, 1997). In fact, while Meszaros et al. (1993) reported the activation by cADPR of Ca^{2+}-release through RyR2 but not RyR1, Williams and co-workers reported cADPR-induced Ca^{2+}-release through RyR1 (Sitsapesan et al., 1995). Recent experiments of single-channel recordings with bovine muscle preparations and muscle microsomes from normal and RyR3 knockout mice (Bertocchini et al., 1997) indicate that cADPR stimulate Ca^{2+}-release also through RyR3, while RyR1 were insensitive (Sonnleitner et al., 1998).

1.1.7 Ryanodine receptor-FKBP12 interaction.

Ryanodine receptor type 1 is associated with a ~12 kD protein, named FKBP12, with which it co-purifies and co-localizes in the junctional SR of skeletal muscle (Collins, 1991; Jayaraman et al. 1992). FKBP12, or FK506 binding protein, is a member of the immunophilin family, ubiquitously expressed proteins that are cytosolic repressors of immunosuppressing drugs (FK506, rapamycin). One FKBP12 is bound to each subunit of the four subunit of the RyR, with a molar ratio of FKBP to RyR of 1:1. A cardiac isoform of FKBP12, named FKB12.6 is selectively associated with the cardiac RyR isoform with the same molar ratio of 1:1 (Timerman et al., 1994; Lam et al., 1995). By treatment with drug FK506, FKBPs can be dissociated from RyR1 or RyR2, but, while RyR2 can rebind only FKBP12.6, RyR1 can associate with both FKBPs. Recently, binding sites for both FKBP12 and FKBP12.6 have been identified

on RyR3. Experiments on purified RyR1 free from FKBP12 demonstrated a stabilization effect of FKBP12 on RyR1 activity (Brillantes et al., 1994).

1.1.8 RyR pattern of expression

As discussed above, RyR1 and RyR2 play a fundamental role for the release of Ca^{2+} from the SR of skeletal and cardiac muscles, where they are respectively expressed at very high levels. RyR3 was originally found to be expressed in many tissues at low levels, but without a preferential association to specific cell types or tissues (Giannini et al., 1992).

A wide analysis of RyR expression in mammals has been performed by different techniques such as RNAse protection, *in situ* hybridization and immunohistochemistry (Nori et al., 1995).

Experiments of RNAse protection on adult mouse tissues confirmed the high level of expression of RyR1 and RyR2 in skeletal and cardiac muscle respectively; in addition they revealed a spread distribution of the two isoforms in many more tissues, which goes together with the large distribution of RyR3 (Giannini et al., 1995). Particularly interesting is RyR expression in brain and muscle systems (smooth, cardiac and skeletal muscle).

All three isoforms are expressed in brain, even though they cover different areas. *In situ* hybridization on adult mouse brain (Giannini et al., 1995) and adult rabbit brain (Furuichi et al., 1994) confirmed RyR2 as the predominant brain isoform (McPherson and Campbell, 1993), and showed a heterogeneous distribution of the three receptors in different areas of brain. These results were also supported by immunohistochemistry experiments. Table 1 summarizes the

Chapter 1-Table 1

Tissue	Methods	RyR1	RyR2	RyR3	Species
Cerebellum	Immunoblot, immunohistochemistry	+	-	-	Mouse
Cerebellum	RNA blot, *in situ* hybridization	+	++	-	Rabbit
Cerebellum	Immunohistochemistry	-	-	+	Rat
Corpus striatum	RmNA blot	-	+	++	Rabbit
Hippocampus	Immunoblot, immunohistochemistry	-	+	-	Cow, mouse, rat
Hippocampus	RNA blot	-	-	+	Rabbit
Hippocampus	*In situ* hybridization	+	++	+	Rabbit, rat
Thalamus	*In situ* hybridization, RNA blot	-/+	++	+++	Rabbit
Thalamus	Immunohistochemistry	-	+	-	Mouse, rat
Cerebral cortex	*In situ* hybridization	++	+++	+	Rabbit, rat
Cerebral cortex	RNA blot	-	+	-	Rabbit
Cerebral cortex	Immunohistochemistry	-	+	-	Rat, mouse
Olfactory bulb	*in situ* hybridization	+	+++	+	Rabbit, rat
Olfactory bulb	RNA blot	+	+	+	Rabbit
Olfactory bulb	Immunohistochemistry	-	+	-	Mouse, rat
Brain stem	*In situ* hybridization	-/+	++	+	Rabbit, rat
Brain stem	Immunohistochemistry	-	+	-	Mouse
Hypothalamus	*In situ* hybridization	+	+	+	Rabbit, rat
Hypothalamus	Immunohistochemistry	-	+	-	Rat, mouse
Amygdala	*In situ* hybridization	+	+	+	Rabbit, rat
Amygdala	Immunohistochemistry	-	+	-	Rat, mouse

pattern of expression of RyR isoforms in different region of the brain (from Nori et al., 1995).

RNAse protection and *in situ* hybridization revealed that RyR3 is expressed in organs containing smooth muscle, such as aorta, esophagus, urinary bladder, spleen, lung, kidney (Hakamata et al., 1992; Giannini et al., 1995). Very low levels of RyR1 and RyR2 mRNA have also been detected in some tissues such as aorta, stomach and spleen (RYR1). Recently, RyRs have been localized in aortic and vas deferens smooth muscle using immunofluorescence confocal microscopy and immunoelectron microscopy (Lesh et al., 1998).

RyR expression in mammalian striated muscles is characterized by the high level of RyR1 in skeletal muscle and RyR2 in cardiac muscle, with the absence of expression of RyR1 and RyR2 from cardiac and skeletal muscle, respectively. The third isoform, RyR3, is expressed in the conduction myocytes of the heart and in skeletal muscles, as revealed by RNAse protection experiments (Giannini et al., 1992; Giannini et al., 1995).

RyR3 protein expression in skeletal muscles has been deeply investigated (Conti et al., 1996). Western blot assays on skeletal muscle microsomes from different mammalian vertebrates (bovine, rat and rabbit) show relatively high levels of RyR3 in diaphragm and a lower level of expression in soleus muscle. A very weak expression has also been detected in tibialis anterior muscle. These experiments also confirmed the high amount of RyR1 in all the skeletal muscles analyzed, and the lack of RyR2. Similarly to RyR1 and the Ca^{2+}-binding protein calsequestrin, RyR3 was localized in the terminal-cisternae region of SR, a region involved in the Ca^{2+}-release mechanism in relation to contraction.

1.1.9 Non-mammalian vertebrate RyR isoforms

RyRs have also been identified in non-mammalian vertebrates such as birds, amphibians, reptiles and fish. Two RyR isoforms, named α and β, have been found in avian, amphibian and piscine skeletal muscle (Sutko and Airey, 1996). These two isoforms have also been found in two reptilian orders, turtles and alligators, while two other orders, lizards and snakes, express only the α isoform (O'Brien et al., 1993). A third isoform has been localized in the avian heart.

The avian isoforms have been isolated, purified and the ion channel properties studied (Airey et al., 1990; Airey et al., 1993; Percival et al., 1994). The two RyR isoforms of fish (blue marlin and toadfish) and amphibian (bullfrog) skeletal muscles have been isolated and the ion channel properties analyzed (Murayama and Ogawa, 1992; O'Brien et al., 1995). The mRNAs for the amphibian and avian α- and β-RyRs have been cloned and sequenced (Oyamada et al., 1994; Ottini et al., 1996). α- and β-RyRs have been shown to be the mammalian homologous of RyR1 and RyR3.

In contrast with RyR expression in mammalian skeletal muscles, in most skeletal muscles from birds and fish both α and β isoforms are expressed at a comparable level. Expression of the α-RyR alone has been demonstrated in muscles with very fast contracting properties, including the toadfish swimbladder muscle, extraocular muscles from toadish, chickens and cats, and the rattler muscle from rattlesnakes (O'Brien et al., 1993). The differential expression of RyR isoforms in non-mammalian vertebrate specialized muscles appears to be a way to regulate Ca^{2+} release in relation to particular contractile properties of those muscles.

1.1.10. Invertebrate ryanodine receptors

A ryanodine receptor has been cloned in *Drosophila melanogaster* (Takeshima et al., 1994). The derived amino acid sequence reveals <50% homology with mammalian isoforms. The *Drosophila* protein has not been isolated and characterized yet. RyRs have been identified in other invertebrates (Sutko and Airey, 1996), by ultrastructure analysis, ryanodine effects on function, [^{3}H]ryanodine binding and lipid bilayer studies. These RyRs have yet to be characterized at a molecular level.

1.2. The striated muscle system

As discussed in the first part of this introduction, Ca^{2+} signalling plays a fundamental role in the regulation of many different cellular functions, and intracellular Ca^{2+} stores are very important in the regulation of intracellular Ca^{2+} concentration. The storage and release of Ca^{2+} from the SR of striated muscle, and its role in muscle contraction represents an example of such regulation.

In striated muscles, contraction is activated by Ca^{2+} released from cytoplasmic stores in response to depolarization of the surface membrane. This process is called excitation-contraction (e-c) coupling, and takes place at intracellular junction between the plasma membrane or its invagination, the transverse (T) tubules, and the internal Ca^{2+} stores of the sarcoplasmic reticulum (SR) (Fig. 2.1). The junctions are named triads, dyads or peripheral couplings, depending on the number and structure of their components. Triads and dyads consist of two SR cisternae or one SR cisterna, respectively, in contact with one T tubule, while in peripheral couplings SR cisternae make contact directly with the plasma membrane (Flucher and Franzini-Armstrong, 1996). These junctions are all equivalent to each other in their composition and function in e-c coupling mechanism. Junctions between the SR and the T tubule have two preferred orientation: transverse or longitudinal. In the transverse orientation, the facing membranes lie in planes transverse to the fiber long axis; in the longitudinal, they lie in planes parallel to fiber long axis. Transversely oriented triads are typical of vertebrate twitch fibers, while longitudinal triads and dyads are in some vertebrate slow tonic fibers and in most fibers from invertebrates. The T-tubule network can be localized at the Z line or at the A-I junctions, resulting in one or two T-tubules per sarcomere. All known mammalian twitch fibers have two T-tubules per sarcomere.

The mechanism of e-c coupling is based on the presence of a "voltage sensor" located in the T tubule that responds to depolarization by gating Ca^{2+}-release from the Ca^{2+} channels localized in the SR.

The molecular basis of this mechanism involves a voltage-dependent Ca^{2+} channel of L-type named dihydropyridine receptor (DHPR) as voltage sensor on the T tubule, and the RyR as the Ca^{2+}-release channel on SR. Although in both skeletal and cardiac muscles the activation of the SR Ca^{2+}-release channel is under the tight control of DHPR, the mechanism of e-c coupling differs in the two muscle types. These two different mechanisms will be described in details in the following sections.
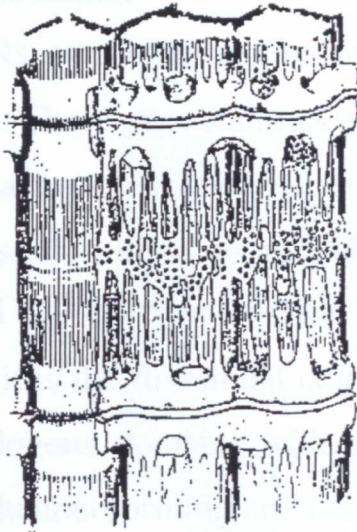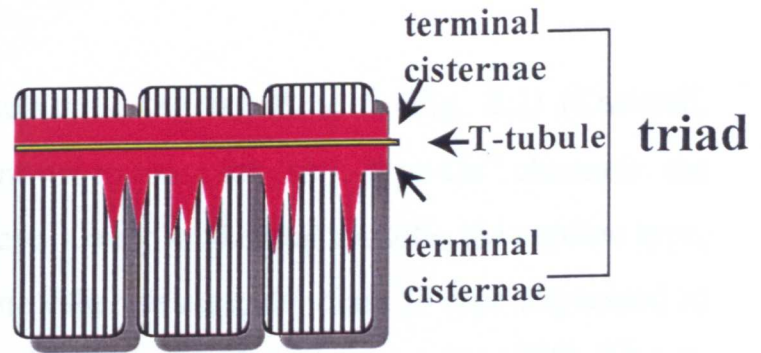
Figure 2.1. A) Frog sartorius muscle. **B)** Schematic representation of muscle in A. The T-tubule with the two adjacent enlargments of SR (terminal cisternae) form the triad.

1.2.1 L-type Ca^{2+} channels.

L-type Ca^{2+} channels, indicated also DHPRs because of the ability to bind the pharmacological agents dihydropyridines (DHPs), are slowly activating Ca^{2+} channels responsible for charge movement across the T-tubule associated with depolarization.

DHPRs are composed of five subunits, α_1, α_2, β, γ, δ (Fig. 2.2) (Catterall, 1991). Three gene families are known to exist for the L-type Ca^{2+} channels, the skeletal type, expressed at high levels only in skeletal muscle; the cardiac type, expressed in heart, brain and some other tissues; the class D type expressed in neural and endocrine tissues (Tanabe et al., 1987; Mikami et al., 1989). The α_1 subunit is the functional component of the complex (Fig. 2.3). It contains four homologous domains with six trans-membrane segments in each, and is the Ca^{2+} channel forming and the DHP-binding portion of the molecule. The role of α_1 subunit in e-c coupling has been established by the use of dysgenic mice. Muscular dysgenesis is a recessive lethal disease due to a point mutation in the α_1 subunit gene, resulting in undetectable levels of the protein. The interruption of e-c coupling in dysgenic fibers and the rescue of functions in fibers transfected with α_1 cDNA provided the evidence leading to the identification of DHPR as the e-c coupling "voltage sensor" (Tanabe et al., 1988, 1990a; Adams et al., 1990).

The β_1 subunit modulates the L-type Ca^{2+} current and it is proposed to modulate the number of α_1 subunit in the membrane (Strube et al., 1996). The role of the other subunits is not clear yet.

Figure 2.2. Subunit structure of DHPR

The mechanism of ex-coupling for skeletal muscle after certain voltage-dependent Ca²⁺ release information have provided that it is based on a mechanical coupling between the sarcolemma and the sarcoplasmic reticulum and the Ca²⁺ release channel (Lamb and Stephenson 1991). The sarcolemma causes the DHPR to undergo conformational changes that may cause activation of the RyR channel (Rios et al. 1991). The Ca²⁺ conductance through DHPR is voltage-dependent and can be blocked by various mechanism (Schneider and Chandler 1973, Rios and Brum 1987). DHPR directly controls the release of Ca²⁺ from the sarcoplasmic reticulum by controlling the opening of RyR. When a voltage change occurs, this mechanism of mechanical coupling takes place in a way that certain conformation is transmitted to the RyR, and yet it unclear and uncertain that DHPR interacts directly with RyR. The direct physical interaction between DHPR and RyR is reported by several researchers because the DHPR cytoplasmic loop between regions II and III of the DHPR α-subunit is able to activate the SR Ca²⁺-release in dysgenic mouse myotubes (Tanabe et al. 1990a (Tanabe et al. 1990a. Tanabe et al. 1990a) further studies have indicated that in a chimeric skeletal muscle DHPR where only the cardiac II-III loop was able to support DCCR. This evidence suggested that the type of DCCR, either skeletal or cardiac, is determined by the DHPR cytoplasmic loop II-III, because transfection in cultured skeletal muscle cells from dysgenic mice with cDNA for cardiac DHPR (re-DHPR) results in a type of DCCR that is very like that of cardiac muscle (Tanabe et al. 1990a). Other studies have shown that deletions of the coupling sequence in the terminal regions of the II-III loop region have no effect on DCCR (Tanabe et al. 1990b).

Figure 2.3. α1 subunit of DHPR. I, II, III, IV represent the four homologous domaind with the six trans-membrane segments in each.

33

1.2.2. The e-c coupling in skeletal muscle

The mechanism of e-c coupling in skeletal muscle, also named voltage-dependent Ca^{2+}-release (Schneider and Chandler, 1973), is based on a mechanical coupling between the surface/t-tubular membrane protein, DHPR, and the Ca^{2+}-release channel on the SR membrane, RyR. The depolarization causes the DHPR to undergo a conformational change that leads to the activation of the RyR channel (Fig. 2.4A). In skeletal muscle, Ca^{2+}-current through DHPR is slow and not required to trigger SR Ca^{2+}-release. This mechanism is also named voltage-dependent, Ca^{2+}-independent Ca^{2+}-release, or directly coupled Ca^{2+}-release (DCCR). DHPR works as a voltage sensor controlling the opening of RyRs via supposed molecular interactions. The mechanism of mechanical coupling, that is how a change in DHPR conformation is transmitted to the RyR, is not yet known. One possibility is that DHPR interacts directly with RyR. This direct molecular interaction between DHPR and RyR is supported by several kinds of observations. The cytoplasmic loop between repeats II and III of α_1-DHPR subunit is required for activation of SR Ca^{2+}-release in dysgenic mouse cultured skeletal muscle cells by DCCR (Tanabe et al., 1990a; Tanabe et al., 1990b). Neither the intact cardiac DHPR nor a chimeric skeletal muscle DHPR containing the cardiac II-III loop was able to support DCCR. This evidence also shows that the type of e-c coupling, skeletal or cardiac, is determined by the DHPR isoform present in the cell, because transfection in cultured skeletal muscle cells from dysgenic mice with cDNA for cardiac DHPR (α_2-DHPR) results in cardiac-type e-c coupling (see below) (Tanabe et al., 1990b). Actually, the RyR isoform also plays its role in determining the e-c coupling type, in fact peptides containing the skeletal II-III loop region have no effect on RyR2 (Lu et al., 1995). Experiments with

34

transgenic mice lacking RyR1 confirm a role of RyR isoforms in determining the e-c coupling type (see below).

In addition, a complex containing DHPR and RyR was precipitated by either anti-DHPR or anti-RyR antibodies (Marty et al., 1994). A second possibility would be that DHPR and RyR do not interact directly, as suggested by unsuccessful attempts to chemically crosslink these two proteins (Caswell and Brandt, 1989). An interaction between DHPR and RyR could be mediated by other proteins. The search for an intermediary protein led to the discovery of an integral protein of the SR membrane, named triadin (Brandt et al., 1990; Kim et al., 1990; Caswell et al., 1991). Triadin is a 95 kD protein enriched in the junctional SR (jSR) and absent from the longitudinal SR. Three triadin isoforms have been detected in both muscle and cardiac muscle (Peng et al., 1994; Guo et al., 1996). Monoclonal antibodies against DHPR and RyR were found to immunoprecipitate triadin (Motoike et al., 1994). Two different interpretations of triadin location in the junctional membrane exist. In the first model triadin repeatedly crosses the jSR with one of its cytoplasmic loop connecting DHPRs and RyRs (Fan et al., 1995) (Fig. 2.5). In the alternative model, triadin has a short cytoplasmic NH2-terminal, a single spanning membrane region and a long, highly charged COOH-terminal tail in the lumenal side (Guo et al., 1996) (Fig. 2.6). In this model triadin does not participate in the DHPR-RyR link. Rather, its lumenal region does interact with calsequestrin and RyR (Guo and Campbell, 1995).

A

DHPR ↙ depolarization

plasma membrane

RyR — calcium release
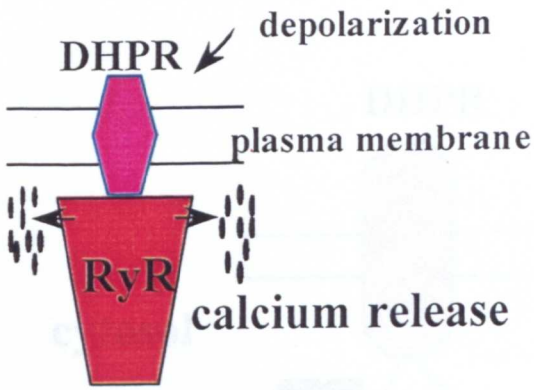
skeletal muscle

voltage-dependent,
calcium-independent calcium-release

B

DHPR ↙ depolarization

plasma membrane

RyR — calcium release
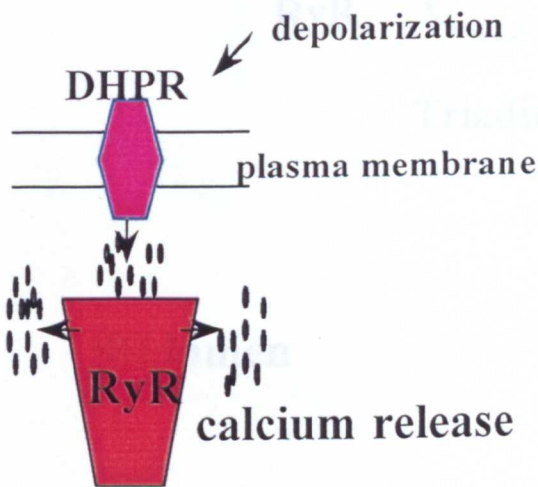
cardiac muscle

calcium-induced calcium-release

Figure 2.4 A and B. The two mechanisms proposed to account for RyR activation in skeletal muscle (A) and cardiac muscle (B).
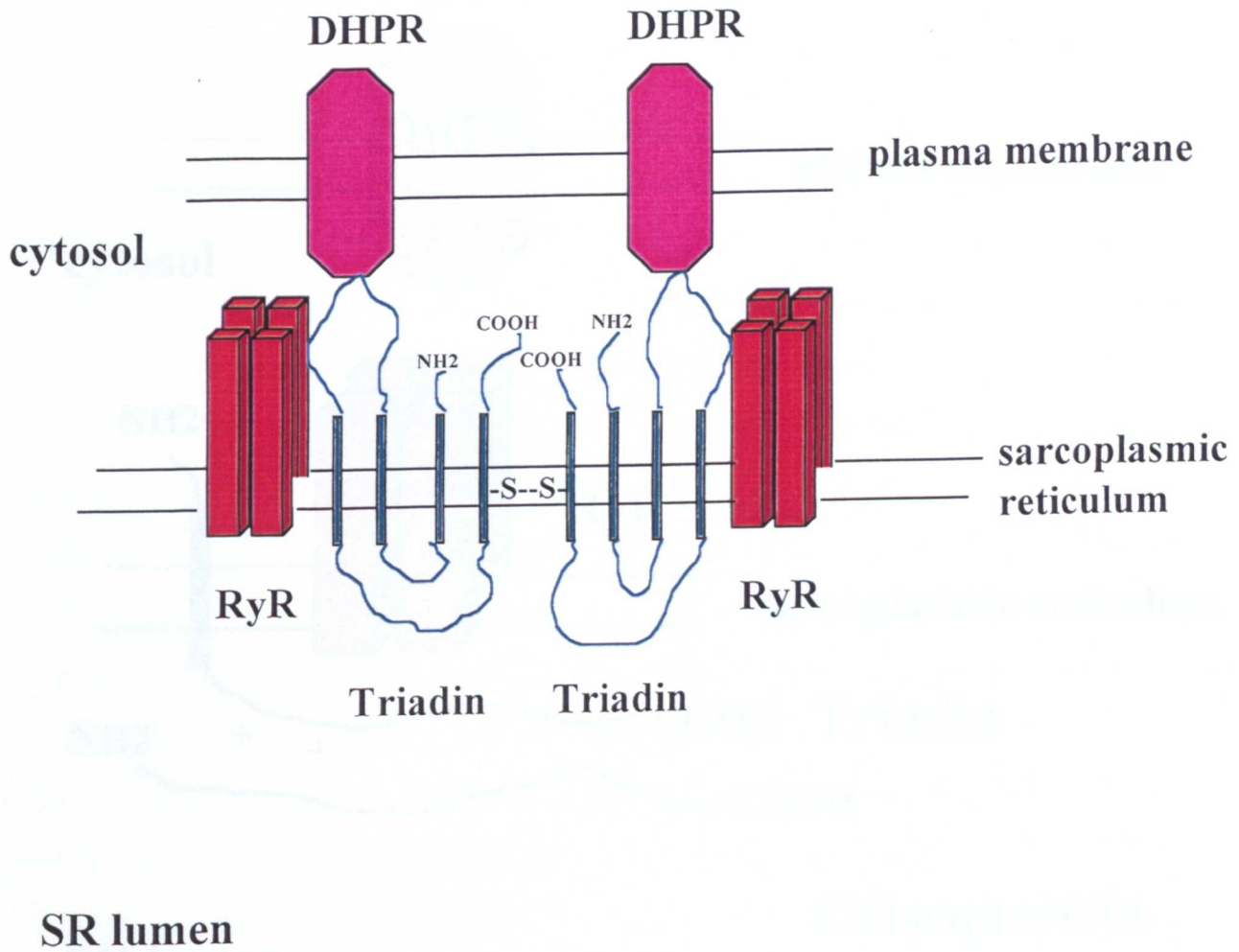
Figure 2.5. Triadin membrane topology. In this model triadin crosses the membrane 4 times. Interaction with RyR and DHPR are indicated. S-S bonds create triadin oligomers. N- and C-terminals are in the cytosol.
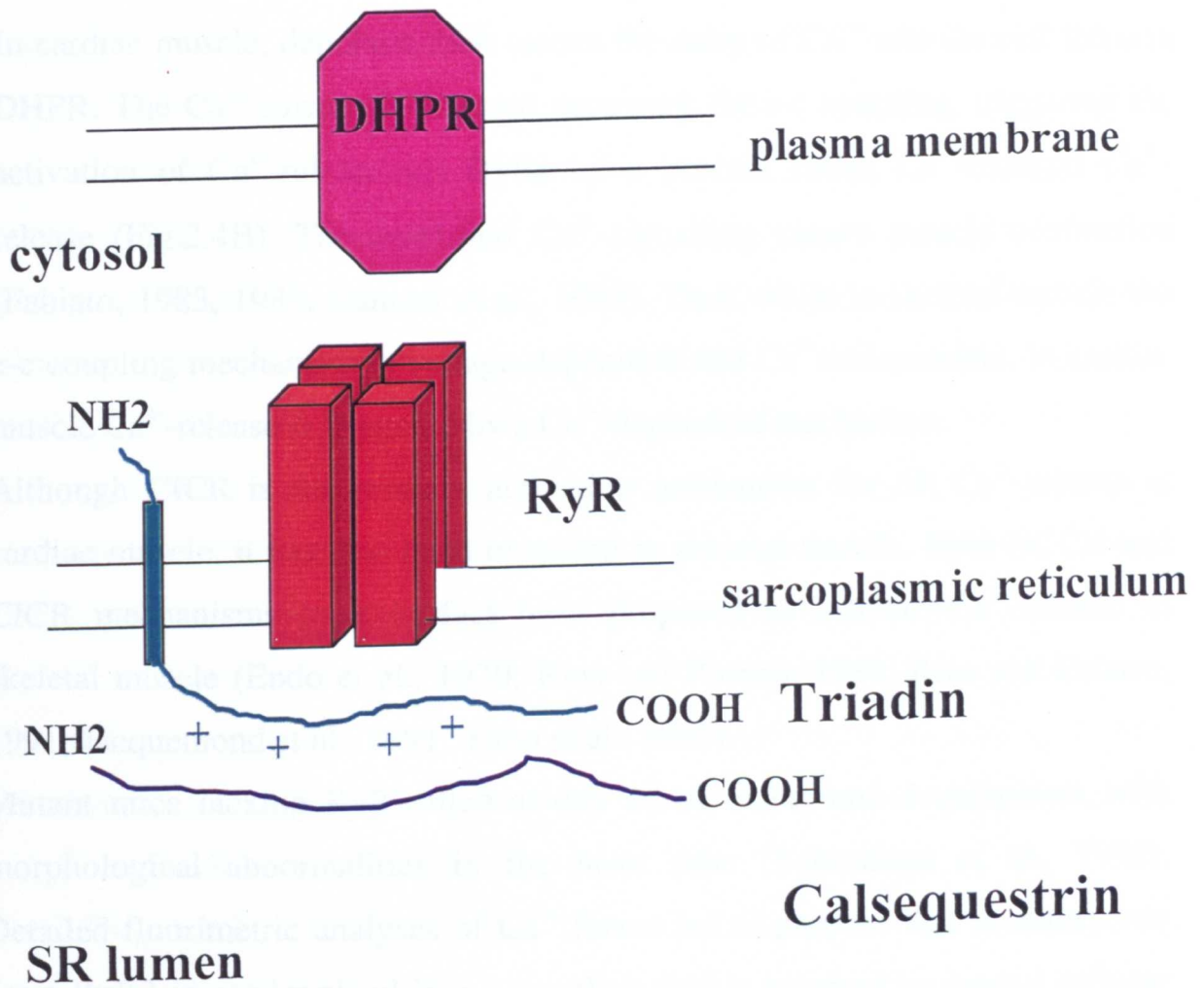
Figure 2.6. Alternative model for triadin topology. In this model triadin has single trans-membrane domain, a short N-terminal region in the cytosol and a highly positive charged C-terminal region. This region would interact with negatively charged calsequestrin and with a lumenal loop of RyR.

1.2.3. e-c coupling in cardiac muscle

In cardiac muscle, depolarization causes the entry of Ca^{2+} into the cell through DHPR. The Ca^{2+} current is fast and necessary for e-c coupling, triggering the activation of Ca^{2+}-release via RyRs by a process called Ca^{2+}-induced Ca^{2+}-release (Fig.2.4B). The amplified Ca^{2+} signalling causes muscle contraction (Fabiato, 1983, 1985; Cannell et al., 1995). Thus, while in skeletal muscle the e-c coupling mechanism is voltage-dependent and Ca^{2+}-independent, in cardiac muscle Ca^{2+}-release is triggered by a Ca^{2+}-dependent mechanism.

Although CICR is the primary activation mechanism for SR Ca^{2+}-release in cardiac muscle, it has also been observed in skeletal muscle. Both DCCR and CICR mechanisms have in fact been proposed to activate Ca^{2+}-release in skeletal muscle (Endo et al., 1970; Rios and Pizarro, 1988; Rios and Pizarro, 1991; Jacquemond et al., 1991; Yano et al., 1995).

Mutant mice lacking RyR2 died at day 10 of embryonic development with morphological abnormalities in the heart tube (Takeshima et al., 1998). Detailed fluorimetric analyses of Ca^{2+} fluxes led to propose that in embryonic heart RyR2 is not involved in e-c coupling, but is required to control cellular Ca^{2+} homeostasis, as a major leak Ca^{2+} channel that has a role in maintaining the SR lumenal Ca^{2+} levels in the physiological range.

1.2.4 Spatial relationship between RyRs and DHPRs.

The structural organization of RyRs and DHPRs in the junctional domains differs in skeletal and cardiac muscles, reflecting the differences between the e-c coupling mechanisms in the two muscles. The main feature common to all

junctions is the "feet", electron-dense periodically distributed structures spanning the narrow junctional gap separating the membrane of SR and either T -tubule or plasma membrane (Franzini-Armstrong, 1970). An individual foot appears as four equal spheres corresponding to the cytoplasmic domain of the homotetrameric RyRs. In skeletal muscles, DHPRs are clustered in groups of fours, or tetrads, positioned in correspondence to the feet so that each DHPR is located in close proximity of one of the fours RyR subunit, localization that allows a direct functional interaction between DHPR and RyR. However, the spacing between tetrads is twice that of the feet, that is, tetrads are associated with alternate feet, resulting in two different population of RyRs, those associated and those not associated to DHPR (Flucher and Franzini-Armstrong, 1996). This disposition has been found in different types of fibers, and does not depend on the presence of two different RyR isoforms (Block et al., 1988; Franzini-Armstrong and Kish, 1995, Flucher and Franzini-Armstrong, 1996). The alternate disposition of tetrads over feet supports the two-component model of Ca^{2+}-release from SR (see below).

In cardiac muscle, DHPRs are also clustered in the junctional domains, but neither are grouped into tetrads, nor have apparent relationship to the position of the feet (Sun et al., 1995; Protasi et al., 1996). Such a disposition is in line with the lack of a direct functional interaction of DHPRs and RyRs. However, in cardiac muscle the concentration of DHPRs in the junctional domain opposite to the RyRs is consistent with a CICR mechanism or cardiac e-c coupling under the control of the L-type Ca^{2+} channel.

1.2.5 RyR1 knockout

Transgenic mice derived from the targeted mutation of RyR1 gene clearly demonstrate a key role of RyR1 as the SR Ca^{2+}-release channel involved in the e-c coupling machinery.

RyR1 knockout mice die perinatally probably because of respiratory failure (Takeshima et al., 1994). e-c coupling is lost in these mutant mice, indicating that RyR1 works as a Ca^{2+}-release channel linked to the T-tubule voltage sensor. Electron microscopy has shown triad junction lacking feet in skeletal muscle fibers of the so-called "dyspedic" mice (Takekura et al., 1995). In addition, RyR1 or RyR2 cDNA transfected into skeletal myoblasts from dyspedic mice has been used in expression experiments in order to establish which RyR type the mechanical coupling depend on (Yamazawa et al., 1996). RyR1 cDNA, but not RyR2 cDNA, was able to restore the skeletal muscle-type coupling. The importance of RyR1 isoform in the DHPR-RyR interaction was also shown by the fact that the II-III loop had no effect on RyR2 (Lu et al., 1995).

The "mechanical" hypothesis of skeletal muscle e-c coupling is supported also by the retrograde signaling interaction, from RyR1 and DHPR, revealed in RyR1 knockout mice (Nakai et al., 1996): dyspedic myotubes lacking RyR1 were shown to express greatly reduced L-type Ca^{2+}-channels. Transfection with RyR1 cDNA re-establishes a normal situation. Thus, a retrograde signal controls DHPR expression.

The presence of RyR3 in dyspedic mouse skeletal muscles could not compensate the lack of RyR1, confirming the non-equivalent function covered by RyR1 and RyR3 in skeletal muscle (Takeshima et al., 1995).

1.2.6. Crooked Neck Dwarf mutation (cn/cn).

A second animal model confirming the role of the skeletal RyR isoform in the mechanical coupling is represented by the chicken recessive lethal mutation Crooked Neck Dwarf (Ivanenko et al., 1995). Although the genetic nature of the mutation has not established, the result is the failure to make a normal α-RyR. +/? and cn/cn skeletal muscle cells formed myotubes in culture, but while +/? cells were able to switch from a Ca^{2+}-dependent to a Ca^{2+}-independent Ca^{2+}-release as observed for cultured neonatal rat skeletal muscle (Cognard et al., 1992), cn/cn were unable to operate this transition. This failure was a confirmation that the α-RyR, the RyR1 homologue, was necessary for skeletal muscle type e-c coupling. Although cn/cn skeletal muscles expressed normal levels of the β-RyR, it was not able to support Ca^{2+}-independent e-c coupling and compensate for the lack of α-RyR.

1.2.7 The model of two-ryanodine receptor Ca^{2+}-release system in skeletal muscle.

The presence of two RyR isoforms in non-mammalian vertebrate skeletal muscle, α and β-RyR, and the expression, although at lower levels, of RyR3 together with RyR1 in mammalian skeletal muscle, has prompted the hypothesis of a two-RyR Ca^{2+}-release system working in skeletal muscles, in which some RyRs are directly activated by the DHPR in a Ca^{2+}-independent manner, while others would be activated by CICR as a consequence of the activation of the first population. A two-RyR system could account for either

specialization of the contractile function associated with different muscle fibers or the amplification of the SR calcium release system resulting in a tune modulation of the contraction machinery (Sutko and Airey, 1996).

Evidences in addition to the biochemical data suggest that two distinct Ca^{2+}-release channels contribute to the regulation of skeletal muscle contraction. Electron microscopy studies (Flucher and Franzini-Armstrong, 1996), physiological analyses of Ca^{2+} from the SR (Rios et al., 1992), and detection of Ca^{2+} sparks in vertebrate skeletal muscles (see below) (Klein et al., 1993), appear consistent with of the existence of a two-release channel system in vertebrate skeletal muscles.

The model will be explained and discussed in the last part of this thesis (Discussion), with the contribution of the reported experimental data.

1.2.8. Skeletal muscle and Ca^{2+} sparks.

Ca^{2+} sparks were originally detected in quiescent rat heart cells as spontaneous local increases in the concentration of intracellular Ca^{2+}, and provide an explanation for both spontaneous and triggered changes in the intracellular Ca^{2+} concentration n the mammalian heart (Cheng et al., 1993). Ca^{2+} sparks represent elementary events underlying e-c coupling in cardiac muscle: the opening of L-type Ca^{2+} channels on the plasma membrane (DHPRs) provides a local increase in Ca^{2+} concentration, that recruits RyRs via CICR (Cheng et al., 1993). If sparks are the result of RyRs opening individually or involve several channels opening in concert is still debated (Shirikova et al., 1999).

Ca^{2+} sparks have also been visualized in skeletal muscle and originate at the level of the triad. In frog skeletal muscles, such unitary triadic Ca^{2+}-release

events occur spontaneously by a voltage-independent mechanism, or are initiated by the voltage sensor (Klein et al., 1996). In the latter, as a consequence of a voltage-gated release process, a secondary activation of Ca^{2+}-release channels occurs, most likely via CICR activated by an increase of Ca^{2+} level near the release channel. These evidences, together with the equal amount of RyR1/α and RyR3/β in frog skeletal muscle support the two-ryanodine receptor Ca^{2+}-release system suggested in the skeletal muscle e-c coupling.

Ca^{2+} sparks have also been detected in mammalian skeletal muscle (Conklin et al., 1999a; Conklin et al., 1999b; Conklin et al., 2000). Ca^{2+} sparks with parameters similar to those reported for adult frog skeletal muscle have been detected, even though at low frequency. The existence of knockout mice for RyR1 (Takeshima et al., 1994), RyR3 (Bertocchini et al., 1997) or both isoforms (Barone et al., 1998), allowed also to analyze separately the involvement of each isoform in the generation of Ca^{2+} sparks. RyR1 and RyR3 are both able to generate Ca^{2+} sparks in the absence of the other isoform, and they are the only intracellular Ca^{2+} channels that participate in sparks activity in embryonic skeletal muscles, because null-mutant mice for both RyR1 and RyR3 abolish any production of Ca^{2+} sparks (Conklin et al., 2000).

1.2.9. RyR expression during muscle development.

The developmental expression of mammalian and non-mammalian vertebrate RyRs has been investigated by Northern blot, Western blot, [^{3}H]ryanodine binding assay, and electron microscopy studies.

In chick myocardium RyRs are detected as early as embryonic day 4 (E4) (Dutro et al., 1993), while the classical "feet" are visible at E2.5 by electron microscopy (Protasi et al., 1996).

The expression of the avian α- and β-RyR proteins in skeletal muscle is differently regulated during development. The α-RyR is detected by E6 in forming skeletal muscle cells, while the β-RyR is detected by E17 (Sutko et al., 1991). At hatching, the level of RyRs increases dramatically, reaching adult levels at day 7 (N7) posthatch. The course of expression of the RyRs and of DHPR, measured in embryonic chicken skeletal muscle by [^{3}H]ryanodine binding and [^{3}H]nitrendipine binding, evolves in parallel: the expression of both proteins remain low before hatching and then increases (Sutko et al., 1991).

In rat and rabbit skeletal muscles the increase of RyR expression is not initiated until well into the period of neonatal development (Arai et al., 1992; Brillantes et al., 1994; Kyselovic et al., 1994).The time of DHPR increase depends on the species: in neonatal rat muscles the rapid increase in DHPR occurs several days in advance of the increase of RyRs. On the contrary, DHPR and RyR mRNA levels were found to increase in parallel during neonatal rabbit skeletal muscle development.

A more detailed analysis of RyR expression during neonatal development was performed on mouse diaphragm muscle (Tarroni et al., 1997). The pattern of expression RyR1 and RyR3 was investigated by Western blot assays. Both proteins are expressed at E18, the first stage analyzed. After birth, RyR1 and RyR3 expression increases, but while RyR1 increases progressively reaching the highest level in the adult, RyR3 is expressed at the highest level from day 5 and 15 after birth, then the expression decreases. Thus RyR3 is expressed at higher levels in neonatal than in adult diaphragm muscle.

1.2.10 Sequential use of cardiac and skeletal e-c coupling mechanism during skeletal muscle development.

A sequential use of DCCR and CICR for activating SR Ca^{2+}-release has been shown to occur in mammalian and chicken skeletal muscle developed in culture (Cognard et al., 1992; Strube et al., 1994; Ivanenko et al., 1995). Initially, SR Ca^{2+}-release depends on extracellular Ca^{2+} and becomes Ca^{2+}-independent as cells mature in culture. The type of e-c coupling depends on the DHPR α-subunit expressed in the cell. This evidence was demonstrated with the already discussed experiments (see above) in which injection of α_1 or α_2-DHPR into dysgenic myocytes resulted in the restoration of either the skeletal-type or the cardiac-type e-c coupling mechanism, respectively (Tanabe et al., 1990a, 1990b). The transient expression of α_1-DHPR in skeletal muscle development and the later replacement with the skeletal DHPR isoform (Chaudhari and Beam, 1993) justifies the transition from one e-c coupling mechanism to the other.

Materials and Methods

Chapter 2

2.1. Molecular Biology techniques

2.1.1 Competent cell preparation

XL1blu E. Coli bacterial strain (Stratagene) was used.

A single colony from a plate was picked and seeded into 5ml of Luria-Bertani Medium (LB). It was grown at 37° o/n and then diluted in 500ml LB. The culture was grown at 37° until 10^8 cells/ml concentration was reached. Cell concentration was checked by measuring absorbance at 600nM wavelength (A600) with spectrophotometer Uvikon 940 (Kontron Instruments): 10^8 cells/ml correspond to A600=0.5. Cells were cooled for 10 minutes (10') in ice and then centrifuged for 10' at 6000 rpm. They were resuspended in 10ml of sterile cold H_2O, diluted to 500ml and spin down again as before. The pellet was resuspended in 200ml of sterile cold H_2O and centrifuged 15' at 3000 rpm. Cells were resuspended in 10ml 10% glycerol in H_2O and spun down 15' at 3000 rpm. Pellet was resuspended in 0.8ml 10% glycerol in H_2O to give 5 x 10^{10} cells/ml, immediately frozen in liquid nitrogen in 40μl aliquots and stored at -80°.

Luria-Bertani Medium (per liter): 10gr Bacto-Tryptone, 5gr Bact-Yeast Extract, 10gr NaCl.

2.1.2 Transformation of competent cells by electroporation

Electroporation was performed to transform competent *XL1blu* bacterial cells prepared as described above with plasmidic DNA.

Biorad Gene Pulser apparatus was used.

10ng of DNA in water was added to 40μl of competent cells in a pre-cooled eppendorf tube. After 1 minute in ice, the suspension was transferred to a cold

electrocuvette (Biorad) and shaken to the bottom. One pulse of 12.5 kV/cm with a time constant of 4.5 to 5.0 msec was applied. The Gene Pulser apparatus was set to the 25μF capacitor and 2.5 kV, and setting the Pulse controller to 200 Ω. One ml of SOC medium was added immediately at room temperature (RT) and cells gently resuspended. Cells were transferred to a 15ml Falcon tube and incubated for 1 h at 37° with shaking. Cells were plated on agar plates containing ampicillin-resistant medium.

SOC medium: LB + 0.4% glucose + 10mM $MgSO_4$ + 10mM $MgCl_2$

2.1.3 Dephosphorylation assay

Dephosphorylation of linearized plasmid DNA was performed with alkaline phosphatase (AP) from calf intestine (Boheringer), an enzyme that removes 5'-phosphate groups from linear DNA.

Linearized 5' protruding plasmid DNA was incubated 1 h at 37°C in 1x AP buffer containing 10mM $ZnCl_2$, 10mM $MgCl_2$, 100mM Tris-HCl pH 8.3, and alkaline phosphatase in the amount of 1 unit/100pmoles of DNA. Linearized 3' protruding or blunt end plasmid DNA was incubated in the same buffer but with 1 unit/2pmoles of AP; the reaction was allowed to proceed 30' at 37°C and, after adding another aliquot of AP, 45' at 55°C .

The reaction was stopped and AP inactivated adding 0.5% SDS, 5mM EDTA, 100μg/ml proteinase K (Sigma), and incubating 30' at 56°C. This step was followed by two rounds of extraction with phenol:chloroform. Aqueous phase was precipitated with two volumes of EtOH absolute and 0.1M NaCl, washed with EtOH 70% and resuspended in a TE 1x at a concentration of about 100ng/μl.

2.1.4 Ligation

The ligation reaction between a linearized dephosphorylated plasmid DNA and a DNA fragment was performed in 10µl of total volume, with 1x T4 DNA ligase buffer, and 1 Weiss unit of T4 ligase (Biolabs) per 100ng of plasmid. T4 DNA ligase from Biolabs was used. The reaction was allowed to proceed at 16°C for 16 hrs. Then, the ligation reaction was dialyzed to remove any salt. 0.025µm-thick filters from Millipore were used. After dialysis, DNA was ready to transform bacterial cells.

2.1.5 Plasmid preparation: miniprep

Plasmid DNA was extracted from bacterial culture using the alkaline lysis method (Molecular Cloning, Second Edition, Sambrook, J., E.F. Fritsch, T. Maniatis, CSHL Press, 1989).

A single colony was grown in 1.5ml of LB with ampicillin 100µg/ml o/n at 37°C with shaking. Bacterial culture was centrifuged in Eppendorf at high speed. Pellet was resuspended in 100µl of a solution containing: 25mM Tris-HCl pH 8, 10mM EDTA, 150mM Glucose, and stored 5' at room temperature. 200µl of a solution containing 0.2N NaOH, 1% SDS were added, and stored 5' in ice. 150µl of a solution containing 3M KAc were added and stored 5' in ice. The solution was centrifuged 5' in Eppendorf at high speed, and the supernatant was extracted with an equal volume of phenol:chloroform. The aqueous phase was precipitated with 1ml of EtOH absolute, washed with EtOH 70%, and resuspended in 20µl of TE 1x.

DNA was ready to be digested with restriction enzyme.

2.1.6 Midiprep

In order to obtain amounts of DNA up to 100μg, plasmid midi preparation was performed using the Qiagen Columns (Promega), starting from 50-100ml bacterial colture. The following protocol corresponds to the Qiagen procedure, supplied by the Qiagen kit.

A single colony was grown in 50-100ml of LB plus ampicillin o/n at 37°C with shaking. The culture was centrifuged at 1000 g in Varifuge RF (Heraeus Sepatech). Pellet was resuspended in buffer P1. 4ml of buffer P2 was added, mixed gently and incubated 5' at room temperature. 4ml of buffer P3 was added, mixed gently and centrifuged 30' at 4°C at a speed>15,000 g. Supernatant was removed and applied onto a Qiagen-tip 100 previously equilibrated with 3ml of buffer QBT. The supernatant was allowed to enter the resin by gravity flow. The Qiagen-tip 100 was washed with 10ml of buffer QC, and then DNA was eluted with 5ml of buffer QF. DNA was precipitated with 0.7 volumes of isopropanol, and centrifuged 30' at room temperature at a speed>15,000 g. DNA was washed with EtOH 70%, and resuspended in a suitable volume of TE 1x.

2.1.7 Caesium Chloride preparation

This protocol of DNA extraction allows to prepare very large and clean amounts of plasmid DNA.

A single colony was incubated in 5ml of LB with ampicillin 100μg/ml 6-8 hrs at 37°C with shaking. The culture was inoculated in 500ml of LB with ampicillin 100μg/ml o/n at 37°C with shaking. The first part of the extraction is

based on the alkaline lysis method previously described (see above), with the difference of the use of large amount of the solutions and the final resuspension of DNA in 8ml of TE 1x. 8ml of CsCl were added, together with Ethidium Bromide at a final concentration of 250μg/ml. Polycarbonate tubes (11.5ml of volume, Kontron Instruments) were used. The samples were put in the quick seal tubes, and filled with a blank solution made with 8gr CsCl, 8ml TE 1x and Ethidium Bromide 250μg/ml. The tubes were sealed with the appropriate apparatus. Samples were centrifuged using the ultracentrifuge Centrikon T-1180 (Kontron Instruments) at a speed of 100,000 g for 16-18 hrs at 20°C. Plasmid circular DNA was removed by aspiration with a syringe, after identification with UV-transilluminator. Sample was collected in a new quick seal tube and centrifuged again at 100,000g for 4 hrs at 20°C. Plasmid DNA was collected again by a syringe, and extracted several times (4-6) with H_2O-saturated butanol. The aqueous phase was dialyzed in TE 1x pH 8.0 to remove all CsCl: o/n at 4°C with a stirrer, followed by 3x3 hrs washes at the same conditions. DNA was precipitated with EtOH absolute and 0.1M NaCl, washed in EtOH 70%, and resuspended in the suitable volume of TE 1x.

2.1.8 Agarose gel Electrophoresis of plasmid DNA (Restriction enzyme digestion)

Plasmid DNA was loaded on a 0.8-1% agarose gel prepared in TAE 1x. Electrophoresis was performed at 80V at room temperature, using a sample buffer containing xylene cyanol 6x. DNA was visualized by UV-transilluminator. Pictures were taken using the Polaroid MP 4+ (250V, ~600W), and Polaroid film (8.5x10.8 cm).

2.1.9 RNA extraction

RNA extraction was performed according to Chomczynski P., and Sacchi N., 1987.

Adult mouse diaphragms were homogenized with Dispergerate X 600W (220V, 50Hz, 600W, Heidolph) for 30", using solution D in the ratio of 1ml/100mg of tissue. Tissue was minced on ice.

Solution D: 4M guanidinium thiocyanate (Fluka), 25mM sodium citrate (Sigma), 0.5% sarcosyl (Sigma), 0.1M β-mercaptoethanol (Sigma).

Sequentially, 0.1ml of 2M sodium acetate pH 7.4 (Sigma), 1ml of H_2O-saturated phenol (Merck), and 0.2ml of chloroform-isoamyl alcohol mixture (49:1) were added to the homogenate, with mixing by inversion after the addition of each component. After cooling 15' on ice, the suspension was centrifuged at 10,000 for 20' at 4°C. The aqueous phase, containing the RNA, was transferred to another tube. After the addition of 1ml of isopropanol the aqueous phase was placed 1 h at -20°C to allow RNA precipitation. After a centrifugation at 10,000 g for 20' at 4°C RNA pellet was resuspended in 0.3ml of solution D. The resuspension was transferred into an eppendorf tube and precipitated again at -20°C after the addition of 1 volume of isopropanol. After centrifugation in Eppendorf centrifuge for 10' at 4°C, and quick washing with EtOH 75%, the RNA pellet was resuspended in a suitable volume of sterile H_2O. Quantitative estimation of RNA was performed by both loading a small aliquot of the resuspension on an agarose gel, and by spectrophotometer analysis. RNA was stored at -20°C.

2.1.10 cDNA synthesis: RT-PCR

10µg of mouse diaphragm RNA plus random examers oligonucleotides 15µM were denatured 2' at 95°C. Then the following components were added: reverse transcriptase buffer 1x, dNTPs 1mM (Pharmacia), DTT 5mM (Sigma), and 200 unit of M-MLV Reverse Transcriptase (Gibco BRL). After an annealing reaction 10' at room temperature, the reaction was allowed to proceed 1 h at 37°C. The neo-synthesized cDNA can be immediately used for an amplification reaction by PCR (5µl), or can be stored at -20°C.

2.1.11 PCR Analysis

PCR assay was performed using the Polymerase Chain Reaction machine Protocol™ thermal cycler (Ams, Biotechnology Ltd). It was used to amplify DNA fragments from plasmids, or mouse genomic DNA. In both cases, small amounts of DNA (10-100ng) was added to a mix containing: Taq Polymerase buffer 1x, 25mM $MgCl_2$, 0.2mM dNTPs, 50 picomoles 3' primer, 50 picomoles 5' primer, and H_2O. Then 2 units of Taq Polymerase (Promega) were added. 100µl of paraffin oil was used to cover the reaction mixture, and avoid evaporation during the denaturing step. To amplify fragments of DNA from plasmids, 5' of denaturation at 95°C preceded 30 cycles at the following conditions: 30" at 95°C (denaturation); 30" at the annealing temperature chosen every time depending on the primers used (annealing); 45" at 72°C (elongation). After 30 cycles, a 5'-long elongation step at 72°C followed. Samples were stored at -20°C before checking amplified DNA on agarose gel.

The annealing temperature was calculated using the melting temperature (TM) of the primers used. The TM was obtained according to this formula:

$$TM = 69.3 + 0.41 \times ((G+C)\%) - 650/L$$

where L=length of the primer. The annealing temperature derives from the lower TM between the two primers, minus 5°C.

2.1.12 DNA sequencing

2.1.12a Sequencing Reaction.

DNA was sequenced using the T7 Sequencing Kit (Pharmacia), based on the method of Sanger (Sanger et al., 1977).

1.5-2.5µg plasmidic DNA was denatured 5' at room temperature with NaOH 0.2N in 20µl of total volume. Then DNA was precipitated with EtOH absolute and 0.3M NaAc ,washed with EtOH 70% and resuspended in 10µl of H_2O. Denatured DNA is ready for sequencing reaction. Three different steps can be distinguished: the annealing reaction, the labelling reaction and the termination reactions. In the annealing reaction, the following components were added to the denatured DNA (10µl): 2µl of primer 0.5pmoli/µg, 2µl of reaction buffer containing 1M Tris-HCl (pH 7.6), 100mM $MgCl_2$ and 160mM DTT, for a final volume of 14µl. The annealing reaction was allowed to proceed for 5' at 65°C, and cooled slowly, first 10' at 37°C and then 10' at room temperature. In the labelling reaction the following components were mixed: the annealed DNA-

primer (14µl), 1µl of DTT 0.1M, 3µl of labelling mix containing 1.375µM each dCTP, dGTP, dTTP and 333.5 mM NaCl, 1µl of [α-^{35}S]-dATP (10 mCi/ml, >1000 Ci/mmol), 2µl of T7 DNA polymerase diluted using the Enzyme Dilution Buffer in a ratio 1:4. Enzyme Dilution Buffer contains: 20mM Tris-HCl pH 7.5, 5mMDTT, 100µg/ml BSA, 5% glycerol. The labelling reaction was allowed to proceed for 5' at room temperature, followed by the termination step. The termination is based on the presence of a dideoxinucleotide, that prevents the further elongation of DNA synthesis. Four different termination mix are used one for each nucleotide, named A Mix, C Mix, G Mix and T Mix. Each mix contains the corresponding dideoxinucleotide. For example, this is the composition of the A Mix: 840µM each DCTP, dGTP, dTTP; 93.5µM dATP; 14µM ddATP; 40mM Tris-HCl (pH 7.6) and 50mM NaCl. The Short-Mix were used. During the 5' incubation time, 2.5µl of each termination mix were aliquoted in different wells of a microtiter plate. 4.5µl of labelling reaction was transferred into each of the four pre-warmed wells, containing the termination solutions, mixed gently, and incubated 5' at 37°C. 5µl of Stop Solution was added to each well. Stop Solution contains 0.3% each Bromophenol Blue and Xylene Cyanol, 10mM EDTA pH 7.5, 97.5% deionized formamide. The samples were ready to be loaded on a polyacrylamide gel.

2.1.12b Electrophoresis

Samples were loaded on a polyacrylamide gel containing 6% acrylamide, 1x TBE, 8M Urea. 6% acrylamide was a mix of acrylamide (DNA-sequencing grade, BioRad) and N,N'-methylenebisacrylamide, in a ratio 30:1.

The solution must be filtered using a 0.45μm filter (Nalgene), degassed, and stored at 4°C. A 4mm-thick gel was used. To allow polyacrylamide polymerization 0.08% APS (Sigma), and 0.05% Temed (BioRad) were added Electrophoresis run was performed at 1500V for 1 h and half (short run), or 4 hrs (long run). Gel was detached from the glasses, transferred to a Whatman 3MM paper and dried by Dryer from Biorad for 1 h at 80°C. Then it was exposed to Hyperfilm™-MP (Amersham) for 12-24 hrs and then developed using the automatic developer machine.

2.1.13 Elution of DNA bands from agarose gels

DNA bands from digested plasmidic DNA were eluted from agarose gel using the Low-Melting Agarose (Sigma).

Digested DNA was loaded on a 0.7% LM-agarose gel in TAE 1x. Electrophoresis run was performed at 4°C (cold room). The specific fragment of DNA was cut from the gel after identification at UV-transilluminator. An equal volume of phenol pH 8.0 was added and put at 65°C for 5-10', until the agarose was completely resuspended. After shaking the mixture was put ice for 15' and then centrifuged at highest speed in Eppendorf centrifuge (14000 rpm). The upper phase was collected and precipitated adding 2 volumes of EtOH absolute and 0.1M NaCl. After precipitation and washing with EtOH 70%, the pellet was resuspended in a small volume of TE 1x.

2.1.14 Genomic DNA extraction from mouse tails

A small piece of tail was cut from a two-week old mouse. It was placed in 750μl of buffer containing 50mM Tris-HCl pH 8, 100mM EDTA, 100mM NaCl, 1% SDS, 0.5 mg/ml Proteinase K, and incubated o/n at 55°C. After cooling at room temperature for 15', it was shaken for 5' and 250μl of saturated NaCl was added (6M NaCl). It was shaken again 5' and spun 10' at full speed in Eppendorf centrifuge. 750μl were taken from the top phase, transferred to a new tube and 500μl of isopropanol were added. After shaking for 2', it was spun 5' at full speed in Eppendorf centrifuge. The pellet was washed with EtOH 70% and allowed to air dry. The pellet was resuspended adding 200μl TE 1x and incubating at 37°C for 2h, with occasionally shaking.

Genomic DNA was stored at 4°C.

This procedure yields 50-100μg of genomic DNA.

2.1.15 Restriction enzyme digestion of plasmid DNA and mouse genomic DNA.

Plasmid DNA was digested with the appropriate restriction enzyme in a concentration of 1 Unit/1μg, in 20μl of total volume containing the restriction enzyme buffer 1x. The reaction was allowed to proceed 2-3 hrs at the temperature suitable for the restriction enzyme used. Most of the digestions were performed at 37°C. The digestion was checked by loading an aliquot of the restriction (1/10) on agarose gel, and visualizing DNA bands at the UV-transilluminator.

Mouse genomic DNA was digested with the appropriate restriction enzyme in a concentration of 1 Unit/1μg, in 60μl of total volume containing the restriction enzyme buffer 1x. The digestion was allowed to proceed for 16 hrs at 37°C. Digested DNA was loaded on an agarose gel for Southern analysis as described (see below).

2.1.16 Southern blot assay

Genomic DNA digested with the appropriate restriction enzyme was loaded on an agarose gel 0.8% in TAE 1x, using a sample buffer containing xylene cyanol 6x. After electrophoresis, the gel was placed in 0.25M HCl for 15'. The gel was rinsed in H_2O and placed in denaturing solution: NaOH 0.5M, 1.5M NaCl. After 30' with shaking, the gel was rinsed again with H_2O and placed in neutralizing solution: NaCl 1.5M, 0.5M Tris-HCl pH 7.2, 0.001M EDTA. After 10' with shaking, the capillary blot is set up: a tray was filled with 20x SSC (blotting buffer), a platform was made and covered with a sheet of Whatman 3MM filter paper saturated with blotting buffer and in direct contact with the blotting buffer in the tray. The gel was placed on the wick and surrounded with parafilm to prevent the blotting buffer being adsorbed directly into the paper towels above (see below). A sheet of Hybond-N membrane (Amersham) is cut to the exact size of the gel, and placed on top of the gel. Three sheets of 3MM paper, wetted with blotting buffer, were placed on top of Hybond-N membrane. A column of adsorbent paper towels was placed over the three 3MM wetted sheets, and a 0.75-1Kg weight was placed on the top. The transfer was allowed to proceed for 16h.

After blotting, the apparatus was disassembled. Before removing the gel the membrane was marked with pencil to allow later identification of wells. The membrane was washed with 2x SSC and allowed to air dry.

DNA was fixed on the membrane using UV-crosslinker apparatus UV-Stratalinker™ 2400 (Stratagene). The membrane was wrapped in SaranWrap™ placed DNA-side up in the crosslinker for 1'.

After fixing, the membrane was ready to be hybridized.

SSC 20X (per liter): NaCl 175.3 gr, sodium citrate 88.2 gr, pH 7

2.1.17 Random primed reaction

A specific fragment of DNA eluted from an agarose gel was radiolabeled using the "High Prime" kit from Boheringer Mannheim, based on the random primed DNA-labelling method. 25-50μg of DNA were denatured at 95°C for 5', and added to 4μl of reaction mixture from High Prime kit. The reaction mixture contains all the components necessary for a random primed reaction: Klenow enzyme and its buffer, deoxyribonucleotides, random hexanucleotides as primers. 5μl of [α-^{32}P]-dCTP (10 mCi/ml, 3000 Ci/mmol) were added to a final volume of 20μl.

The reaction was allowed to proceed for 30', and then stopped by adding 1mM EDTA. The radiolabeled DNA fragment was separated from non-incorporated deoxynucleotides by passing the reaction mixture in a packed Sepharose G-50 column. The column was made as follows. Sephadex G-50 resin was suspended in TEN buffer: 10mM Tris-HCl pH 7.5, 1mM EDTA pH 8, 100mM NaCl, 0.1% SDS. The equilibrated resin was packed over a small amount (200μl) of glass

beads (Sigma,425-600 microns, acid-washed), equilibrated in TEN buffer, and packed in a holed eppendorf tube. The column was put in a 15ml Falcon tube. The volume of the random primed reaction mixture was brought to 100µl, loaded on the column, and spun 5' at 1000 rpm. The eluate was collected at the bottom of the Falcon tube. 1µl of the eluate was counted at the β-counter machine in order to know the amount of incorporated radioactivity.

Before using, the radiolabeled DNA was denatured 5' at 95°C.

2.1.18 Hybridization

The hybridization of a membrane was performed using tubes in a heater with roller. The Hybond-N membrane with UV-crosslinked DNA was pre-hybridized at 65°C in Church buffer: 0.5% Na2HPO4 (H2O)2 pH 7.2, 7% SDS, 1mM EDTA, 1% BSA. After 30' of pre-hybridization, the membrane was hybridized in 5-10ml of Church buffer adding the radioactive probe prepared as described (see above). The probe was added at a concentration of 5×10^6 cpm/ml. The hybridization was allowed to proceed for 16 hrs at 65°C. Then the membrane was washed 2x20' at 65°C using the following wash buffer: 40mM Na2HPO4 (H2O)2 pH 7.2, 1% SDS. After washing the membrane was wrapped in SaranWrap™ and exposed o/n with Hyperfilm™-MP (Amersham) in an autoradiography cassette at -80°C. The film was then developed using the automatic developing machine.

Church buffer: Na_2HPO_4 0.5 M, SDS 1%, EDTA 1mM

2.2 Transgenic mouse techniques

Materials

All reagents utilized are from Gibco BRL, unless otherwise indicated.

β-mercaptoethanol: β-mercaptoethanol 14.3mM (Sigma) was dissolved in PBS 1x at a final concentration of 10mM. The solution was filtered with a 0.22μm filter (Millipore), and stored at +4°C.

LIF: Leukaemia Inhibitory Factor was dissolved in 10ml of ES cell medium at a final concentration of 10^5U/ml, filtered with a 0.22μm filter (Millipore), and stored at 4°C.

Gelatin: 1%(w/v) tissue culture grade gelatin (Sigma) was mixed in H_2O and sterilized by autoclaving. The working solution is 0.1% and is made by diluting the stock solution in sterile H_2O.

Mytomicin D: mytomicin D (Sigma) was dissolved in PBS 1x at a concentration of 2mg/ml, and stored at -20°C. Stocks for use were made diluting 0.25ml into 50ml of MEF, and storing at -20°C.

G-418: G-418 sulphate (Geneticin[R]) was dissolved in HEPES 0.1M pH 7.4 at a concentration of 50mg/ml, filtered with 0.2μm filters, and stored at 4°C.

PBS 1x: phosphate-buffered saline. For 1 liter the following component were mixed: 8g NaCl, 0.2g KCl, 0.2g KH_2PO_4, 1.072g $Na_2HPO_4.7H_2O$ in water. pH was adjusted to 7.2 using a saturated solution of $Na_2HPO_4.7H_2O$. It was filter sterilized and stored at room temperature.

DMEM: Dulbecco's modified Eagle's medium.

2.2.1 Culture of feeder layers and mytomicin D treatment.

Feeder layers are primary embryo fibroblasts. They were prepared from 13.5 day post-coitum (d.p.c.) neo-resistant mice, aliquoted on freezing vials and stored in liquid nitrogen.

Feeder layers were grown in MEF (mouse embryonic fibroblasts) medium: DMEM + 4.5µg/l glucose, 10% foetal calf serum (FCS) heat-inactivated (56°C for 30'), glutamine 2mM, penicillin/streptomycin 100µg/ml.

A vial of fibroblasts was thawed quickly in a bath at 37°C. Fibroblasts were put in a 15ml falcon containing 6ml of MEF medium, and centrifuged 3' at 1000rpm. Pellet was resuspended in 10 ml of MEF medium and plated on a 10-cm diameter plate. Feeder layers were allowed to grow and expand before treatment with mytomicin D. Fibroblasts were treated with mytomicin D before being used as substrate to plate Embryonic Stem (ES) cells. MEF medium was sucked off, and MEF + mytomicin D 10µg/ml was added, in a volume suitable to cover the plate. After 3 hrs at 37°C, 5% CO_2, the medium was removed and cells were washed with PBS 1x. Cells were trypsinized a few minutes at room temperature, and then MEF medium was added. Fibroblasts were centrifuged at 15°C for 3' at 1000rpm in a Minifuge T (Hearaeus Sepatech). Cells were resuspended in the suitable volume of ES cell medium, and plated to be used as feeder layers for ES cells.

2.2.2 ES cell culture

ES cells were grown in the following culture medium: DMEM + 4.5μg/l glucose, 15% FCS heat-inactivated (56°C for 30'), glutamine 2mM, penicillin/streptomycin 100μg/ml, β-mercaptoethanol 100 μM, Leukaemia Inhibitory Factor (LIF) 10^3 u/ml. This medium is suitable for E14 ES cells. ES cells R1 require, in addition, Na-pyruvate 1mM, and NEAA (Non Essential Amino Acid, Seromed) 1% of stock solution. ES cells were grown on feeder layers, that is fibroblasts from neo-resistant mice, treated with mytomicin D as described.

A vial of ES cells previously frozen was thawed quickly in a bath at 37°C. ES cells were put in a 15ml falcon tube containing 6ml of ES cell medium, and centrifuged 3' at 1000rpm. Pellet was resuspended in 5ml of medium and plated on a 6-cm diameter plate with feeder layers. Medium was changed daily. ES cells were allowed to grow until they reached the suitable amount to be used in a round of electroporation of plasmid DNA.

2.2.3 Electroporation of plasmid DNA into ES cells

Es cells, grown as described (see above), were washed with PBS 1x 1' at room temperature; after trypsinization 5' at room temperature, cells were collected, diluted in 5ml of ES medium and centrifuged 3' at 3000rpm. Cells were resuspended in ES medium and plated 30' at 37°C in a plate without feeder layer. This pre-plating step allows the elimination of fibroblasts that attach to the plate. Cells were collected and centrifuged again 1' at 3000rpm. Cells were resuspended in ml PBS 1x and counted using the appropriate counting glass. In

order to get a concentration of 1×10^7 cells/ml, cells were centrifuged again and resuspended in the suitable volume of PBS 1x. Biorad Gene Pulser apparatus was used. 0.9ml of cells were added to a cuvette, followed by addition of DNA. 10µg, 25µg or 50µg of linearized plasmid DNA was used, in a volume not greater than 50µl. Electroporation was performed in the following conditions: 240V, 500µF.

After electroporation cells were stored 5' at room temperature, and then were plated, distributing the 0.9ml into 8-cm diameter plates.

24 hrs after electroporation, the medium was changed.

2.2.4 Selection with G-418 and gancyclovir

48 hours after electroporation G-418 selection started. G-418 was used at a concentration ranging from 0.325mg/ml to 0.350mg/ml, depending on the ES cells used. Medium was replaced every day with fresh medium. 6 days after the beginning of G-418 selection, gancyclovir selection started, and proceeded together with G-418 selection. 500mg of powder gancyclovir (Cytovene, Sintex) were dissolved in 10ml PBS 1x, to a final concentration of 196mM. It was diluted in ES medium (containing also G-418) in the following concentration: 1µl/98µl ES medium, to get a final concentration of 2mM. 10ml of gancyclovir 2mM in ES medium were prepared, filtered with 0.2µm filters, and stored at 4°C. Gancyclovir for the selection was used at a concentration of 2µM, so diluting 1/1000 the 2mM stock. Gancyclovir selection was allowed to proceed for two days. On the second days, colonies resistant to both G-418 and gancyclovir were started to be picked up. The plate containing the colonies was washed with PBS 1x. PBS 1x was added to cover the plate. The plate was placed on an inverted microscope, and individual colonies were picked up by a

mouth-controlled pipette. Once picked up, the resistant colony was allowed to grown in a well of a 96-well plate according to Ramirez-Solis et al. 1993. ES cells were grown on feeder layers treated with mytomicin D as described . 150μl of ES cell medium per well was used. Cells were allowed to grow at 37°C, 5% CO_2 for 3-5 days. Medium was changed if necessary (when it started turning yellow). When approaching confluence, cells in the wells were washed with PBS 1x, and 50μl of trypsin per well were added and sucked off immediately. After 1', the remaining trypsin was removed. 150μl of ES cell medium was added, followed by gently pipetting. 75μl of resuspended cells were transferred to a gelatinized 96-well plate (0.1% gelatin), where they were grown to extract DNA. The other 75μl remained in the wells of the original 96-well plate. where they were allowed to grow for 2-4 days before being frozen. To allow the growing, some ES cell medium (75μl) was added to the wells of both the gelatinized plate and the original one.

2.2.5 DNA extraction from ES cells in 96-well plates

Cells on the gelatine -coated plates were allowed to grow until they turned the medium yellow every day (4-5 days). Wells were rinsed twice with PBS 1x. 50μl of lysis buffer per well were added. The plate was incubated o/n at 60°C in humid atmosphere. The next day, 100μl per well of a mix of NaCl and EtOH were added. The mix was prepared adding 150μl of 5M NaCl to 10ml of EtOH absolute. After 30' at room temperature nucleic acids precipitate as a filamentous network. The solution was discarded inverting the 96-well plate. Nucleic acids were rinsed three times with EtOH 70%. After drying, DNA was ready to be digested with restriction enzymes.

2.2.6 Digestion with restriction enzyme of DNA on 96-well plates.

The restriction digestion mix was prepared as follows: 1x restriction buffer, 1mM spermidine, 100μg/ml bovine serum albumin (BSA), 100μg/ml RNase A and 10 units of the chosen restriction enzyme per sample. 30μl per well of restriction digest mix were added, and the reaction was incubated o/n at 37°C in humid atmosphere. The next day, digested DNA was ready for conventional electrophoresis and Southern analysis (as described in section 1).

2.2.7 Freezing of selected clones

The freezing of selected clones in 96-well plates was performed according to Ramirez-Solis et al., 1993.

Medium was changed 4 hrs before freezing. Medium was discarded by aspiration and cells were rinsed twice with PBS 1x. 50μl of trypsin per well were added using the multichannel pipettor, followed by incubation of the 96-well plate for 10' at 37°C, 5% CO_2. 50μl of 2x freezing medium per well were added, and cells were dissociated gently pipetting up and down. 100μl of sterile light paraffin oil per well were added to prevent degassing and evaporation during storage at -70°C. The 96-well plate was sealed by Parafilm, and stored at -70°C.

Freezing medium 2x: 60% DMEM, 20% FCS, 20% DMSO (Sigma).

2.2.8 Thawing of selected clones

The 96-well plate was taken out of the freezer and placed for 10'-15' at 37°C, 5% CO_2. Once identified the selected clones, the entire content of the well was put into a well of a 24-well plate containing 2ml of medium. The medium was changed the next day to remove the DMSO and the oil.

2.2.9 Blastocyst recovery

Blastocysts were recovered by C57 mouse strain. The pregnant C57 mouse was killed on the fourth day of pregnancy (3.5 d.p.c.) by cervical dislocation. At this time blastocysts are present in the uterine lumen, and were recovered by removal and flushing of the uterine horns with the appropriate culture medium (see below). A cut through the utero-tubal junction on each side was made, freeing the entire tract. The tract was spread out in a dry sterile Petri dish and any remaining mesentery and fat was trimmed away. A cut across the cervix was performed to expose the entrance to both uterine horns. Inserting a Pasteur pipette tip into the cervical end 0.5ml of medium was flushed through each horn. Medium, together with blastocysts, flowed freely through the tract.

PB-1 medium + 10% heat-inactivated foetal calf serum (56°C for 30').

PB-1 solution was prepared as follows:

Stock solution	(g/100ml)	Volume (ml)
$NaCl$	0.9	68.96
KCl	1.148	1.84
$Na_2HPO_4.12H_2O$	5.5101	5.44
KH_2PO_4	2.096	0.96
$CaCl_2.2H_2O$	1.1617	0.88
$MgCl_2$	3.131	0.32
Na pyruvate	0.020	22.40

The following were added to make up 104ml of medium:

penicillin	6.2mg
glucose	104mg
H_2O	2.16ml
phenol red (1%)	0.1ml

Foetal calf serum at a final concentration of 10% was added. Complete medium was filter sterilized, and refrigerated until use.

2.2.10 Injection of selected clone into mouse blastocyst

The ES cell clone selected to be injected was grown in ES medium in a plate with feeder layers as described, until they reach the exponential phase of growing. The day of injection ES cells were fed. One hour later they were washed with PBS 1x, and trypsinized 1' at room temperature. After dilution with ES medium, trypsinized cells were centrifuged 3' at 1000rpm. They were resuspended in ES medium and plated 30' at 37°C on a plate without feeder

layers. The pre-plating step allowed the removal of feeder layer cells. Cells were collected and centrifuged again 3' at 1000rpm. Pellet was resuspended in 50µl of ES cell medium and stored at 4°C. 13-15 ES cells were injected into mouse blastocysts previously withdrawn (see above). Injection was performed using mechanical force micromanipulators and a standard microscope, and a micromanipulator chamber in which the embryo and the ES cells were kept in hanging drops. Microinstruments for use in blastocyst injection are fashioned out of glass capillary fitting the instrument holders (for example, Drummond custom capillary, 1mm outside diameter, 0.75 inside diameter). Only two instruments are necessary, a holding pipette to hold and stabilize the blastocyst, and a cell injection pipette to pick up and inject the ES cells. Both pipettes were made by a pipette puller. For the injecting pipette, a bevelled-tip pipette is preferred. In this case, after pipette puller treatment, the pipette is placed under a dissecting microscope and a scalpel blade is used to brake off the tip.

Blastocyst and a cell suspension of ES cells were introduced into drops in the manipulation chamber using a mouth-controlled Pasteur pipette. This can be done under a dissecting microscope. The injection instruments can be set-up in the micromanipulator, and filled with oil by positive pressure. The tips of the two pipettes were put in the same focus field. The manipulation chamber was introduced. 12-15 ES cells were picked up at the tip of the injecting pipette using suction. A blastocyst was picked up with the holding pipette by suction, positioning it so that the ICM (inner cell mass) could be seen in profile against the pipette. The injected pipette was allowed to penetrate the trophoectoderm layer, the ES cells were expelled into the blastocoelic cavity, and the pipette was removed. When all the available blastocysts had been injected, they were transferred to culture medium for a brief period of culture before being transferred to pseudo-pregnant hosts.

2.2.11 Transferring of injected blastocyst into foster CD1 mother

CD1 female mice (white-colored) were rendered pseudo-pregnant by mating with sterile males during oestrus, because they displayed the hormonal profile of a pregnant female when the stimulus of mating occurs during oestrus. Sterile males were produced by vasectomy, that is the cut of vas deferens. In general embryos can be transferred to a synchronous host, but, since *in vitro* manipulation of embryo cause a delaying embryonic development, the more efficient method is to transfer embryos to host that are one day asynchronous. Thus, fourth day blastocysts were transferred to the uterus of females in the third day of pseudo-pregnancy. 4-5 injected blastocysts were transferred in each horn of the pseudo-pregnant female. An embryo transfer pipette was used. It was made like the holding pipette, but the overall diameter at the tip was larger so that the opening could easily accomodate embryos (110-130μm). After a skin incision performed on the dorsal side of the female, a needle was inserted through the muscle layer of the uterus, about 2mm from the utero-tubal junction. After removing the needle without taking the eyes off the hole, the tip of the transferred pipette was inserted into the hole, and embryos were expelled into the lumen together with air bubbles that served as indicators of embryo expulsion. Skin incisions were closed by small wound clip.

2.3. Biochemical techniques

2.3.1 Microsomal membrane preparation from mouse tissues

Mouse tissues were homogenized with Dispergerate X 600W (220V, 50Hz, 600W, Heidolph) at setting, followed by dounce homogeniser using 5ml/gr of a solution containing 320mM sucrose, 5mM Hepes-NaOH pH 7.4 and 0.1mM PMSF (homogenizing buffer). The homogenate was centrifuged at 10,000 g for 5' at 4°. Supernatant was centrifuged at 100,000 g for 1 h at 4°. Pellet was resuspended in the homogenizing buffer using a 2ml dounce. Aliquots of microsomes were immediately frozen in liquid nitrogen and stored at -80°. Protein concentration of the microsomal fraction was quantified using a protein assay kit (Bio Rad).

2.3.2 Western blot assay of mouse tissue microsomal membranes

A 1.5 mm gel was prepared, with 5% acrylamide in the resolving gel and 4% in the stacking gel. Microsomal membranes were loaded after adding Laemmli buffer (1x final) and denaturing at 95°C for 2'. Laemmli buffer: 0.0025M Tris-HCl pH 6.8, 2% SDS, 10% glycerol, 5% 2-mercaptoethanol, 0.001% bromophenol blue (Laemmli, U.K., 1970). Electrophoresis was allowed to proceed for 16 hrs at 60 V at 4°C (cold room), in the following running buffer: 25mM Tris, 192mM glycine, 0.1% SDS, pH 8.3. Then electro-blot was performed at 400 mA at 4°C for 6 hrs, using nitrocellulose membrane Protran BA 85 (Scheicher & Schuell) and electro-blotting apparatus (Hoefer scientific instruments), in blotting buffer: 25mM Tris, 192mM glycine, 0.01% SDS, 10% methanol, pH 8.3. After blotting, the membrane was blocked 3 hrs at room

temperature in blocking buffer: 50mM Tris-HCl pH 7.4, 150mM NaCl, 0.2% Tween 20, 5% dry milk. The membrane was incubated with the primary antibody o/n at room temperature in blocking buffer. All the antibodies used were diluted 1:3000 (Giannini et al., 1995). The membrane was washed 4x15' in wash buffer: 50mM Tris-HCl pH 7.4, 150mM NaCl, 0.2% Tween 20, 0.5% dry milk, followed by incubation with the biotin-conjugated anti-rabbit secondary antibody. The biotin is conjugated to the alkaline phosphatase. The secondary antibody incubation was performed in wash buffer without tween. The membrane was washed 4x15' in wash buffer, and then it was incubated with streptavidin-biotin complex (Amplified Alkaline Phosphatase Immunoblot reagents from Biorad). The membrane was washed again 4x15' before development. The two substrates bromochloroindolyl phosphate (BCIP) and nitro blue tetrazolium (NBT) are added to the alkaline phosphatase buffer: 100mM NaCl, 5mM $MgCl_2$, 100mM Tris-HCl pH 9.5. 33µl of 5% NBT in 70% dimethylformamide, and 66µl of 5% BCIP in H_2O were added to 10ml of alkaline buffer. 10ml of alkaline buffer are suitable for 15x15 cm^2 membrane. The blot was developed for 10' at room temperature with shaking, and the colorimetric reaction was blocked rinsing the membrane with H_2O.

2.3.3 Binding analysis with radioactive ligand

2.3.3a Saturation curve and Scatchard analysis

50μg microsomal membranes from mouse tissues were incubated for 1 h at 37°C with the following concentrations of [^{3}H]ryanodine (Dupont, 0.1μCi/μl, specific activity: 68 Ci/mmol): 0.5nM, 1nM, 1.5nM, 2.5nM, 5nM, 7.5nM, 10nM, 15nM, 20nM, 25nM, 30nM. The reaction was performed in 200μl of binding buffer containing 1M KCl, 20mM Hepes-NaOH pH 7.4, 100μM CaCl$_2$ and a mixture of protease inhibitors: 76.8nM aprotinin (Sigma), 0.83mM benzamidine (Sigma), 1mM iodoacetamide (Sigma), 1.1μM leupeptin (Sigma), 0.7μM pepstatin (Sigma) and 0.1mM PMSF (Sigma). The bound [^{3}H]ryanodine was separated from free ligand by filtering through Whatman GB/F glass fiber microfilters. The filters were washed with 3x5ml of ice-cold binding buffer, and 2x5ml EtOH 10%. Radioactivity remaining with the filters was measured by liquid scintillation counting, using β-counter machine.

Specific binding was calculated as the difference of total and nonspecific binding measured in parallel assays in the presence of 10μM unlabeled ryanodine (Calbiochem). Experiments were performed in duplicate.

Scatchard analysis was performed using the computer program MacLigand.

2.3.3b Ca^{2+}-dependence Curve

Ca^{2+}-dependence experiments were performed using 10nM [^{3}H]ryanodine in the following binding buffer: 0.3M KCl, 20mM Hepes-NaOH pH 7.4, the

mixture of protease inhibitors as described above and different concentration of Ca^{2+}: 10nM, 100nM, 1μM, 10μM, 100μM, 1mM, 10mM, 100mM.

.

2.4. Contracture analysis

Diaphragm strips including the insertion on the rib and on the central tendon were dissected and mounted between a force transducer (AE 801 Sensonor Horten, Norway) and a movable hook in a perfusion bath containing bicarbonate Krebs solution (volume 2ml). The solution was bubbled with O_2-CO_2 mixture and the temperature was kept constant at 22°C. The preparations were stretched just above slack length (resting tension ~5% of twitch tension) and supramaximally activated with field stimulation. The output of the tension transducer was stored in a PC after A/D conversion and recalled for analysis. CEA 1401 A/D converter and CEA Spike2 software were used. After stabilization at 0.1 Hz, twitch and tetani (0.5 s duration) at frequencies of 5, 10, 20 and 50 Hz were recorded.

The depressing effect of external Ca^{2+} removal was studied on twitches produced at the rate of 0.1 Hz.

After the electrical responses, the response to pharmacological agents able to release Ca^{2+} was tested. For pharmacological agents, increasing doses of caffeine (range 10-30mM) or 10μM of ryanodine were used. Each contracture was followed by washing with Krebs solution without caffeine or ryanodine to produce a complete relaxation of the preparation.

To analyze the ability of the myofibrils to develop tension in response to direct Ca^{2+} activation, the following procedure was used. The preparation was immersed for 1 h in skinning solution containing EGTA and Triton X-100 at low temperature (10°C). Membranes were removed with this treatment. The solution in the chamber was then replaced with a relaxing solution at pCa 8. After a few minutes the preparation was activated to develop tension by filling the chamber with activating solution (pCa 4.5). When tension reached a stable level, the preparation was relaxed by filling the chamber with relaxing solution.

The composition of skinning, relaxing and activating solution were previously described (Bottinelli et al., 1994).

Results

Chapter 3

3.1. The construction of the targeting vector C1

3.1.1 Introduction

The 3' region of the murine *RyR3* gene was previously cloned from a 129/Sv mouse strain genomic library by G. Giannini and A. Nori.

The region is represented in Fig.1.1A. The region used for the construct spans from the HindIII site upstream the exon B to the EcoRI site just upstream of the exon G and the 3' UTR (Fig. 1.1B). This genomic region was cloned in two plasmids using pBluescript (Stratagene, Fig. 1.2) by G. Giannini and A. Nori:

- pBS H/H 1.6: 1.6 kb containing the region from the HindIII site upstream and the HindIII site just downstream exon B, cloned in the HindIII site of plasmid Bluescript KS (Fig.1.4A).

- p• 1.3: 5.2 Kb containing the region from the HindIII site downstream the exon B and the EcoRI site upstream the exon H and the 3' UTR, cloned in the HindIII and the EcoRI sites of pBluescript (Fig. 1.4B).

These two plasmids were modified to make a suitable construct useful to knockout the murine *RyR3* gene.

A

GENOMIC DNA

Hind III

Hind III

EcoRI
Hind III

exo A

EcoRI

Hind III

exo B

EcoRI
Hind III

Hind III
Kpn I

Dra II

exo C

Sac I

Pst I

exo D   exo E   exo F

Xba I

EcoRI

exo G

Hind III

3´UTR

EcoRI

B
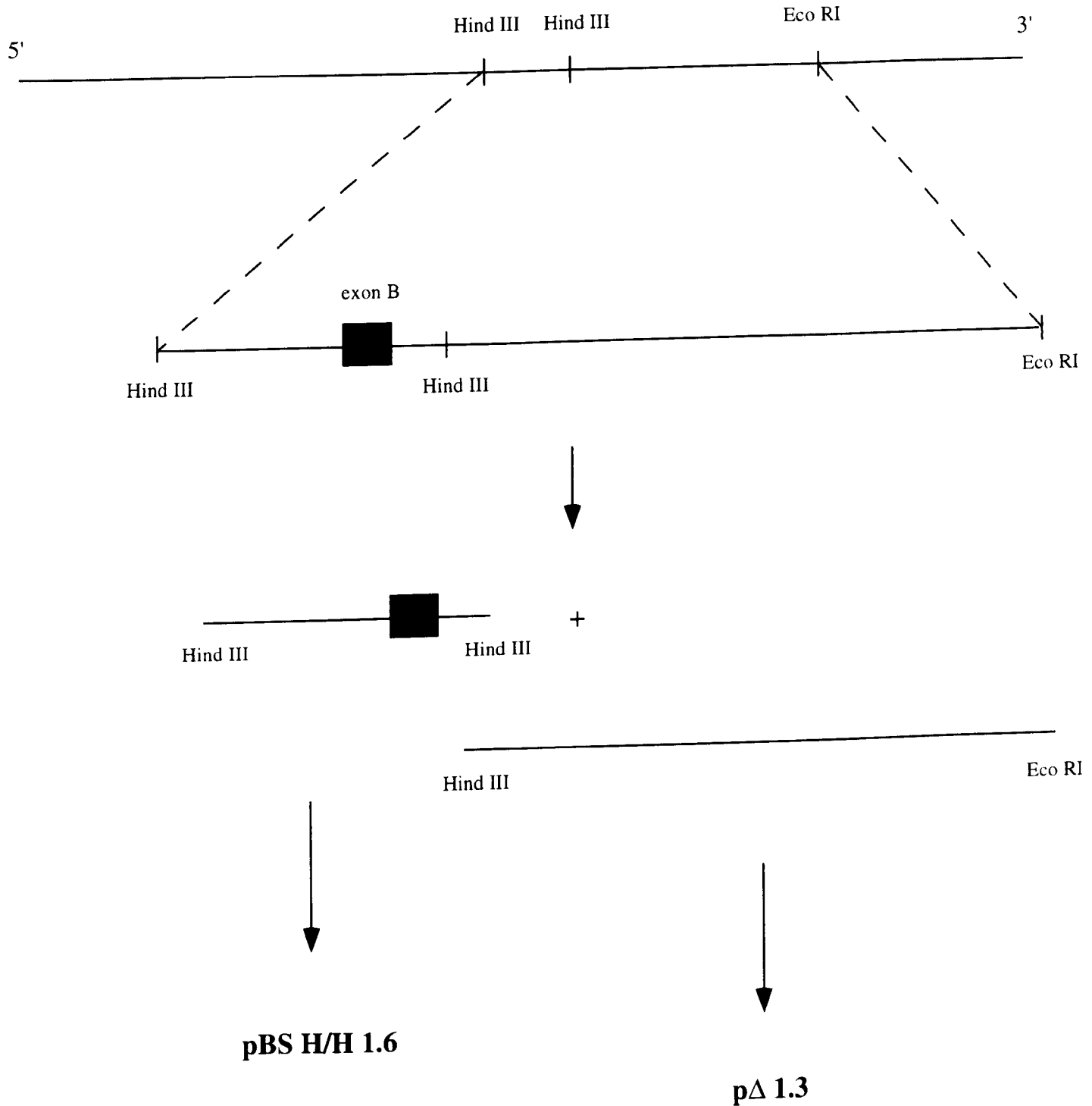
Figure 1.1A and B. A)The 3' region of the murine RyR3 gene. The exons, some restriction enzyme sites and the 3' UTR region are indicated. B) The region used for the construct is indicated: the 1.6 Kb HindIII/HindIII region containing the exon B was cloned in pBluescript to originate pBSH/H 1.6; the 5.2 Kb HindIII/EcoRI region was cloned in pBluescript to originate pΔ1.3.
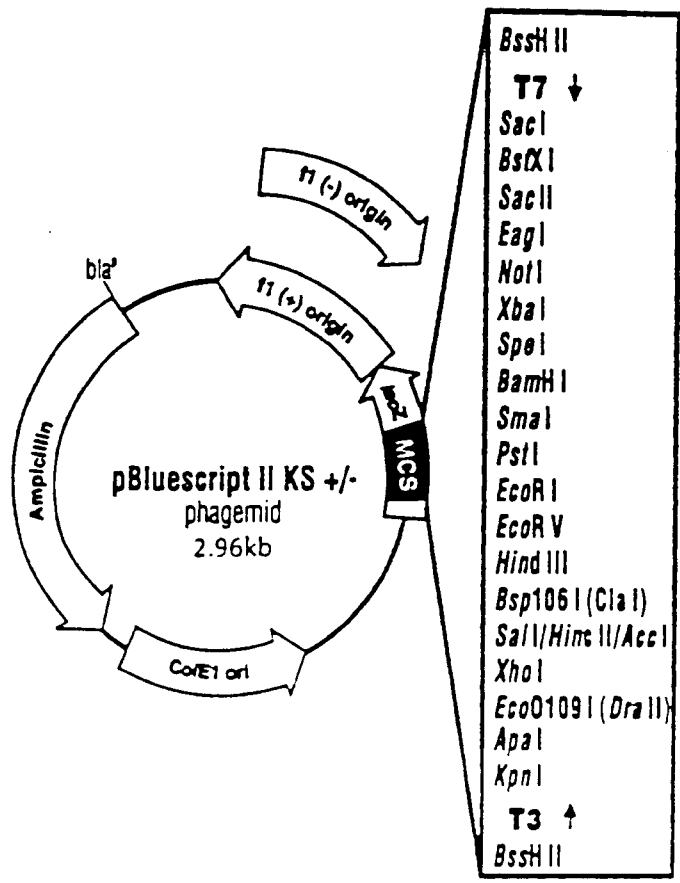
Figure 1.2. Plasmid pBluescript KS +/- (Stratagene).
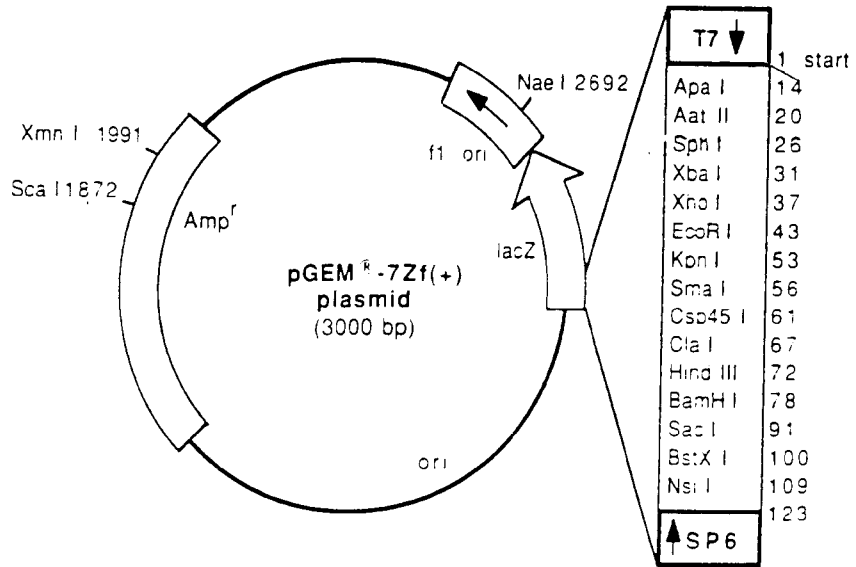
Figure 1.3 Plasmid pGEM 7Zf(+) (Promega).

A

HindIII   exon B   HindIII   pBluescript

pBS H/H 1.6

B

HindIII   EcoRI   pBluescript
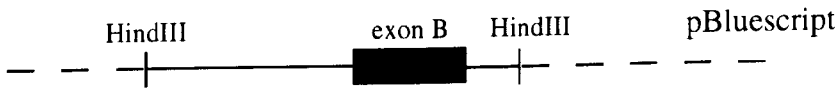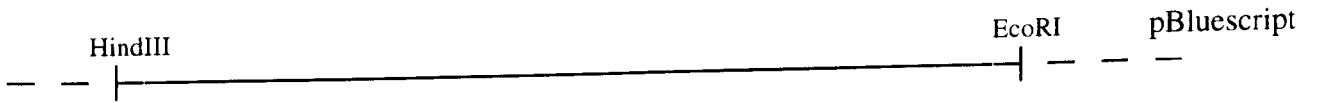
pΔ 1.3

Figure 1.4 A and B. The genomic region used for the construct was cloned in two plasmids, pBS H/H 1.6 (A) and pΔ 1.3 (B).

89

3.1.2 Strategy

The targeting vector to be transfected into murine ES cells was designed in order to obtain a high recombination frequency with the chromosomal locus, and to increase the chance of, and maximize the selection for, clones with a targeted integration event and against clones with random insertion events. For the first point, the length of the homologous sequences in the vector was chosen between 5 and 10 Kb. Concerning the second point, the positive-negative selection technique (PNS) was used as enrichment strategy for gene targeting events (Mansour et al., 1988). In this scheme, in addition to the positive selection permitting the isolation of all the clones which stably incorporate the plasmid DNA, the vector contains a negative selectable gene at one end: in a targeted gene replacement event this gene is lost and degraded, whereas clones in which the vector has been randomly integrated incorporate it. Negative selection works by killing clones of cells expressing the negatively selectable gene, i.e. the clones of cells which have integrated the vector at a random location and clones which have integrated all of the vector components into the target locus by homologous recombination. The enrichment achieved with negative selection is highly variable, ranging between 2 and 20-fold.

3.1.3 The DNA plasmid PCR-neo

The PCR-neo plasmid was built by using the PGK-neo plasmid on one side, and the pBS H/H 1.6 on the other side.

3.1.3a PGK-neo plasmid

The PGK-neo plasmid (Fig. 1.5) was made by cloning in pGEM-7Z(f)+ (Promega, Fig. 1.3) the 1745 bp EcoRI-HindIII fragment from pKJ1 containing the PGK-neo cassette (Tybulewicz et al., 1991), to get a 4.7 Kb plasmid. The PGK-neo cassette has all the components necessary for the autonomal expression of the *neo* gene, that is a promoter, the *neo* coding region, and a polyadenylation site. It was built as follows (Tybulewicz et al., 1991): a 511 bp fragment from the mouse PGK-1 promoter (Adra et al., 1987), the coding portion of the *neo* gene as a 823 bp fragment from pMC1neo (Thomas and Capecchi, 1987), and 404 bp fragment containing the mouse PGK-1 poly(A) addition site (Adra et al., 1987).

10µg of PGK-neo plasmid were cut with the restriction enzymes ApaI for 3 hrs at 37°C. The linearized plasmid was loaded on an agarose gel in TAE 1x, 0.8%, and eluted by low-melting agarose method. Then the plasmid was cut with XbaI for 3 hrs at 37°C; this step was followed by plasmid dephosphorylation. After AP inactivation, followed by precipitation with EtOH absolute and NaCl 0.1M and washing with EtOH 70%, the digested and dephosphorylated plasmid was resuspended in 10µl of TE 1x. 1/10 of the resuspension was loaded on an agarose gel in order to have a quantitative estimation of the linearized plasmid.

pBS H/H 1.6 Kb   PGK-neo

1.6 kb
exon B
                                          pBluescript   ApaI XbaI   pGEM 7Zf(+)

ApaI/NotI   XbaI   neo cassette 1.7 Kb

primer a   primer b

amplification by PCR   digestion by ApaI and XbaI

1.2 k amplified fragment   dephosphorilation

digestion by ApaI and XbaI

ligation

1.2 amplified fragment
                                                                    pGEM 7Zf(+)

                                       neo cassette 1.7 Kb

1/4"   1/4"
primer PR2   primer pUC M13 reverse
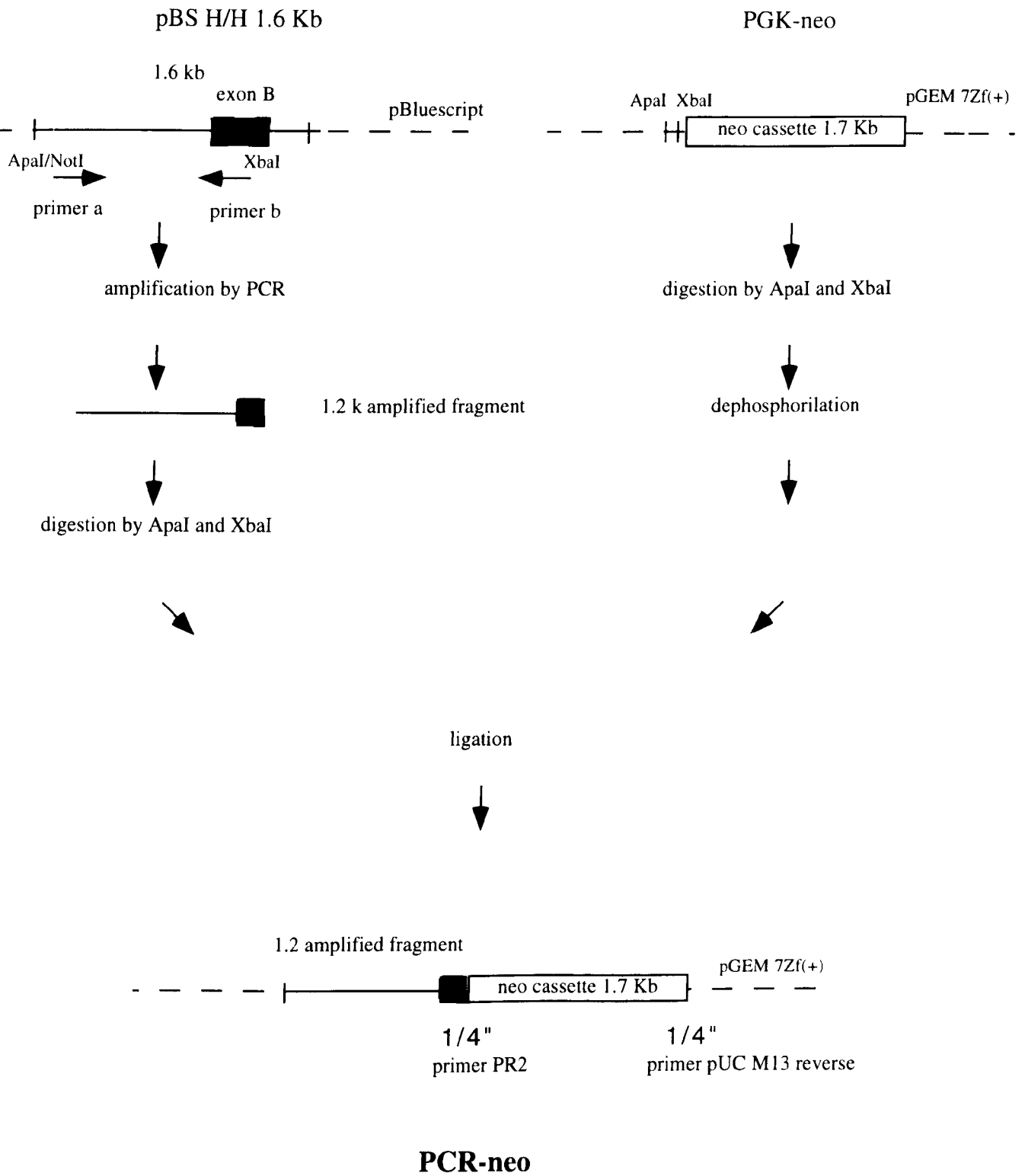
PCR-neo

Figure 1.5. Cloning strategy to get the plasmid PCR-neo

3.1.3b pBS H/H 1.6 plasmid

The pBS H/H 1.6 plasmid was used to amplify a 1.2 Kb band from the 1.6 Kb genomic fragment. The two oligonucleotides designed for the amplification are named primer a and primer b. The two primers are localized as shown in Fig 1.5. The first 5' nucleotide of primer a maps at nucleotide 164 of the 1.6 Kb fragment. The first 5' nucleotide of primer b maps at nucleotide 17 upstream the 3' end of the exon B (nucleotide 1373 from the 5' of the 1.6 Kb fragment). The 1.2 Kb fragment will contain only a portion of the exon B.

These are the sequences of the two primers utilized:

     5'   **ApaI/NotI**   3'

primer a: TA<u>GGGCCC</u>**GCGGCCGC**CCTCCTGCTAAAGCACCTCTTAT

     5'   XbaI   3'

primer b: GG<u>TCTAGA</u>ATATCCGGCTCATCGTCATC

The ApaI and XbaI sites are underlined, the NotI site is in bold.

The amplification conditions were described in Materials and Methods. The calculated annealing temperature was 61°C. 1/10 of the amplification reaction was loaded on an agarose gel to check the amplification of the expected band. 10µl of amplified DNA were digested with ApaI for 3 hrs at 37°C. After inactivation of the enzyme for 15' at 65°C, the DNA was digested with XbaI, appropriately modifying the ionic strength of the reaction. After 3 hrs at 37°C, the double digested DNA fragment was extracted once with phenol-chloroform to inactivate the enzyme, precipitated with EtOH absolute and NaCl 0.1M, washed with EtOH 70%, and resuspended in 10µl of TE 1x. 1/10 of the resuspension was loaded on an agarose gel to check the amount of the digested DNA band.

3.1.3c Ligation of 1.2 Kb ApaI/XbaI digested fragment to ApaI/XbaI digested, dephosphorylated PGK-neo plasmid.

The ApaI/XbaI digested 1.2 Kb fragment was ligated to the ApaI/XbaI digested, dephosphorylated PGK-neo plasmid. We used a molar ratio plasmid:fragment of 1:3.

After dialysis, 1/3 of the ligation was used to transform competent XL1blue cells. 24 colonies were inoculated in 5ml of LB + ampicillin, and allowed to grow 2 hrs at 37°C. 5μl of each bacterial growth were analyzed by PCR in the same condition used to amplify the 1.2 genomic fragment. 19 out of 25 colonies were positive to the amplification of the 950 bp expected band. 10 positive clones were allowed to grow in a larger volume of LB + ampicillin, and DNA was extracted by mini preparation. DNA of all 10 minipreps was digested with EcoRI; according the genomic map, an EcoRI site is present at the position 420 in the 1.6 Kb genomic fragment. The digestion with EcoRI of PGK-neo plus the 1.2 Kb fragment would result in a band of 950 bp. Such expected band was present in all the DNA analyzed, but not in the EcoRI digested plasmid PGK-neo, which was simply linearized. One colony, number 3, was chosen and grown in a larger volume of LB + amp, to get a larger amount of DNA recovered by midi preparation. The DNA recovered by a midiprep was used for further check of the cloning. Plasmid was digested with different restriction enzymes: ApaI, HindIII, NotI, XbaI. PGK-neo was also digested as control. The restriction analysis confirm the presence of the 1.2 Kb fragment cloned in PGK-neo: ApaI, HindIII and XbaI linearized both the plasmids, but PGK-neo gave a lower band (lower molecular weight); NotI cut the new plasmid, but not PGK-neo, as expected. To confirm the cloning, DNA from colony 3 was sequenced, using the following two primers:

- universal forward primer pUC/M13 (17 MER): 5′ GTTTTCCCAGTCACGAC 3′

- primer PR 2: 5′ GTGGTGGCCTTCAACTTCTTCCGCAAGTTC 3′

The two primers are localized as shown in Fig. 1.5. The first 5′ nucleotide of primer PR2 maps at nucleotide 1301 of the 1.6 Kb fragment (nucleotide 50 downstream the 5′ end of exon B).

The sequencing analysis confirmed the presence of the 1.2 Kb fragment cloned in ApaI/XbaI in PGK-1 plasmid.

This new plasmid was named PCR-neo. Figure 1.5 summarizes the cloning strategy.

3.1.4 The DNA plasmid pΔ 1.3-tk

The p• 1.3-tk plasmid was built by A. Nori by using the PGK-tk plasmid from one side, and the pΔ1.3 on the other side.

The strategy utilized will be briefly described.

3.1.4a PGK-tk plasmid

The PGK-tk plasmid (Fig. 1.6) was made by cloning in pGEM-7Zf(+) the 2740 bp EcoRI-HindIII fragment from pKJtk containing the PGK-tk cassette (Tybulewicz et al., 1991), to get a 5.7 Kb plasmid. The PGK-tk cassette has all

the components necessary for the autonomal expression of the *tk* gene, that is the murine PGK promoter and poly(A), and the coding portion of the *tk* gene as an 1823 bp fragment from pMC1tk (Tybulewicz et al., 1991).

The PGK-tk plasmid was digested with XhoI and NsiI, so as to excise the tk cassette from the pGEM-7Z(f)+ plasmid. The fragment containing the tk cassette was blunted by Klenow enzyme, followed by digestion with BamHI. This procedure created a fragment with a blunt end from one side, and a ΔBamHI end on the other side.

3.1.4b The pΔ 1.3 plasmid

The pΔ 1.3 plasmid was digested with SmaI, which created a blunt end, and BamHI. So, the linearized plasmid presented a blunt end and a BamHI end suitable for the tk cassette fragment ends.

The digested pΔ 1.3 plasmid was ligated to the tk cassette fragment. The cloning was checked by restriction enzyme analysis and sequencing, and the new plasmid was named pΔ 1.3-tk (Fig. 1.6).

PGK-tk

pΔ 1.3

tk cassette 2.7 Kb

pGEM7Zf(+)

BamHI NsiI

XhoI

digestion by XhoI and NsiI

Klenow reaction to make blunt ends

digestion by BamHI

pBluescript

EcoRI

SmaI BamHI

5.2 Kb fragment

HindIII

digestion by SmaI and BamHI

ligation

HindIII

EcoRI

HindIII

tk cassette 2.7 Kb

pBluescript
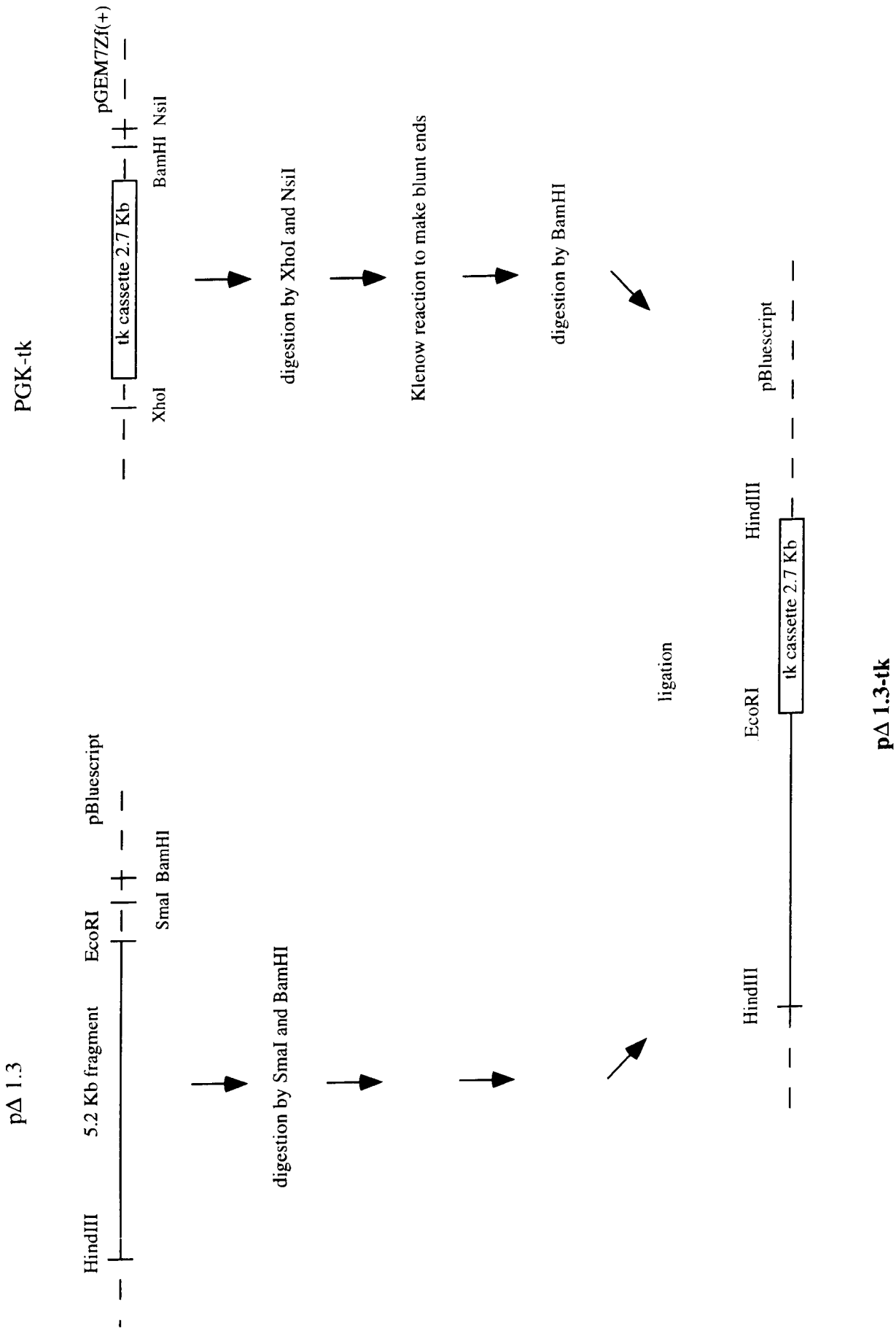
pΔ 1.3-tk

Figure 1.6. Cloning strategy utilized to obtain the plasmid pΔ 1.3-tk.

3.1.5 The DNA plasmid C1

The targeting vector was built by using the PCR-neo plasmid from one side, and the pΔ 1.3-tk on the other side.

3.1.5a HindIII digestion of PCR-neo and pΔ 1.3-tk

10μg of PCR-neo were digested with the restriction enzyme HindIII for 3 hrs at 37°C. The linearized plasmid was eluted from an agarose gel through the low-melting agarose technique, step followed by dephosphorylation. After inactivation of AP, precipitation with EtOH absolute and NaCl 0.1M, and washing with EtOH 70%, the linearized and dephosphorylated plasmid was resuspended in a suitable volume of TE 1x. DNA concentration was checked by loading 1/10 of the resuspension on an agarose gel.

20μg of the pΔ 1.3-tk plasmid were digested with HindIII for 3 hrs at 37°C. The HindIII digestion separated a 8 Kb DNA fragment from the plasmid. The 8 Kb fragment contains the 5.2 Kb HindIII/EcoRI genomic region plus the tk cassette. The digestion was loaded on a low-melting agarose gel, the 8 Kb band was eluted, and resuspended in a suitable volume of TE 1x. DNA concentration was checked by loading 1/10 of the resuspension on an agarose gel.

3.1.5b Ligation of the 8 Kb DNA fragment to the linearized pΔ 1.3-tk plasmid

The HindIII digested 8 Kb fragment was ligated to the HindIII linearized, dephosphorylated PCR-neo plasmid. We used a molar ratio plasmid:fragment of 1:3. 1/3 of dialyzed ligation was used to transform XL1blue competent cells. 14 colonies were inoculated in 5ml of LB + ampicillin, and allowed to grow 2 hrs at 37°C. 5μl of each bacterial growth were analyzed by PCR using the primers named PR 2 and PR 6, that map in the 5.2 genomic region, spanning a 70 bp portion of exon C (Fig 1.7). The first 5' nucleotide of PR 6 maps at the position 68 downstream the first nucleotide of exon C, the first 5' nucleotide of PR 31 maps at the position 1 of exon C. The orientation of the two primers is shown in Fig. 1.7. These are the sequences of the two primers:

5'   3'
PR 6: GGGTCTTCAATTTCATGACCAATGCC

5'   3'
PR 31: TGCTACCTCTTCCACATGTAC

The amplification conditions were described in Materials and Methods. The annealing temperature was calculated at 52°C.

11 out of 14 colonies were positive to the amplification of a 70 bp band. 10 positive clones were allowed to grow in a larger volume of LB + ampicillin, and DNA was extracted by mini preparation. DNA of all 10 minipreps was digested with HindIII. 8 out of 10 minipreps contained the 8 Kb fragment, separated from the plasmid by the HindIII digestion. One colony, number 7, was chosen and grown in a larger volume of LB + amp, to get a larger amount

of DNA, recovered by midi preparation. The DNA recovered by midiprep was used for further check of the cloning. Plasmid was digested with different restriction enzymes: ApaI, NotI, XbaI, SacI, EcoRI. PCR-neo was also digested as control. The restriction analysis confirm the presence of the 8 Kb fragment cloned in PCR-neo. In addition, the restriction analysis revealed that the 8 Kb fragment was inserted in the right orientation. To confirm the cloning and the orientation, DNA from colony 7 was sequenced. The sequencing analysis was performed with different primers (Fig. 1.7), using both short and long runs:

- universal forward primer pUC/M13 (17 MER) (see above)

<div align="center">5'   3'</div>

- universal reverse primer pUC/M13 (17 MER): CAGGAAACAGCTATGAC

- PR 6 (see above)

<div align="center">5'   3'</div>

- PR 2: GTGGTGGCTTTCAACTTCTTCCGAAAGTTCTAC

The new plasmid represented the complete targeting vector, and was named pC1. The cloning strategy of the pC1 construct is summarized in Fig. 1.7.

Figure 1.7. Cloning strategy to obtain the targeting vector pC1.
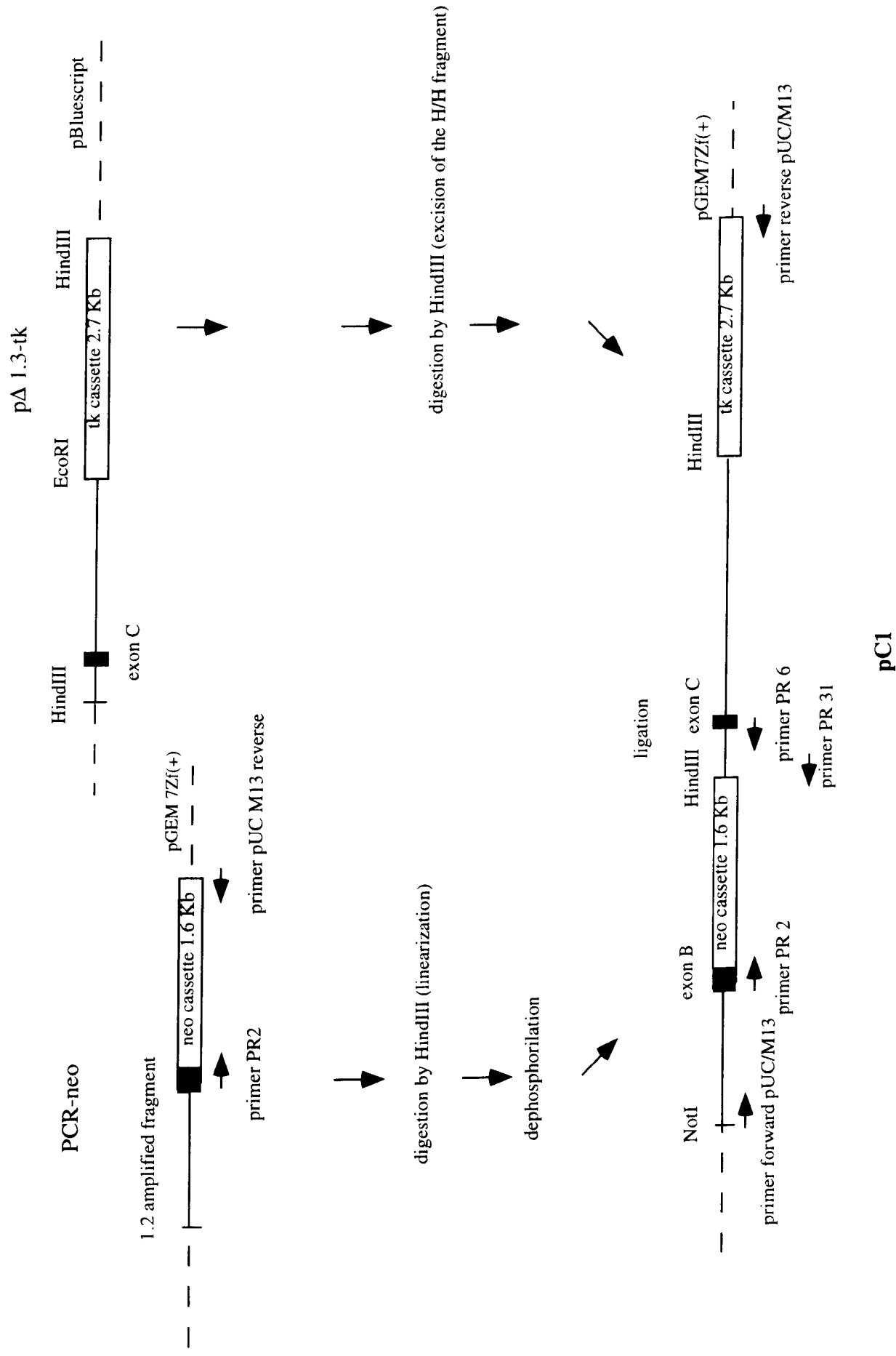
To get a large amount of highly purified targeting vector pC1, DNA extraction was performed starting from a large culture (500ml of LB + amp) and using caesium chloride DNA extraction method.

3.1.6 Linearization of the plasmid C1 to be transfected into ES cells

Plasmid DNA to be transfected into ES cells must be linearized.

The NotI site, deriving originally from the oligonucleotide a of PCR-neo, was used as unique site to linearize the targeting vector pC1 (Fig. 1.7). Two different aliquots of DNA were digested with NotI: 25µg and 50µg. The digestion was allowed to proceed o/n at 37°C, and then was checked loading 1/100 of the reaction on an agarose gel. After phenol-chloroform extraction, precipitation with EtOH absolute and NaCl 0.1M, and washing with EtOH 70%, the linearized C1 was resuspended in a suitable volume of buffer to be transfected into ES cells, as will be described (see below).

3.2. Restriction map of murine RyR3 3' genomic region

3.2.1 Introduction

Gene targeting experiments are based on a homologous recombination event in which the targeted wild-type genomic region is substituted with the mutated one contained in the targeting vector. One of the most important aspects of the gene targeting experiments is to confirm that the desired genetic change has occurred. Two methods are available to screen for a specific recombination allele: PCR or Southern blot analysis.

For PCR-based screenings, the primers are chosen to amplify a specific junction fragment following a cross-over on the short arm of the vector.

Southern blot analysis is based on cutting genomic DNA with an appropriate restriction enzyme, and choosing a probe that can distinguish the wild-type from the predicted targeted allele. In order to avoid the identification of false positives, two tricks are currently used:

- a restriction digest with an enzyme that does not cut in the vector;

- the use of a probe that is not contained in the target vector.

As a consequence, a simple gene replacement event will increase the length of the wild-type fragment by the length of the positive selection marker. So it is easy to detect the integration of the entire vector by a significant increase of the fragment size. The use of an enzyme that cuts inside the vector, together with an external probe, allows the analysis of one arm of the target locus. Therefore it is important to analyze both the 5' and the 3' of the target locus to be able to discriminate a simple gene replacement event from the integration of the entire vector or concatenamers of the vector.

Internal probes detect also random integration events, which is the reason why external probes are preferred.

The deep knowledge of the restriction map of the region interested by the homologous recombination event results determinant

3.2.2 The 5' and 3' probes

The choice of the probes to be used in Southern blot analysis on mouse genomic DNA was conditioned by the need of external probes. As a consequence we decided to use the following genomic fragments:

5' probe: a 150 bp fragment just upstream the genomic region used to make the targeting vector (Fig. 2.1);

3' probe: a 900 bp fragment immediately downstream the 3' end of the region included in the targeting vector (Fig. 2.2).

3.2.2a The 150 bp as 5' probe

The chosen 5' probe maps in the 5' portion of the 1.6 HindIII/HindIII genomic fragment, that was cloned in pBluescript, producing the plasmid named pBS H/H 1.6. This plasmid was used as template to amplify the 150 bp fragment to be used as 5' probe (Fig. 2.3). The following primers were used:

5'   3'

primer d: TTGCCACACCTCAGGTACTGAGTC

primer c: GGCAAAGGTTGTAGGATCTACCTATGC

The first 5' nucleotide of primer d maps at the nucleotide 7 of the 1.6 H/H fragment; the first 5' nucleotide of primer c maps at nucleotide 151 of the same fragment.

The annealing temperature was 60°C.

The amplified 150 bp fragment was eluted from a low-melting agarose gel and, after resuspension in a suitable volume of TE 1X, it was used in a random primed labeling reaction.

3.2.2b The 900 bp as 3' probe

The 900 bp EcoRI/HindIII fragment to be used as 3' probe had already been cloned in pBluescript, producing the plasmid pBS E/H 0.9 Kb. The plasmid was double-digested with the restriction enzymes EcoRI and HindIII. The 900 bp DNA fragment, separated from the plasmid, was eluted from a low-melting agarose gel, and, after resuspension in a suitable volume of TE 1x, it was used in a random primed labeling reaction.

The strength of the two probes was checked in a Southern blot assay. Genomic DNA from wild-type mice, extracted as described (see Materials and Methods), was digested with HindIII and EcoRI. After Southern blot, DNA was hybridized first with the 5' probe, the 150 bp fragment, and then with the 3' probe, the 900

Wild-type
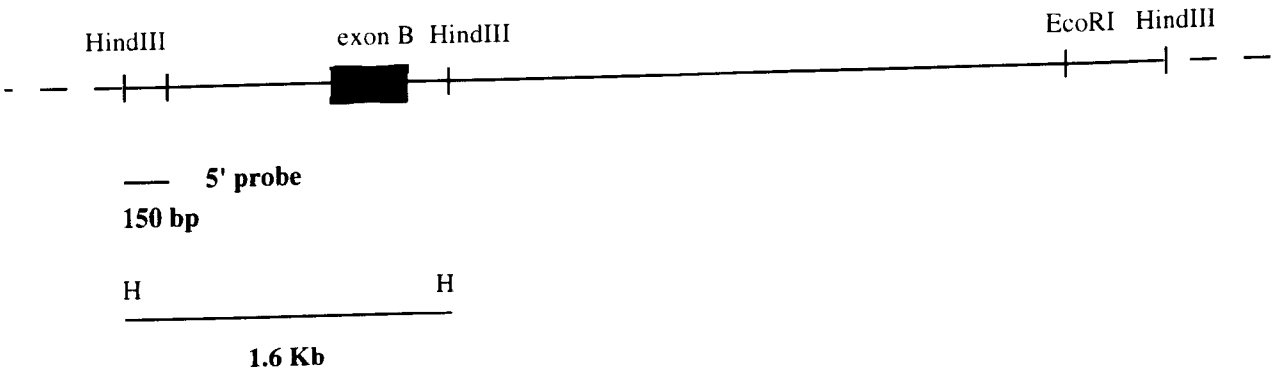
Mutated allele
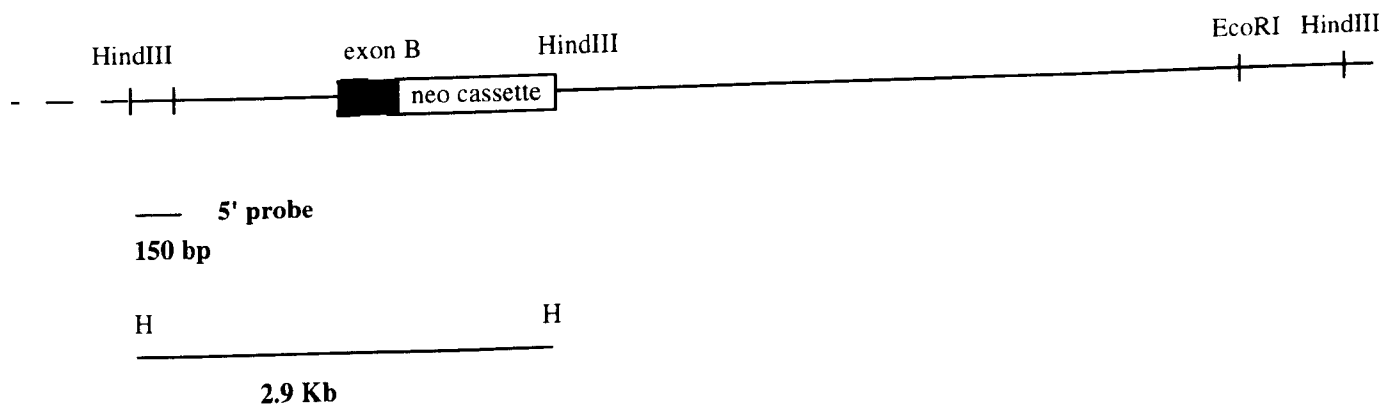
Figure 2.1. The 150 bp long 5' probe just upstream the genomic region included in the targeting vector pC1. In the wild-type allele (top) the 5' probe recognizes a 1.6 Kb band in HindIII digested genomic DNA. In the mutated allele (bottom), a 2.9 Kb band is identified.

Wild-type
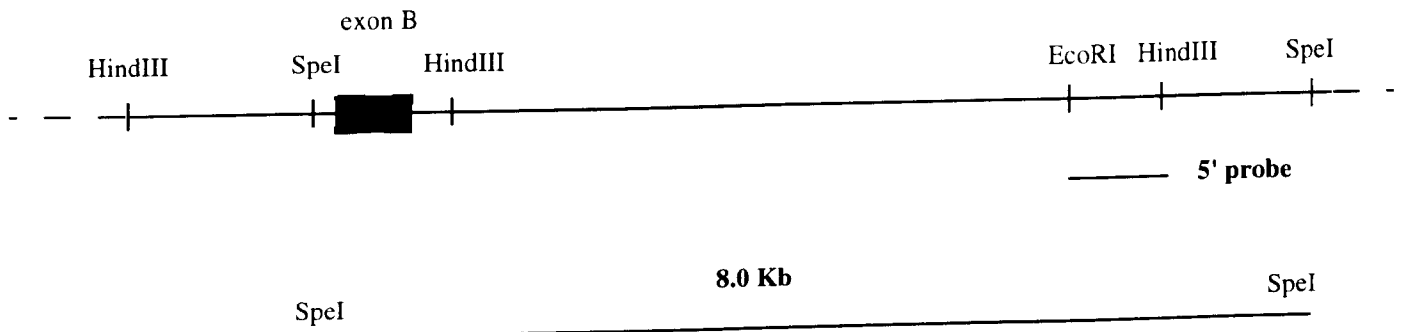
Mutated allele
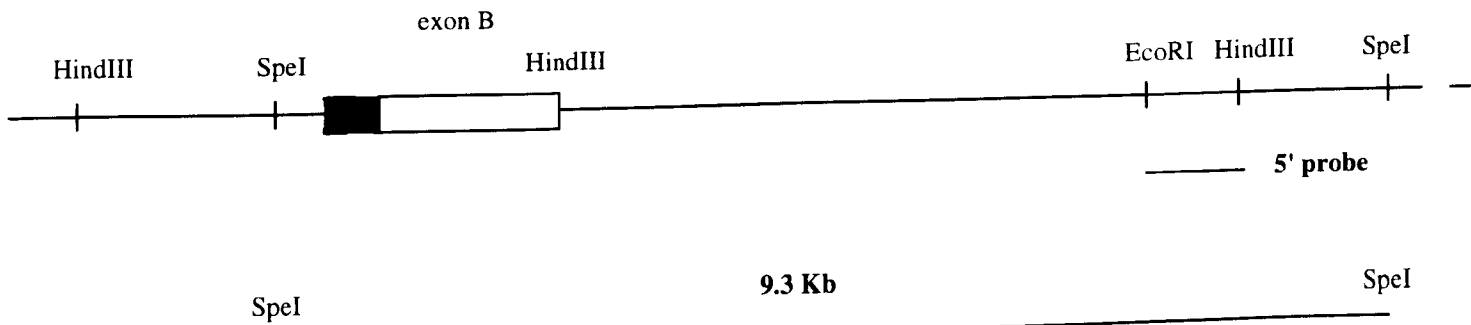
Figure 2.2. The 900 bp long 3' probe just downstream the genomic region included in the targeting vector pC1. In the wild-type allele (top) the 5' probe recognizes a 8.0 Kb band in SpeI digested genomic DNA. In the mutated allele (bottom), a 9.3 Kb band is identified.
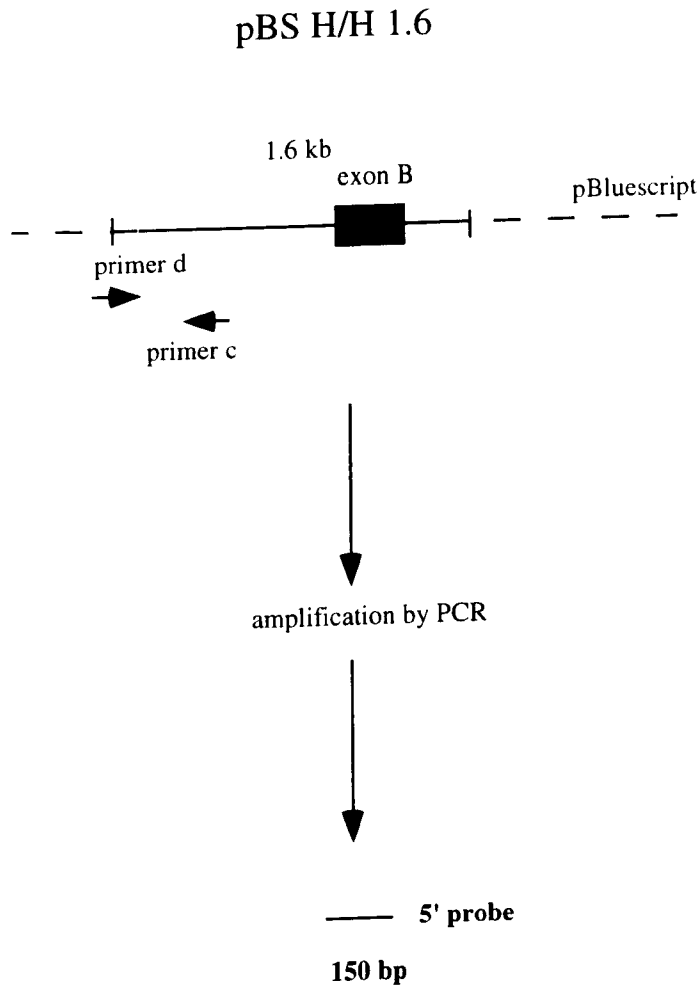
pBS H/H 1.6

Figure 2.3. The 5' probe derives from the amplification of 150 bp from pBS H/H 1.6 as indicated. Primers d and c were used for the amplification.

109

Figure 2.4. Southern blot analysis on mouse genomic DNA digested with the indicated restriction enzymes, and hybridized with the5' external probe 0.15 Kb fragment.
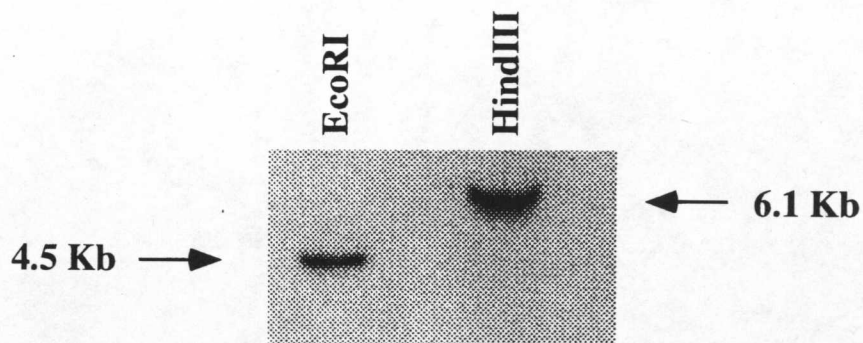
Figure 2.5. Southern blot analysis of mouse genomic DNA digested with the indicated restriction enzymes, and hybridized with the 3' external probe 0.9 Kb fragment

Figure 2.6. Southern blot analysis of mouse genomic DNA digested with different restriction enzymes and hybridized with the 3' probe. The different sized bands recognized by the probe allow to draw the restriction map of the region. The size of some of the bands is indicated.

bp E/H fragment. These are the results of the Southern blot assays (Fig. 2.4. 2.5, 2.6):

HindIII digestion, 5' probe: 1.6 Kb band, as expected;

EcoRI digestion, 5' probe: 6.6 Kb band;

HindIII digestion, 3' probe: 6.1 Kb band, as expected;

EcoRI digestion, 3'probe: 4.5 Kb band;

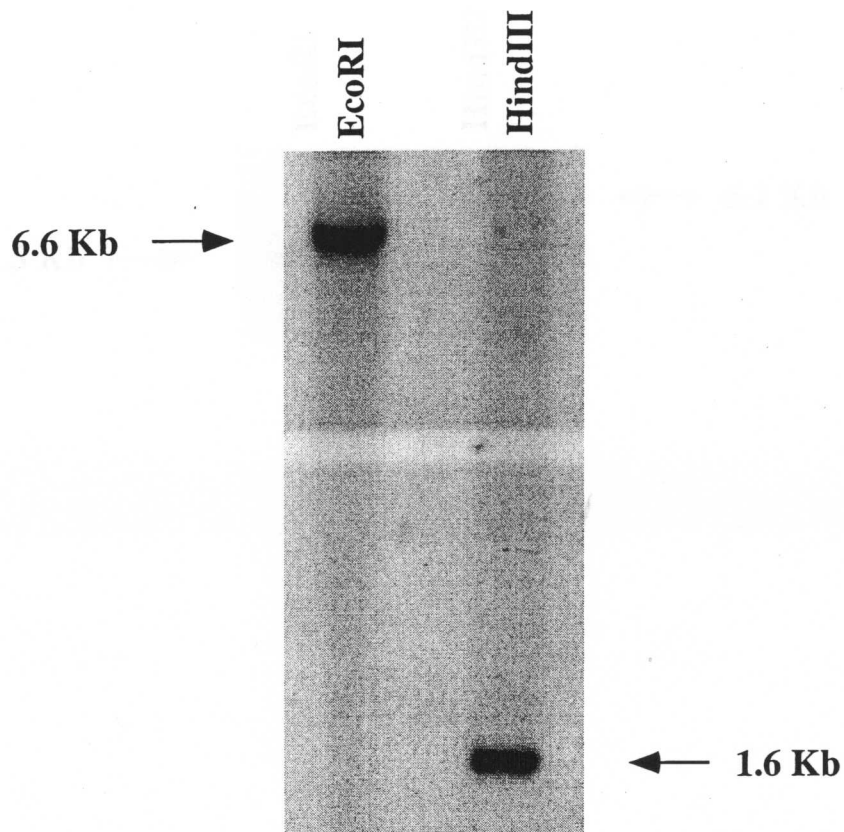The Southern blot assay is shown in Fig. 2.4 and 2.5.

If on one side this assay confirmed the functionality of the two probes, on the other side it gave the first information about the restriction map of this genomic region. The restriction map was further investigated, as described below.

3.2.3 Digestion of genomic murine DNA by restriction enzymes

Genomic DNA from wild-type mice was digested with the following restriction enzymes:

DraII, NcoI, SfiI, ScaI, Mlu, NotI, SpeI, SphI, XhoI, SacI, XbaI, ScaI/SpeI, ScaI/EcoRI, ScaI/HindIII, ScaI/XbaI, ScaI/SacI, SpeI/EcoRI, SpeI/HindIII, SpeI/XbaI, SpeI/SacI

The digested DNA was assayed by Southern blot and hybridized with the two probes. Figure 2.6 represents an example of this analysis. The resulting restriction map is represented in Fig. 2.7.

Figure 2.7. Restriction map of the murine RyR3 3' genomic map (5' ➔ 3'). The restriction enzymes in bold represent the HindIII and EcoRI sites present in the previous map shown in figure 1.1.

3.2.4 Restriction digestion chosen to distinguish between the wild-type and the mutated form of RyR3 allele

Once the restriction map of the genomic region of interest was known, the subsequent step was to choose the restriction enzyme that gives a different restriction pattern between the wild-type and the mutant RyR3 allele, and that is recognized by the used probe.

3.2.4a Differential restriction digestion recognized by the 5' probe

Mouse genomic DNA was digested by HindIII, assayed by Southern blot and hybridized by the 5' probe, 150 bp fragment: the wild-type allele gives a 1.6 Kb band, while the recombinant allele gives a 2.9 Kb band (Fig. 2.1).

3.2.4b Differential restriction digestion recognized by the 3' probe

Mouse genomic DNA was digested by SpeI, assayed by Southern blot and hybridized by the 3' probe, 900 bp fragment: the wild-type allele gives a 8.0 Kb band, while the recombinant allele gives a 9.3 Kb band (Fig. 2.2).

The restriction digestion by SpeI and the hybridization with the 3' probe 900 bp E/H was further used to genotype mice, as described below.

3.3. The making of RyR3$^{-/-}$ mouse

The procedure is based on several sequential steps that can be so summarized:

- transfection of the targeting vector into ES cells

- selection of transfected ES cells with G-418 and gancyclovir

- genotype analysis of selected clones by Southern blot assay

- injection of positive clones into mouse blastocysts for the production of chimeras
- proper crossbreeds to obtain heterozygous mice for RyR3, and, subsequently, homozygous mutant mice for RyR3.

3.3.1 Introduction

ES cell lines derive directly from embryo. This derivation was an extension of the study on the stem cells of teratocarcinomas. The latter are tumors of germ cells, and are most prevalent in the testes of 129 mice and in the ovaries of LT mice. On this line of study, Stevens developed substrains of 129 mice with enhanced rates of germ cell tumor formation (Stevens, 1983). As a consequence, these strains were chosen in the first attempts to derive embryonic cell lines (Evans and Kaufman, 1981). The method was extended to other strains, but the 129 ES cell lines remain the most used. There is, however, a certain degree of heterogeneity in ES cell lines, because in deriving these lines different 129 substrains were used.

We used two different ES cell lines:

ES cell lines	Substrains
E14	129/Ola
R1	(129/Sv x 129/SvJ)F1

All of the ES cell lines in common use were derived from male embryos. Male ES cells are preferred because they produce a high proportion of phenotypic male chimeras, and male chimeras can be bred quickly to test for germ line transmission. Also in combination with a female embryo, male cells often produce a fertile male chimera. This sex conversion is probably due to the colonization by XY ES cells of various tissues determining sex in the developing embryo. However, germ line transmission from female chimeras has been reported in the literature, probably due to the loss of part of all the Y chromosome; the resulting XO cells are able to form ova (Papaioannou V. and Johnson, R., 1993). The positive, recombinant clone will be injected into a mouse blastocyst. ES cells will contribute to the embryo, giving rise to a chimera. The choice of the host embryo is determinated by two specific, fundamental requirements:

- high probability of chimera formation (compatible host)
- difference in some genetic loci, useful as genetic markers to know the contribution of injected ES cells to the whole animal.

C57BL/6J mouse embryos are compatible hosts for 129 ES cells. They guarantee an efficient chimera formation and germ line transmission. C57BL/6J mice differ from 129 mice in several genetic loci which are useful as markers of chimerism. One of the best genetic marker of chimerism is represented by the coat colour. Chimeric combinations of strains differing at coat colour loci allow

a simple visual appreciation of proportion of the coat that expresses the ES cell allele. In general, the more is the degree of coat colour chimerism, the more is the contribution of the ES cells to the germ line. The difference in some coat colour loci between the ES cell strains and the C57BL/6J strain make the last one particularly suitable as host recipients embryos.

The following table summarizes the differences in coat colour alleles between the ES cell strain used and the C57BL/6J strain:

Substrain	ES cell line	Locus	Locus	Locus
		Agouti	Albino	Pink-eyed dilution
129/Ola	E14	A^w	c^{ch}	p
(129/Sv x 129/SvJ)F$_1$	R1	A^w	$c/+^c$	$p/+^p$
C57BL/6J		a	$+^c$	$+^p$

The following table demonstrates the phenotypic effects of the alleles in the mentioned loci (from Papaioannou and Johnson, 1993):

Locus	Alleles	Cell type affected and phenotypic effect

Agouti	A^W, A, a, a^e	Affects hair follicle function, alleles differ in the amount and distribution of yellow pigment; wild-type (A^W or A) hair has a yellow sub-apical band
Albino	c, c^{ch}	Affects melanocytes; homozygous albino (c/c) will mask any other coat colour allele; c^{ch} causes a reduced pigmentation and affects yellow pigment more than black; c/c^{ch} is intermediate between c/c and c^{ch}/c^{ch}.
Pink-eyed dilution	p	Affect melanocytes; causes a reduced pigmentation but affects black pigment more than yellow.

In summary, a C57BL/6J blastocyst produces a black-coated mouse, a 129 mouse will be brown-coated, due mainly to the alleles in the Agouti locus. Chimeras from C57BL/6J blastocysts plus injected ES cells will be characterized by a mosaic of black regions and brown regions. The level of chimerism will determine the extension of brown colour.

To get germline transmission is necessary that injected ES cells contribute to the germline. To check it, sexually mature chimeric mice (60 days old) were crossbred to C57BL/6J mice. If ES cells contribute to the germline, mice will be heterozygous in the locus Agouti (A^W/a): the dominant allele A^W determines the formation of brown-coated mice. If ES cells do not contribute to the germline, both alleles at the locus Agouti are from C57BL/6J (a/a), determining black-coated mice.

Once heterozygous mice for *RyR3* (RyR3$^{+/-}$) have been identified, they were crossbred with each other to get homozygous mice (RyR3$^{-/-}$).

3.3.2 ES cell proceeding

These experiments were performed with the collaboration of Catherine Ovitt, at EMBL, Heidelberg, Germany.

3.3.2a Transfection

Three rounds of transfection by electroporation of C1 targeting vector into ES cells were performed. As positive control, 10μg of linearized PGK-neo plasmid were transfected into ES cells. As negative control, non-transfected ES cells were used.

In the first experiment we used E14 ES cells. 25μg and 50μg of linearized DNA were transfected into 10^7 cells. After G-418 and gancyclovir selection, 215 positive clones were identified. One clone out of 215 resulted positive by

screening for homologous targeting events by Southern blot analysis (see below). It was named C1-134. The frequency of a homologous recombination event was 0.4%.

In the second experiment we used R1 ES cells. 25μg of linearized C1 were electroporated into 10^7 cells. Two out of 54 clones positive to G-418 and gancyclovir resulted positive by Southern blot analysis. They were C1-9 and C1-49. With R1 ES cells the frequency of homologous recombination was 3.7%.

In the third round of transfection both E14 and R1 ES cells were used. 50μg of linearized C1 were transfected into 10^7 E14 cells. No positive clones were selected. 25μg and 50μg of linearized C1 were transfected into 10^7 R1 cells. Two clones out of 119 positively selected contained the mutated allele as the result of a homologous recombination event. They were C1-112 and C1-116. The frequency of recombination was 1.6%.

In all, five ES cell clones heterozygous for the mutated form of *RyR3* were identified, one E14 ES cell clone, four R1 ES cell clones.

3.3.2b Screening for homologous targeting events by Southern blot analysis

Colonies that survived positive-negative selection were screened by Southern blot analysis for the recombination allele. These screenings were performed on the small amount of DNA obtained from cells grown in 96-well plates. An aliquot of DNA from resistant clones was firstly digested with SpeI and assayed with the 3' external probe EcoRI/HindIII 0.9 Kb fragment. The clones in which an homologous recombination event had occurred gave two different bands: the

wild-type 8.0 Kb band and the 9.3 Kb band from the recombinant allele (Fig. 3.1). A second aliquot of DNA from the positive clones was digested with HindIII and analyzed with the 5' external probe 0.15 HindIII/HindIII fragment. The real positive clones gave the wild-type 1.6 Kb band plus the 2.9 Kb band from the recombinant allele (Fig. 3.2).

Figure 3.3a shows the result of the homologous recombination event, together with the 3' probe and the difference of SpeI digestion between the wild-type and the mutated allele.
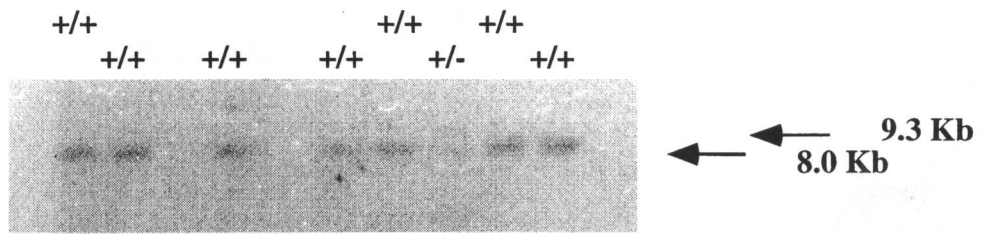
Figure 3.1. Southern blot analysis of genomic DNA digested with SpeI. The 3' external probe 0.9 Kb fragment was used. The wild-type clones (+/+) originates the 8.0 Kb band, the heterozigous clone (+/-) gives the 8.0 wild-type band and the 9.3 Kb band from the recombinant allele.
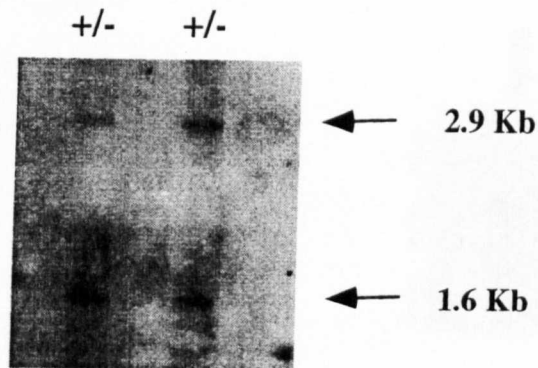
Figure 3.2. Southern blot analysis of genomic DNA digested with HindIII
The 5' external probe 0.15 Kb fragment was used. The heterozygous clones
(+/-) originate the wild-type 1.6 Kb band and the the 2.9 Kb band from the
recombinant allele.
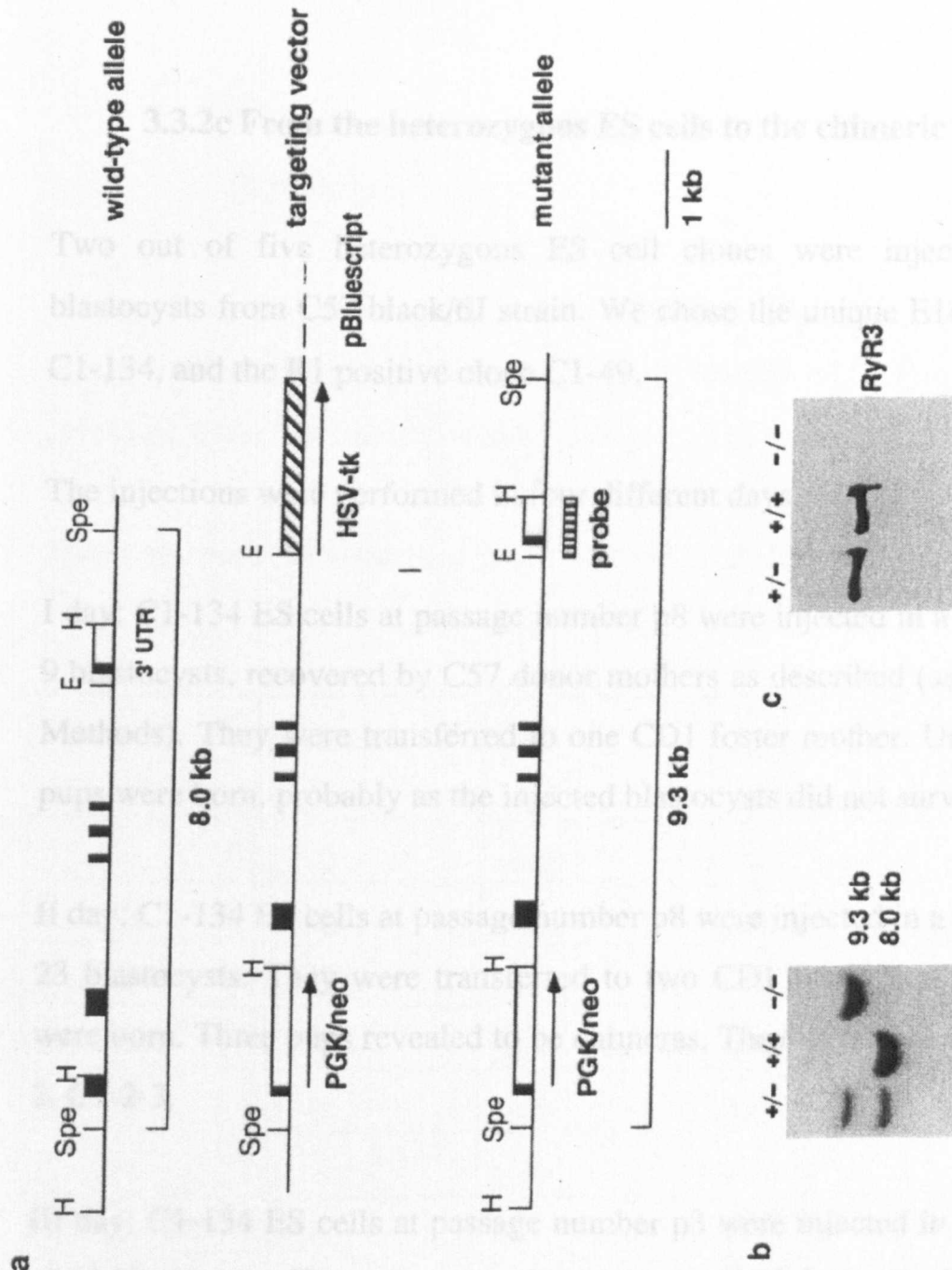
Figure 3.3. Gene targeting of the RyR3 locus. a) Wild-type allele (top), targeting vector (middle) and the homologous recombination product (bottom).

H: HindIII site; E: EcoRI site. Exons are represented by black boxes. b) Southern blot analysis. Genomic DNA was digested with SpeI and hybridized with the 3' probe. The wild-type and mutated allele result in a 8.0 Kb and 9.3 Kb band respectively. In heterozygous both are present. c) Immunoblot analysis. Diaphragm microsomes from +/+, +/- and -/- mice were analyzed by western blot with RyR3-specific antibody.

3.3.2c From the heterozygous ES cells to the chimeric mice

Two out of five heterozygous ES cell clones were injected into mouse blastocysts from C57 black/6J strain. We chose the unique E14 positive clone, C1-134, and the R1 positive clone C1-49.

The injections were performed in four different days.

I day: C1-134 ES cells at passage number p8 were injected in a total number of 9 blastocysts, recovered by C57 donor mothers as described (see Materials and Methods). They were transferred to one CD1 foster mother. Unfortunately, no pups were born, probably as the injected blastocysts did not survive.

II day: C1-134 ES cells at passage number p8 were injected in a total number of 23 blastocysts. They were transferred to two CD1 foster mothers. Four pups were born. Three pups revealed to be chimeras. They were called C1-2-1, C1-2-2, C1-2-3.

III day: C1-134 ES cells at passage number p3 were injected in a total number of 14 blastocysts. They were transferred to two CD1 foster mothers. Two pups revealed to be chimeras. They were named C1-3-1, C1-3-2.

IV day: C1-49 ES cells at passage number p4 were injected in a total number of 23 blastocysts. They were transferred to two CD1 foster mothers. One pup resulted to be a chimera. It was named C1-4-1.

We got six chimeras in total.

3.3.3 From chimeras to homozygous mice for the mutated *RyR3* allele (RyR3$^{-/-}$)

Among the six chimeras, five were male, as expected, while C1-2-3 was female. All six chimeras were mated to C57BL/6J mice. Four chimeras gave germ line transmission, revealed by brown-coated pups.

These results are summarized in the following table:

Clone	chimera	sex	degree of chimerism	germline transmission
C1-134	C1-2-1	male	75%	yes
C1-134	C1-2-2	male	95%	no
C1-134	C1-2-3	female	100%	yes
C1-134	C1-3-1	male	60%	yes
C1-134	C1-3-2	male	100%	no
C1-49	C1-4-1	male	90%	yes

The four chimeras were renamed with alphabetical letters as follows:

C1-2-1=A

C1-2-3=B

C1-3-1=C

C1-4-1=D

Pups from the crossbreed chimera x C57BL/6J were allowed to grow. When they were 15 days old, the tip of the tails were cut, DNA was extracted, digested with SpeI and the Southern blot analysis was performed using the 3' external probe EcoRI/HindIII 0.9 Kb fragment. Mice heterozygous for the mutated *RyR3* allele were identified because of the presence of two bands from the Southern blot assay: the wild-type 8.0 Kb band and the 9.3 Kb band from the recombinant allele. These RyR3$^{+/-}$ mice were allowed to grow, and, when sexually mature, they were crossbred to get homozygous mice for the mutated *RyR3* allele. Mouse DNA was analyzed by Southern blot assay as described above. RyR3$^{-/-}$ mice could be identified for the presence of the only recombinant 9.3 Kb band (Fig. 3.3b).

3.3.4 The RyR3$^{-/-}$ mouse

RyR3$^{-/-}$ mice were obtained in the 25% of the progeny, according to the mendelian genetics. Their embryonic development was normal, as well as the post-natal life. They could not be distinguished from wild-type mice. RyR3$^{-/-}$ mice were allowed to grow until they reached sexual maturity, and then were crossbred. They could give progeny as well as wild-type mice. We took advantage of the non-sterility of the RyR3$^{-/-}$ mice to establish a RyR3$^{-/-}$ mouse line. The line was established using mice of the group A.

3.3.5 The control of RyR3 knockout mouse: looking for RyR3 mRNA and protein

3.3.5a RyR3 mRNA in the RyR3$^{-/-}$ mouse.

We proceeded in parallel with both RyR3$^{-/-}$ mice and wild-type mice as control. Total RNA was extracted from adult mouse diaphragm. An amount of 10μg was used for RT-PCR reaction. 5μl of synthesized cDNA was amplified using the oligonucleotides, eI and fI. These two primers amplify a 290 bp long fragment at the 5' of RyR3 cDNA.

These are the sequences of eI and fI primers:

5'   3'

eI: CGGAATTCGAGGGAGGCGAGGACGAGATCCA

5'   3'

fI: CCCAAGCTTCCTGTGGCCACCCCCTTGTGC

A 290 bp was amplified by both cDNA from control mice and cDNA from knockout mice (not shown). The presence of the 290 bp fragment, that is the presence of RyR3 mRNA in knockout mice, was not an unexpected result. In fact the RyR3 gene was interrupted in its 3' portion, and, unless a strong instability due to the interruption, mRNA should be synthesized. Evidently RyR3 mRNA was not unstable.

3.3.5b RyR3 protein in the RyR3$^{-/-}$ mouse.

In order to determine if RyR3 protein had been knocked out, Western blot analysis was performed on diaphragm and brain microsomes from RyR3$^{-/-}$ and wild-type mice as control. Using the anti-RyR3 antibody, the band corresponding to RyR3 monomer was absent in RyR3$^{-/-}$ mice, confirming the positive outcome of the knockout technique (Fig. 3.3c).

RyR1 and RyR2 antibodies were also used as control: the absence of RyR3 does not affect the expression of RyR1 and RyR2 isoforms in Western blot assay (see below, Fig. 4.2).

Chapter 4

Pattern of expression of RyR3 protein in adult skeletal muscle and during neonatal phase of skeletal muscle development

These experiments were performed together with Antonio Conti, researcher in my same laboratory, Growth Factors and Signal Transduction Unit, DIBIT, HSR.
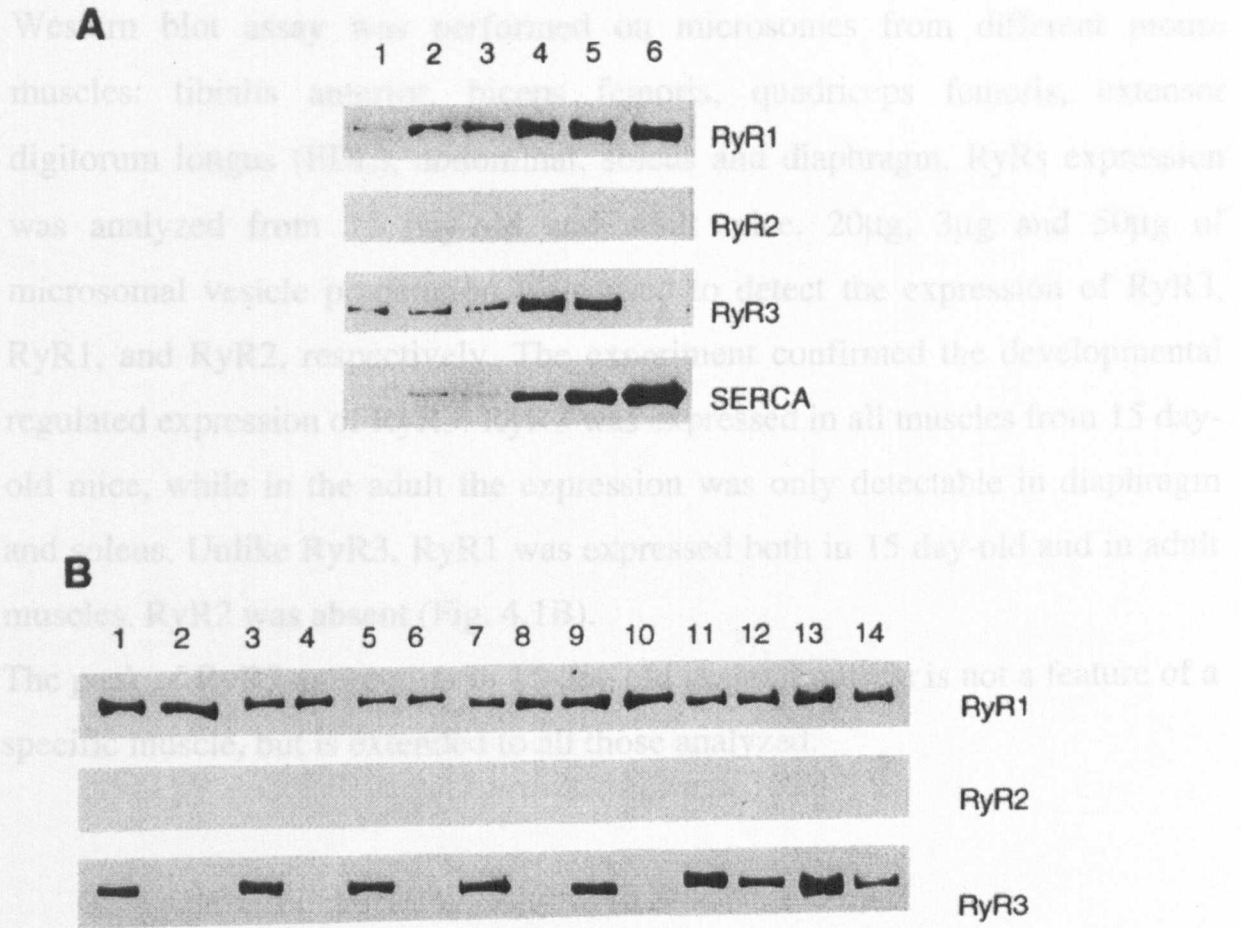
4.1 Introduction

As described in the introduction, preliminary results about RyR3 expression in adult mouse tissues had revealed a wide spread distribution of mRNA, without an apparent preferential localization in a specific tissue or cell type (Giannini et al., 1995). However, the presence of RyR3 mRNA and protein in skeletal muscle together with the type 1 isoform resulted to be particularly interesting. The presence of RyR1 in skeletal muscle has been largely studied, and its role in e-c coupling is universally accepted. Previous results revealed the expression of RyR3 protein in such specific skeletal muscles as diaphragm and soleus (Conti et al., 1996). In addition, RyR3 seems to be regulated during mouse diaphragm development, because of the higher level of expression in 5 day old mice diaphragm than adult tissue, as revealed by Western blot experiments on mouse diaphragm (Tarroni et al., 1997). As described in details in the introduction, the first 3-4 weeks after birth represent a critical phase for skeletal muscle development: during this phase many muscle-specific proteins start to be expressed, or switch from one isoform to another; the e-c coupling machinery completes its structural and functional development after birth. Because of the key role of this period for skeletal muscle development, and the described preliminary results, we decided to further investigate the profile of RyR3, and also RyR1 and RyR2, in the neonatal phase of development.

4.2a Western blot assay on microsomes from total hindlimb muscles

Western blot assay was performed as described (see Materials and Methods). 20μg of microsomal vesicles from total hindlimb mouse muscles were used in a Western blot assay with the anti-RyR3 policlonal antibody. Muscles for microsomal preparation were dissected from mice at different stages of development: 18 days of foetal development (F18), 2 day-old mice, 5 day-old, 25 day-old, adult mice. The same experiment was performed in parallel to investigate RyR1 and RyR2 expression with the suitable anti-RyR policlonal antibodies, using 3μg and 50μg of microsomal vesicle preparation, respectively. SERCA (Ca^{2+}-ATPase) was used as control. RyR3 was weakly expressed at F18, increased at 2 day-old and reached the highest level of expression at 15 day-old. Then the expression decreased (25 day-old) and disappeared in the adult. Unlike RyR3, RyR1 was expressed at progressively higher levels from F18, reaching the peak of expression in the adult. RyR2 was absent as expected (Fig. 4.1A).

The experiment confirmed a regulated expression of RyR3 during the neonatal phase of skeletal muscle development, evidencing the maximum level of expression in 15 day-old mice.

Figure 4.1. Developmental expression of RyRs isoforms in skeletal muscles. A) Western blot on microsomes from total hindlimb muscles of day 18 embryos (lane 1), 2-day-old (lane 2), 5-day-old (lane 3), 15-day old (lane 4), 25-day-old (lane 5) and adult mice (lane 6). Specific antibodies to distinguish the three isoforms were used. SERCA (Ca^{2+}-ATPase) was used as control. B) Western blot analysis on microsomes from single skeletal muscles from 15-day-old and adult mice: tibialis anterior (lanes 1 and 2), biceps femoris (lanes 3 and 4), quadriceps femoris (lanes 5 and 6), extensor digitorum longus (lanes 7 and 8), abdominal (lanes 9 and 10), soleus (lanes 11 and 12), and diaphragm (lanes 13 and 14).

4.2b Western blot assay on microsomes from single muscles

Western blot assay was performed on microsomes from different mouse muscles: tibialis anterior, biceps femoris, quadriceps femoris, extensor digitorum longus (EDL), abdominal, soleus and diaphragm. RyRs expression was analyzed from 15 day-old and adult mice. 20μg, 3μg and 50μg of microsomal vesicle preparation were used to detect the expression of RyR3, RyR1, and RyR2, respectively. The experiment confirmed the developmental regulated expression of RyR3: RyR3 was expressed in all muscles from 15 day-old mice, while in the adult the expression was only detectable in diaphragm and soleus. Unlike RyR3, RyR1 was expressed both in 15 day-old and in adult muscles. RyR2 was absent (Fig. 4.1B).

The peak of RyR3 expression in 15 day-old skeletal muscle is not a feature of a specific muscle, but is extended to all those analyzed.

4.3 Expression of the RyR1 and RyR2 during development in RyR3$^{-/-}$ mouse

In order to verify if the lack of RyR3 could affect the level of RyR1 and RyR2 expression during skeletal muscle development, Western blot assay was performed on microsomes from 5 day-old, 15 day-old and adult skeletal muscles. Total hindilimb muscles and diaphragm were chosen. While the absence of RyR3 in the assayed muscles was confirmed, RyR1 and RyR2 expression was unaffected: RyR1 was expressed at higher levels in adult muscles than in 2 day-old and 5 day-old tissues, RyR2 was still absent (Fig. 4.2).

The pattern of expression the two other isoforms did not result to be modified as a consequence of the lack of type 3.
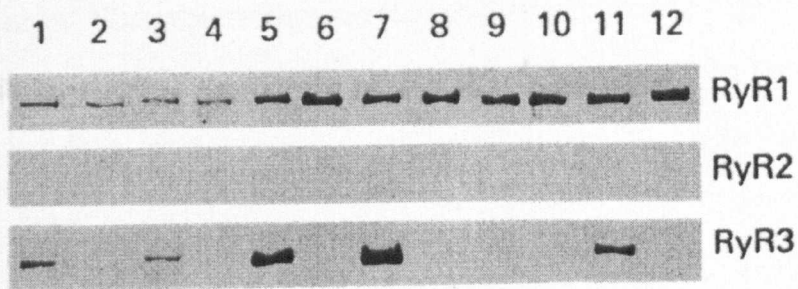
Figure 4.2. Immunoblot analysis of RyR1, RyR2 and RyR3 from wild-type (lanes 1, 3, 5, 7, 9, 11) and RyR3$^{-/-}$ mice (lanes 2, 4, 6, 8, 10, 12) at different developmental stage: 2-day-old (lanes 1-4), 5-day-old (lanes 5-8), and adult mice (lanes 9-12). Microsomes were prepared from total hindlimb (lanes 1, 2, 5, 6, 9, 10) and diaphragm (lanes 3, 4, 7, 8, 11, 12) muscles.

Chapter 5

Functional analysis of RyR3$^{-/-}$ mouse

5.1 Contractile function analysis

These experiments were performed in collaboration with R. Bottinelli and C. Reggiani at the Department of Human Physiology, University of Pavia.

In order to address the contribution of RyR3 to the excitation-contraction machinery, we studied the contractile properties of skeletal muscles from wild-type and RyR3$^{-/-}$ mice. The experiments were performed to investigate both the contractile response to physiological electrical stimulation and to caffeine, an activator of RyRs.

5.1a Analysis of contractile activity in response to electrical stimulation

Muscle strips were dissected from diaphragm of neonatal (15 day-old) and adult (60-90 day-old) mice, wild-type and RyR3$^{-/-}$.

A high frequency stimulation (50 Hz) was applied and fused tetani were evoked. No significant differences were evident between wild-type and RyR3$^{-/-}$ mice, although the preparation from neonatal mice developed less tension than the preparation from adult mice (Fig. 5.1A). The experiment was repeated using a low stimulation frequency (0.1 Hz): in 15 day-old mice tension developed during the twitch was significantly lower in RyR3$^{-/-}$ than in wild-type mice (Fig. 5.1B): expressed as a fraction of tetanic tension (twitch/tetanus ratio), it represented 0.23±0.03 in wild-type (n-10) and 0.15±0.01 in RyR3$^{-/-}$

134

(n=10, P<0.05). The measurement of tension developed during unfused tetani (5 and 10 Hz) confirmed the results. At higher stimulation rates, the difference was cancelled by fusion and summation of the responses. Figure 5.1 (C and D) summarizes the result: in 15 day-old mice (Fig. 5.1C) the tension developed in unfused tetani was lower in RyR3$^{-/-}$ mice than in wild-type (force-frequency curve shifted downward and rightward in mutant mice); in the adult (Fig. 5.1D) the difference disappeared.

The time necessary to peak tension was investigated. The time course of the twitch was age-dependent, in fact it became shorter in the adult muscles. No difference was detectable between wild-type and RyR3$^{-/-}$ mice, neither in the 15 day-old nor in the adult mice (Fig. 5.1E).

The analysis of the contractile properties was repeated after removing extracellular Ca^{2+}. Tension developed after lowering Ca^{2+} concentration in the perfusing medium was lower in neonatal than in adult muscles, but, again, no difference was detectable between wild-type and RyR3$^{-/-}$ mice, both in the 15 day-old and in the adult mice (Fig. 5.1F).
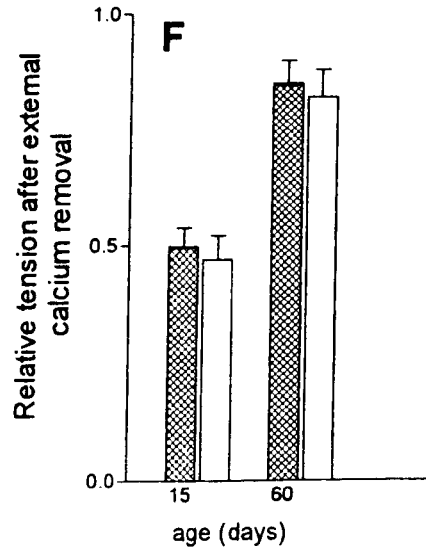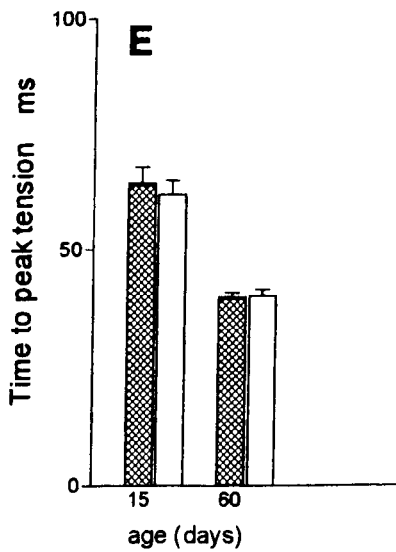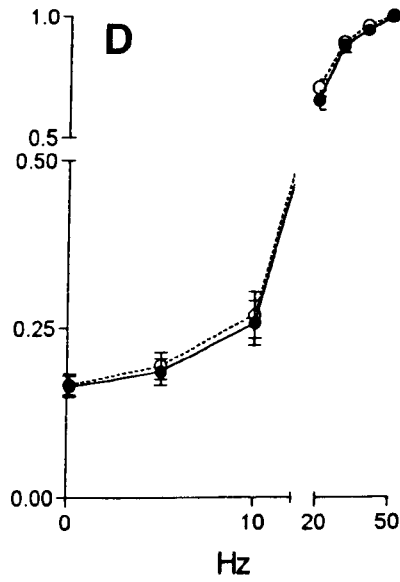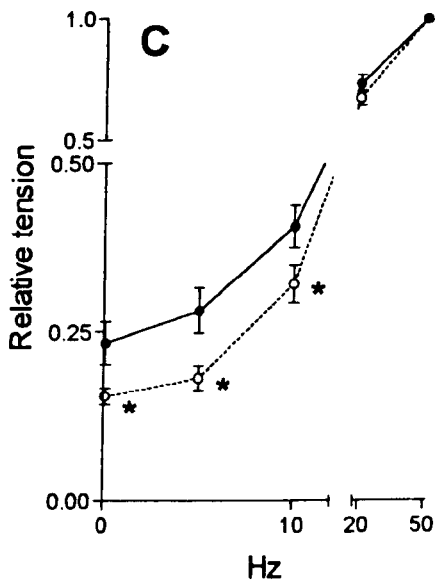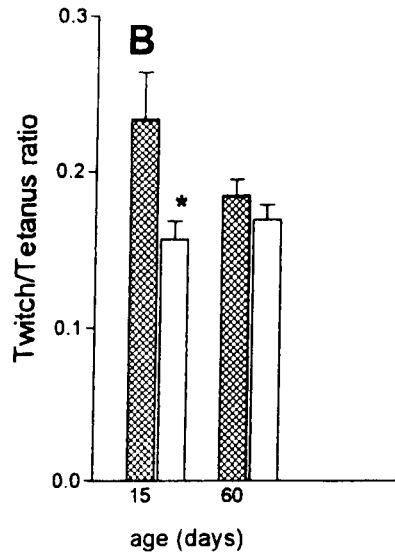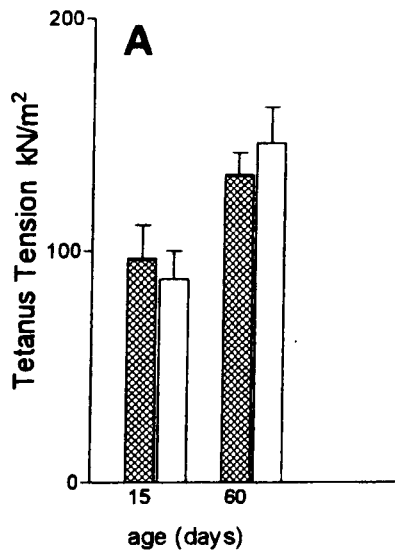
Figure 5.1. Contractile properties of diaphragm strips from RyR3$^{+/+}$ (filled symbols and columns) and RyR3$^{-/-}$ mice (empty symbols and columns) at 15 and 60 days. A) Tension developed during tetanic stimulation at 50 Hz. B) Twitch/tetanus ratio at the stimulation frequency of 0.1 Hz. C) Force-frequency relationships in diaphragm strips from 15-day-old mice. D) Force-frequency relationships in diaphragm strips from 60-day-old mice. E) Time to peak tension in twitch responses. F) Effect of Ca^{2+} removal expressed relative to twitch tension in basal conditions. Means and standard errors of 10 neonatal and 20-28 adult RyR3$^{+/+}$ preparations, and 10 neonatal and 16-22 adult RyR3$^{-/-}$ preparation. *P<0.05.

5.1b Analysis of contractile activity in response to stimulation by caffeine

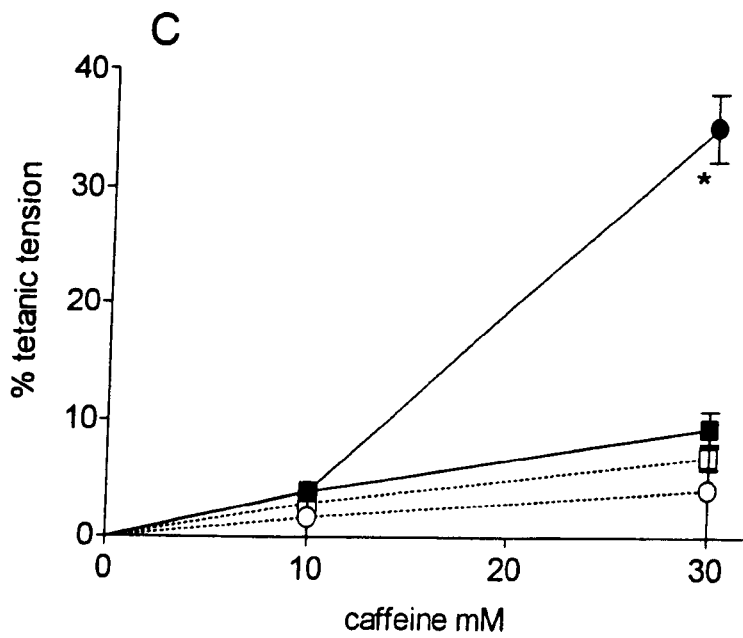As for previous experiments, muscle strips were dissected from the diaphragm of 15 day-old and adult (60-90 day-old) mice, wild-type and RyR3$^{-/-}$. Tension development was induced by exposure to millimolar caffeine concentration. In wild-type mice, at caffeine concentration >10mM, 15 day-old diaphragm strips developed much more tension than adult diaphragm strips; at 30mM caffeine tension induced was four times greater in neonatal than in adult strips (Fig. 5.2A, B, and C). In addition, the kinetics of tension development was much slower in neonatal than in adult diaphragm strips: the time to peak tension was 400-600 s in neonatal and ~10 s in adult (Fig. 5.2A and B).

The large response to caffeine produced in neonatal diaphragm strips from wild-type mice was completely abolished in neonatal diaphragm strips from RyR3$^{-/-}$ mice (Fig. 5.2A and B). No difference was detectable between adult wild-type and mutant mice. The kinetics of tension development was not altered in RyR3$^{-/-}$ mice compared to wild-type, both in neonatal and in adult mice. The abolishment of the large response to millimolar caffeine in RyR3$^{-/-}$ diaphragm strips was the most important difference between wild-type and RyR3$^{-/-}$ muscles.

These experiments were also performed in EDL and soleus muscles (not shown). The difference of the responses to caffeine between preparation from 15 day-old wild-type and RyR3$^{-/-}$ mice was confirmed: in EDL 51% of tetanic tension was measured in wild-type and 7.4% in mutant mice; in soleus 38% of tetanic tension was measured in wild-type and 8.6% in mutant mice. In EDL from adult mice the tension developed in response to caffeine was barely detectable, and ranged between 5 and 10% in soleus. No difference between

wild-type and RyR3$^{-/-}$ mice was detected, confirming the results obtained with diaphragm.

A neonatal

+/+

30

20

10

0

100 s

↑   ↓

30

20

10

0

−/−

↑   ↓

% tetanic tension

B adult

+/+

30

20

10

0

7 s

↑   ↓

30

20

10

0

−/−

↑   ↓

C

40

30

20

10

0

% tetanic tension

*

0   10   20   30
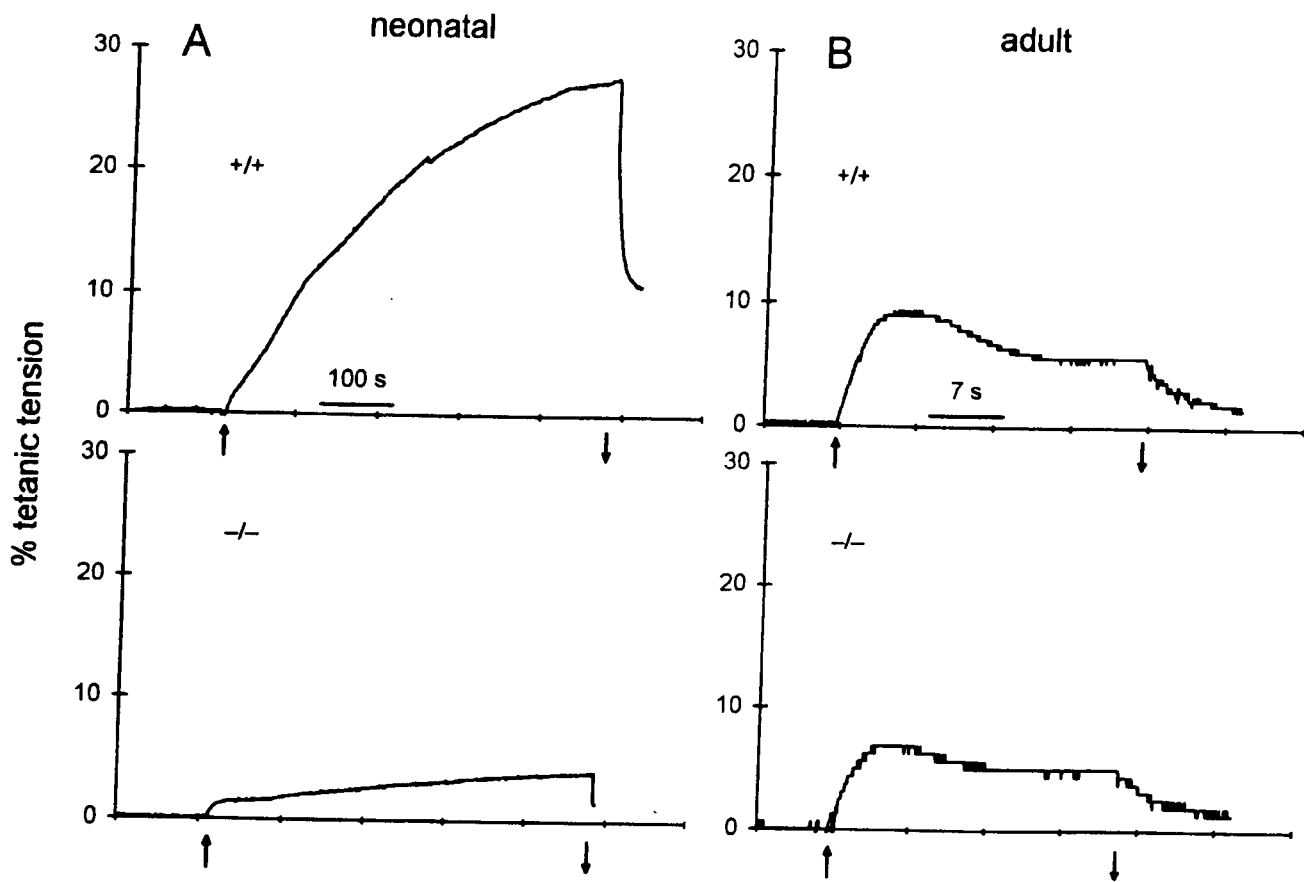
caffeine mM

Figure 5.2. Response to caffeine of diaphragm strips from 15-day-old (neonatal) (A) and 60-day-old (adult) mice (B). Diaphragm strips were exposed to 30mM caffeine. Tension is expressed as the percentage of tetanic tension. Arrows indicate addition and washing out of caffeine. C) Tension developed in contractures elicited by exposing muscle strips to 10 and 30mM caffeine. Means and standard errors of 10 neonatal and 30 adult RyR3$^{+/+}$ preparations, and 10 neonatal and 30 adult RyR3$^{-/-}$ preparations. Circles: neonatal mice; squares: adult mice; filled symbols: RyR3$^{+/+}$; empty symbols: RyR3$^{-/-}$. *P<0.05.

5.2 Biochemical characterization of knockout RyR3$^{-/-}$ mouse

5.2a Introduction

The biochemical characterization of skeletal muscles from RyR3$^{-/-}$ mice was performed through binding experiments on microsomal preparations from total hindlimb and diaphragm muscles.

Binding analysis was performed by the use of the specific [^{3}H]-labeled ligand ryanodine, which interacts with the channel in the open state.

Because of the specific interaction between the radiolabel led ryanodine and ryanodine receptors, the binding assay was used as a tool to quantify the amount of ryanodine receptors in the analyzed skeletal muscles. In fact, the availability of RyR3$^{-/-}$ mice gave the possibility to compare binding data from wild-type skeletal muscles to binding data from RyR3$^{-/-}$ skeletal muscles, estimating the contribution of RyR3 to the total amount of ryanodine receptors in the skeletal muscles analyzed.

Finally, binding experiments were performed on skeletal muscles from mice at different developmental stages: 5 day-old, 15 day-old, and adult mice. By the profile of expression of ryanodine receptors in skeletal muscles (RyR1 and RyR3) during neonatal development, it was interesting to study the same profile by binding experiments, again taking advantage of the comparison between RyR3$^{+/+}$ and RyR3$^{-/-}$ mice.

To evaluate the amount of ryanodine receptors in the skeletal muscles, we chose experimental conditions that are known to stimulate the maximum binding of ryanodine, such as high salt concentration (1M KCl), and 100μM Ca^{2+} (Ogawa and Harafuji, 1990; Murayama and Ogawa, 1996).

5.2b Saturation experiments on microsomes from diaphragm and total hindlimb of RyR3+/+ and RyR3-/- mice

Binding experiments were performed as described (see Materials and Methods).

Experiments on diaphragm from adult RyR3+/+ mice

Five experiments with four different batches of microsomes from adult wild-type diaphragms were performed. The following table summarizes the results:

Ry (nM)	I exp. pmoles/mg	II exp. pmoles/mg	III exp. pmoles/mg	IV exp. pmoles/mg	V exp. pmoles/mg	Media pmoles/mg	S.D.
2.5	0.18	0.24	0.26	0.49	0.59	0.35	0.173
3.5	0.25		0.55	0.61		0.47	0.038
5	0.39	0.42	0.6	0.74	0.72	0.57	0.147
6.5	0.52		0.69	0.67		0.63	0.014
7.5	0.72	0.45	0.68	0.89	0.9	0.73	0.211
8.5	0.84	0.78	0.8	1.03		0.86	0.136
10	0.68	0.87	0.77	0.76	0.98	0.81	0.103
12.5	0.67	1.1	0.99	0.89	1.21	0.97	0.138
15	0.82	1.17	0.96	0.86		0.95	0.158
17.5	0.82		0.84	0.86		0.84	0.014
20	1.08	1.42	0.93	0.99		1.1	0.267
25	1.66	1.49	1.11	0.95		1.3	0.277
30	0.76	1.28	1.06	1.33	1.93	1.27	0.372

The resulting saturation curve and Scatchard plot analysis are shown in Fig. 5.3. The values of K_d and B_{max} calculated were respectively 8.79 nM and 1.55 pmol/mg.
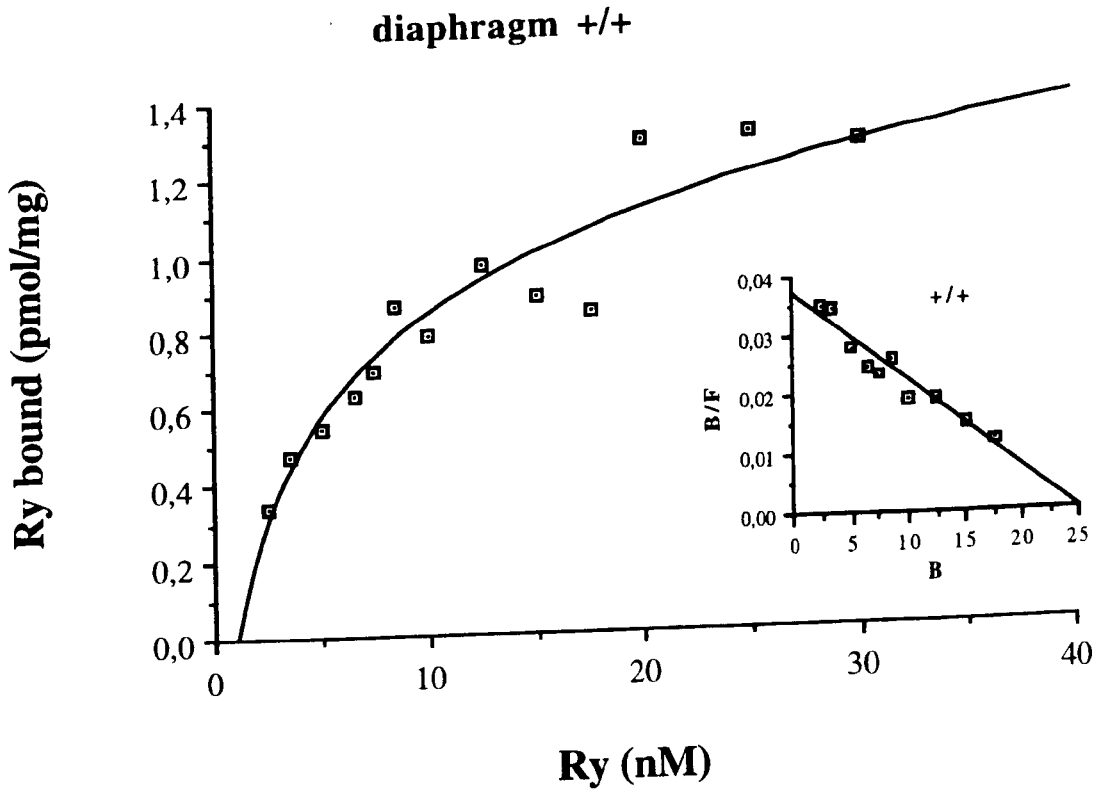
Figure 5.3. Specific binding of [3H]ryanodine to diaphragm microsomal membranes from +/+ mice. [3H]ryanodine binding in the presence of 2.5-30nM [3H]ryanodine as indicated in Materials and Methods. *Inset*, Scatchard plot of saturation data of the specific binding. Data represents the mean of 5 experiments in duplicate.

Experiments on diaphragm from adult RyR3$^{-/-}$ mice

Four experiments with three different batches of microsomes from adult knockout RyR3$^{-/-}$ diaphragms were performed. The following table summarizes the results:

Ry (nM)	I exp. pmoles/mg	II exp. pmoles/mg	III exp. pmoles/mg	IV exp. pmoles/mg	Media pmoles/mg	S.D.
2.5	0.07	0.16	0.15	0.13	0.13	0.036
3.5	0.09	0.14			0.11	0.031
5	0.12	0.18	0.28	0.41	0.24	0.126
6.5	0.31	0.26			0.28	0.04
7.5	0.31	0.25	0.26	0.49	0.33	0.114
8.5	0.36	0.26			0.31	0.071
10	0.3	0.46	0.2	0.48	0.36	0.133
12.5	0.37	0.43			0.39	0.041
15	0.38	0.54	0.24		0.38	0.152
17.5	0.32	0.37			0.34	0.034
20	0.35	0.43		0.48	0.42	0.069
25	0.27	0.54			0.4	0.19
30	0.2	0.72	0.79	0.55	0.56	0.264

The resulting saturation curve and Scatchard plot analysis are shown in Fig. 5.4. The values of K_d and B_{max} calculated were respectively 10.7 nM and 0.7 pmol/mg.
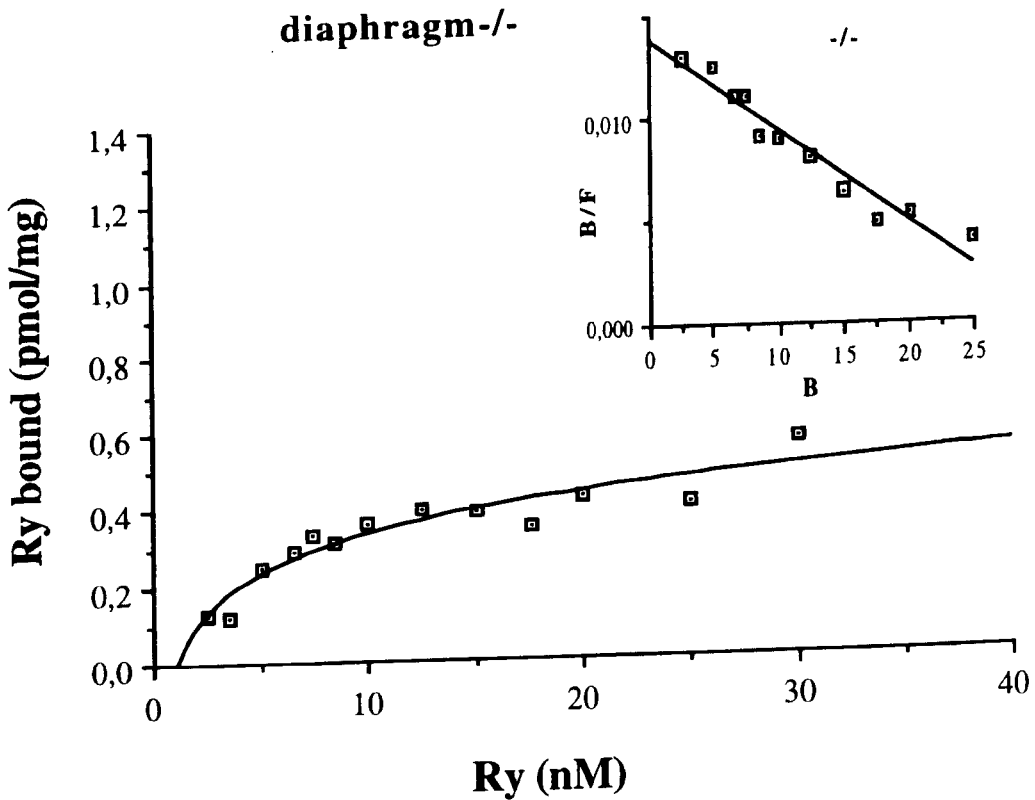
Figure 5.4. Specific binding of [^{3}H]ryanodine to diaphragm microsomal membranes from -/- mice. [^{3}H]ryanodine binding in the presence of 2.5-30nM [^{3}H]ryanodine as indicated in Materials and Methods. *Inset*, Scatchard plot of saturation data of the specific binding. Data represents the mean of four experiments in duplicate.

These results point out a strong difference between diaphragm from wild-type and mutant mice. In particular, despite the similar values of K_d, the value of B_{max} from the RyR3$^{-/-}$ diaphragm was about half the wild-type diaphragm B_{max}, suggesting a strong contribution of RyR3 to the total amount of ryanodine receptors in mouse diaphragm.

Experiments on hindlimb from adult RyR3$^{+/+}$ mice

Two experiments with two different batches of microsomes from adult wild-type total hindlimbs were performed. The following table summarizes the results:

Ryanodine (nM)	I exp. pmoles/mg	II exp. pmoles/mg	Media pmoles/mg	S.D.
0.5	0.31	0.36	0.33	0.033
1.5	0.57	0.43	0.49	0.101
2.5	0.67	0.42	0.55	0.178
5	0.79	0.53	0.66	0.185
7.5	1.12	0.87	0.99	0.178
10	1.44	0.89	1.17	0.388
15	2.36	1.35	1.85	0.714
20	2.85	1.57	2.21	0.906
30	2.55	1.63	2.08	0.652

The resulting saturation curve is shown in Fig. 5.5. The preliminary calculated values of K_d and B_{max} were respectively 5 nM and 1.94 pmol/mg.
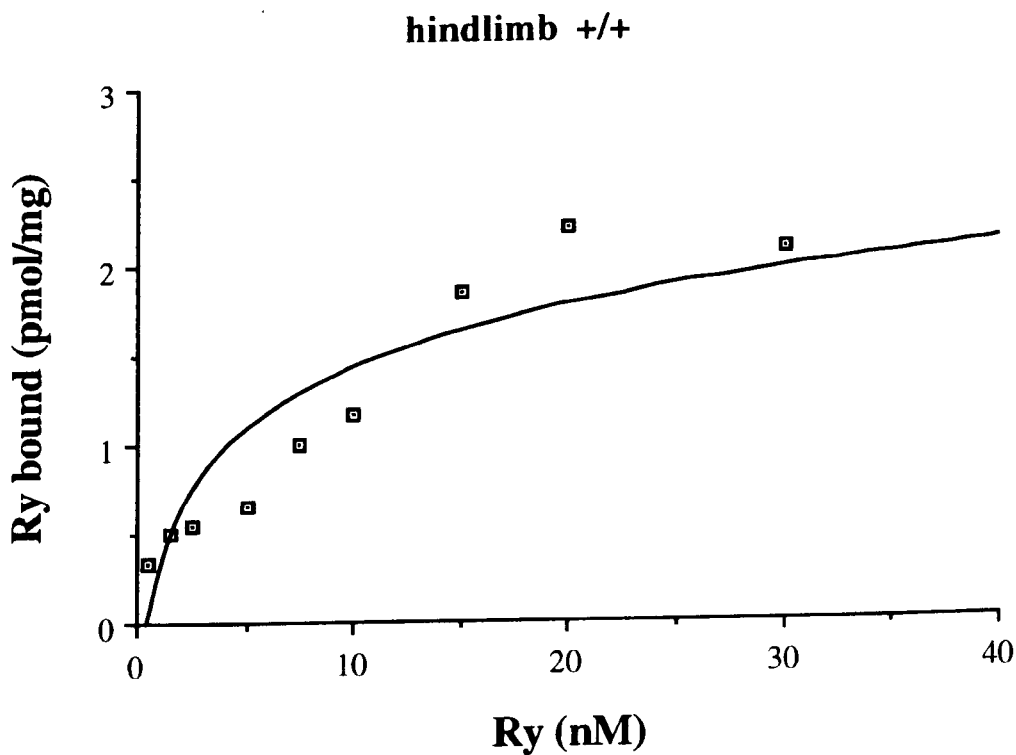
Figure 5.5. Specific binding of [3H]ryanodine to total hindlimb microsomal membranes from +/+ mice. [3H]ryanodine binding was performed in the presence of 0.5-30nM [3H]ryanodine as indicated in Materials and Methods. Data represents the mean of two experiments in duplicate.

Experiments on hindlimb from adult RyR3$^{-/-}$ mice

Two experiments with two different batches of microsomes from adult knockout RyR3$^{-/-}$ total hindlimbs were performed. The following table summarizes the results:

Ryanodine (nM)	I exp. pmoles/mg	II exp. pmoles/mg	Media pmoles/mg	S.D.
0.5	0.27	0.26	0.27	0.011
1.5	0.38	0.44	0.41	0.043
2.5	0.48	0.45	0.46	0.026
5	0.71	0.81	0.75	0.072
7.5	0.98	0.99	0.98	0.008
10	1.08	1.26	1.17	0.123
15	2.82	1.82	2.32	0.707
20	3.45	1.82	2.66	1.105
30	3.93	1.65	2.78	1.613

The resulting saturation curve is shown in Fig. 5.6. The preliminary calculated values of K_d and B_{max} were respectively 9.1 nM and 2.55 pmol/mg.

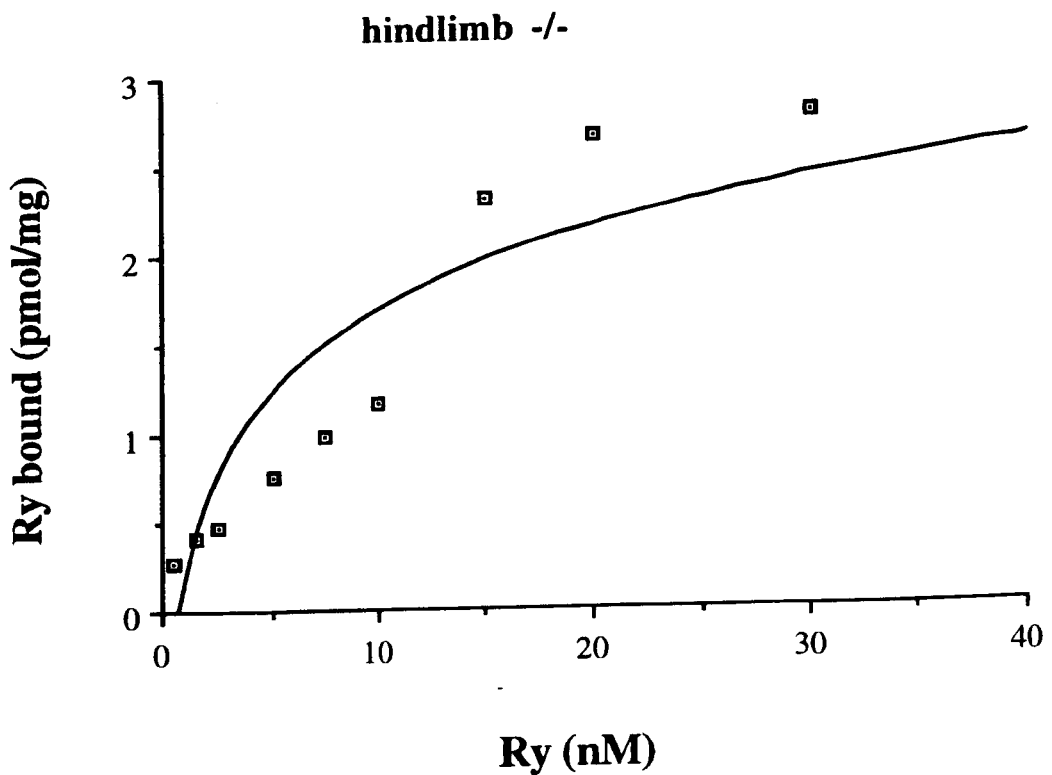**Figure 5.6.** Specific binding of [3H]ryanodine to total hindlimb microsomal membranes from -/- mice. [3H]ryanodine binding was performed in the presence of 0.5-30nM [3H]ryanodine as indicated in Materials and Methods. Data represents the mean of two experiments in duplicate.

Because of the low number of trials and the few batches utilized, the result of binding experiments performed on microsomes of total hindlimbs from +/+ and -/- mice are preliminary, as suggested by the large value of the standard deviation (see S.D. in the tables). Although preliminary, the data suggest a substantial equality between the wild-type and the mutant hindlimb muscles, as if the contribution of RyR3 to the total amount of RyRs in adult hindlimb muscles were minimum. This conclusion is in agreement with the Western blot assays described (see above).

5.2c Ca^{2+}-dependence of [^{3}H]ryanodine binding on diaphragm microsomes from RyR3$^{+/+}$ and RyR3$^{-/-}$ mice

Binding experiments were performed as described (see Materials and Methods). The data presented are the result of preliminary experiments.

Experiments on diaphragm from adult RyR3$^{+/+}$ mice

Two experiments with two different batches gave the following results:

Ca^{2+}	specific binding pmol/mg I experiment pmoles/mg	specific binding pmol/mg II experiment pmoles/mg		average value in % relative to the 100% binding
10nM	0.054	/		4
100nM	0.297	/		22.5
1µM	0.515	0.194		83.3
10µM	0.593	0.194		89.2
100µM	0.66	0.219		100
1mM	0.565	0.133		73.2
10mM	nd	0.1212		55.3
100mM	0.04	0.034		3

The last column of the table represents the average values in % relative to the 100% of maximum binding. The peak of [3H]ryanodine binding was obtained at Ca^{2+} concentration of 100µM, as shown in Fig. 5.7.
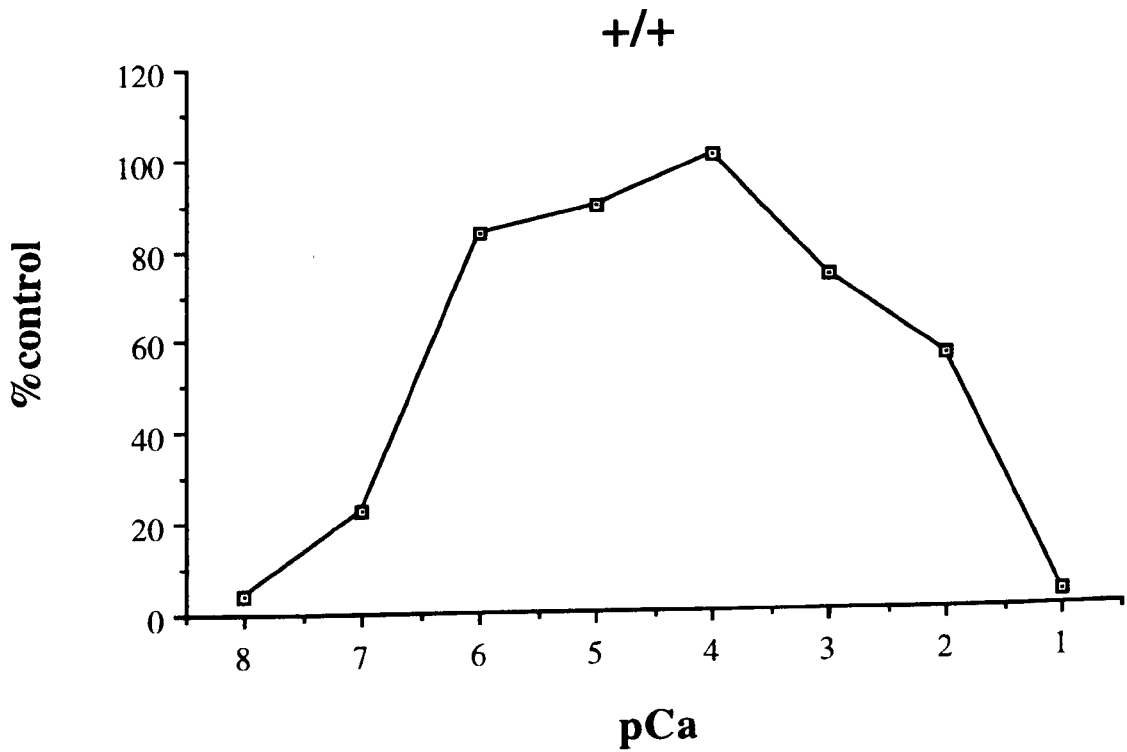
Figure 5.7. Dependence of [^{3}H]ryanodine binding on Ca^{2+} concentration. Experiments were performed on diaphragm microsomes from RyR3$^{+/+}$ adult mice.

Experiments on diaphragm from adult RyR3$^{-/-}$ mice

Two experiments with two different batches gave the following results:

Ca^{2+}	specific binding pmol/mg I experiment pmoles/mg	specific binding pmol/mg II experiment pmoles/mg	average value in % relative to the 100% binding (I)	average value in % relative to the 100% binding (II)
10nM	/	0.025	/	14.8
100nM	0.073	0.09	21.5	53.2
1µM	0.34	0.124	100	73.4
10µM	0.314	0.169	92.3	100
100µM	0.319	0.148	93.8	87.6
1mM	0.187	0.112	55	66.3
10mM	0.013	/	3.8	/
100mM	/	/	/	/

The last 2 columns of the table represent the average values in % relative to the 100% of maximum binding. In this case, the 100% of [3H]ryanodine binding was different in the two experiments. The curves of the single experiments are shown in shown in Fig. 5.8 A and B. A larger number of experiments will help to clear the picture.

A

-/-

B

-/-
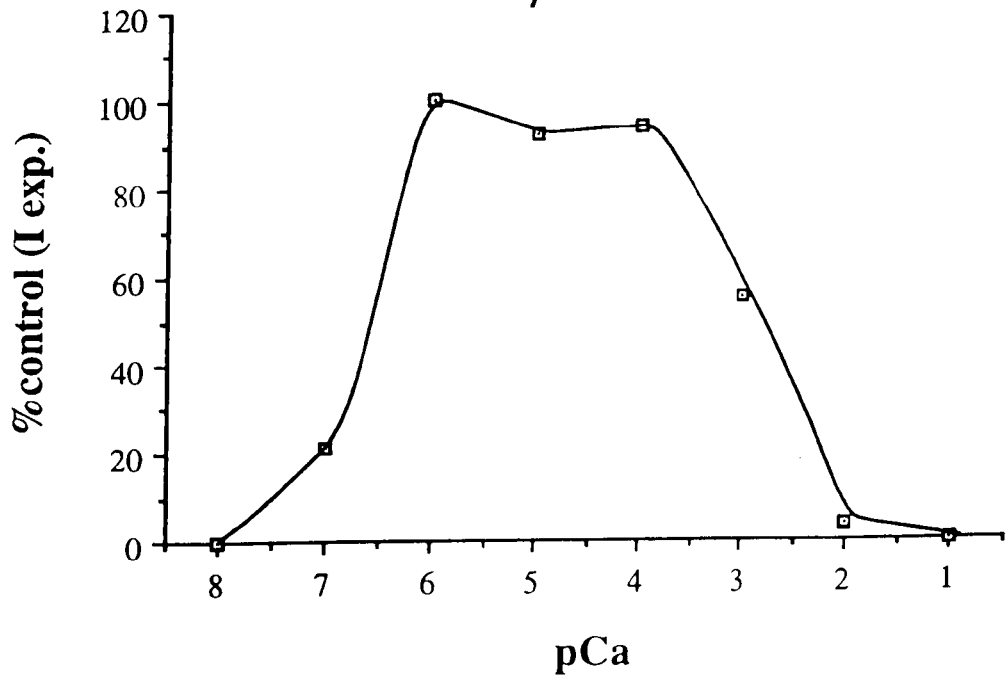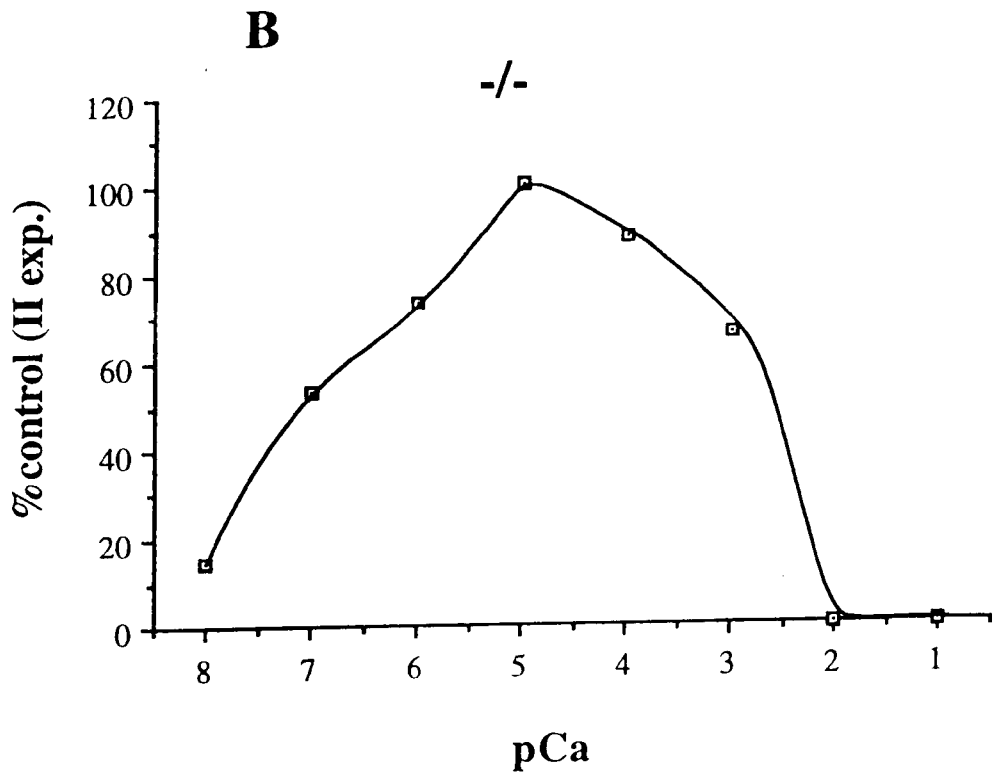
Figure 5.8 A and B. Dependence of [³H]ryanodine binding on Ca²⁺ concentration. Experiments were performed on diaphragm microsomes from RyR3⁻/⁻ adult mice.

5.2d [^{3}H]ryanodine binding experiments on microsomal preparations from RyR3$^{+/+}$ and RyR3$^{-/-}$ mice at different stages of neonatal skeletal muscle development

[^{3}H]ryanodine binding experiments on diaphragm

Microsomes from 5 day old, 15 day-old and adult diaphragm mice were utilized in [^{3}H]ryanodine binding assays. 4 experiments were performed using three different batches for 5 day-old diaphragms, four different batches for 15 day-old diaphragms and four different batches for adults.

Figure 5.9 schematizes the results reported in the following table:

diaphragm +/+

+/+	I exp.	II exp.	III exp.	IV exp.	V exp.	media ± S.D.
5d		1.06		1.01	0.73	0,93 ± 0,17
15d	0.86	0.77	0.86		1.06	0,88 ± 0,12
adult	1.1	1.16	1.44	1.13	0.96	1,16 ± 0,17

diaphragm -/-

-/-	I exp.	II exp.	III exp.	IV exp.	V exp.	media ± S.D.
5d	0.47	0.52		0.58	0.67	0,56 ± 0,08
15d	0.48		0.44	0.25	0.25	0,35 ± 0,12
adult	0.2	0.47	0.24	0.54	0.31	0,35 ± 0,14

The value of [^{3}H]ryanodine binding (pmol/mg) in 5 day-old diaphragm is similar to the value in 15 day-old muscle, and again, very similar to the adult value. From these data, it seems that no change in the total level of RyRs occurs during neonatal diaphragm development, both in RyR3$^{+/+}$ and in RyR3$^{-/-}$ mice. Although the profile of [^{3}H]ryanodine binding does not change, in knockout RyR3$^{-/-}$ mice there is a strong reduction of the binding values (Fig. 5.9). As for the saturation experiments, these data suggest a strong contribution of RyR3 to the total amount of RyRs in diaphragm during the analyzed neonatal phases of development.

[^{3}H]ryanodine binding experiments on total hindlimb

The same experiments described for diaphragm microsomes were performed on microsomes from total hindlimb muscles. 6 experiments with three different batches of 5 day-old, 15 day-old and adult hindlimb muscles were made. The following table summarizes the results:

leg +/+

+/+	I exp.	II exp.	III exp.	IV exp.	V exp.	VI exp.	VII exp.	media ± S.D.
5d		0.56	0.35	0.18	0.39	0.19	0.36	0,34 ± 0,14
15d	0.7	0.95	1.19	2.29	2.5	2.11	2.96	2 ± 0,86
adult	2.47	1.86	2.41		2.5		3.66	2,6 ± 0,65

leg -/-

-/-	I exp.	II exp.	III exp.	IV exp.	V exp.	VI exp.	VII exp.	media ± S.D.
5d	0.48	0.25		0.18	0.38	0.19	0.42	0,28 ± 0,12
15d	0.97	1.1	1.05	3.11	1.5	2.35	3.16	2,04 ± 0,97
adult	2.04	1.43	1.07		2.26	3.33		2,02 ± 1,15

Figure 5.10 shows the profile of [^{3}H]ryanodine binding during neonatal development of hindlimb muscles. At difference with the picture described in diaphragm, [^{3}H]ryanodine binding values (pmol/mg) increase progressively during development, without any detectable difference between wild-type and RyR3$^{-/-}$ mice.
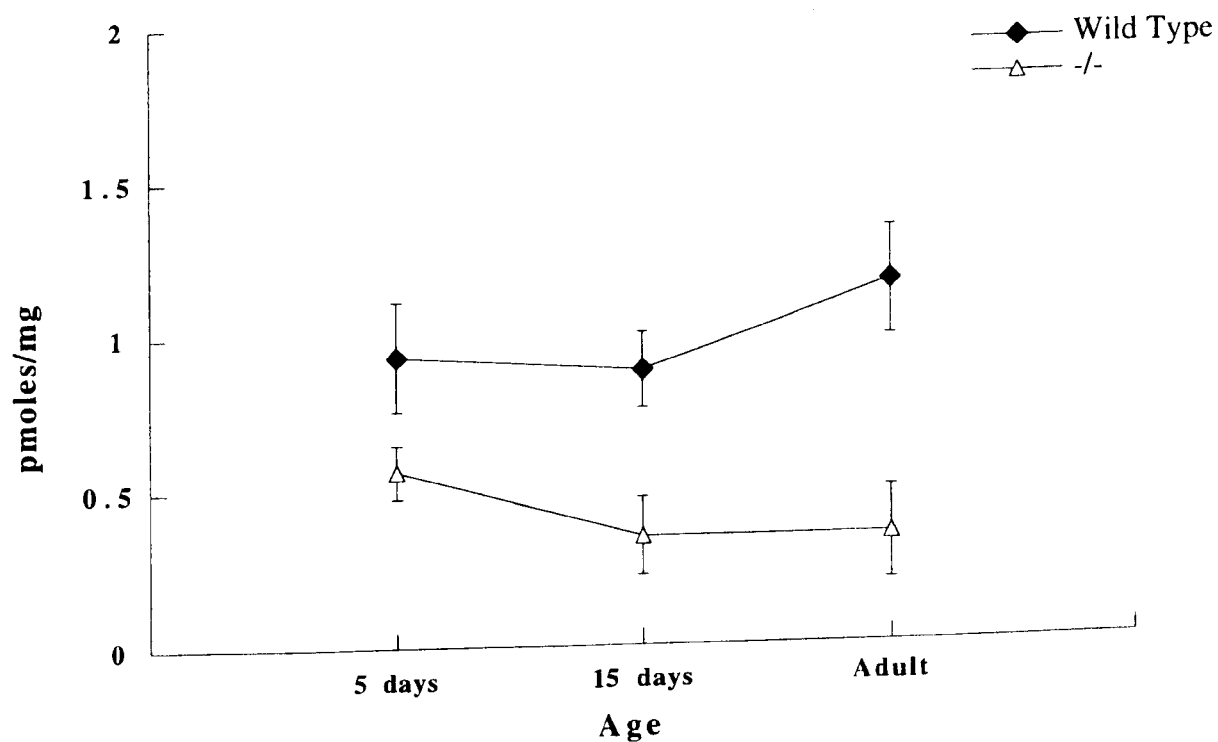
Figure 5.9. [^{3}H]ryanodine binding during development of diaphragm muscle in +/+ and -/- mice. Data represent the mean of four experiments in duplicate. For each stage, the mean ± S.D. is represented.
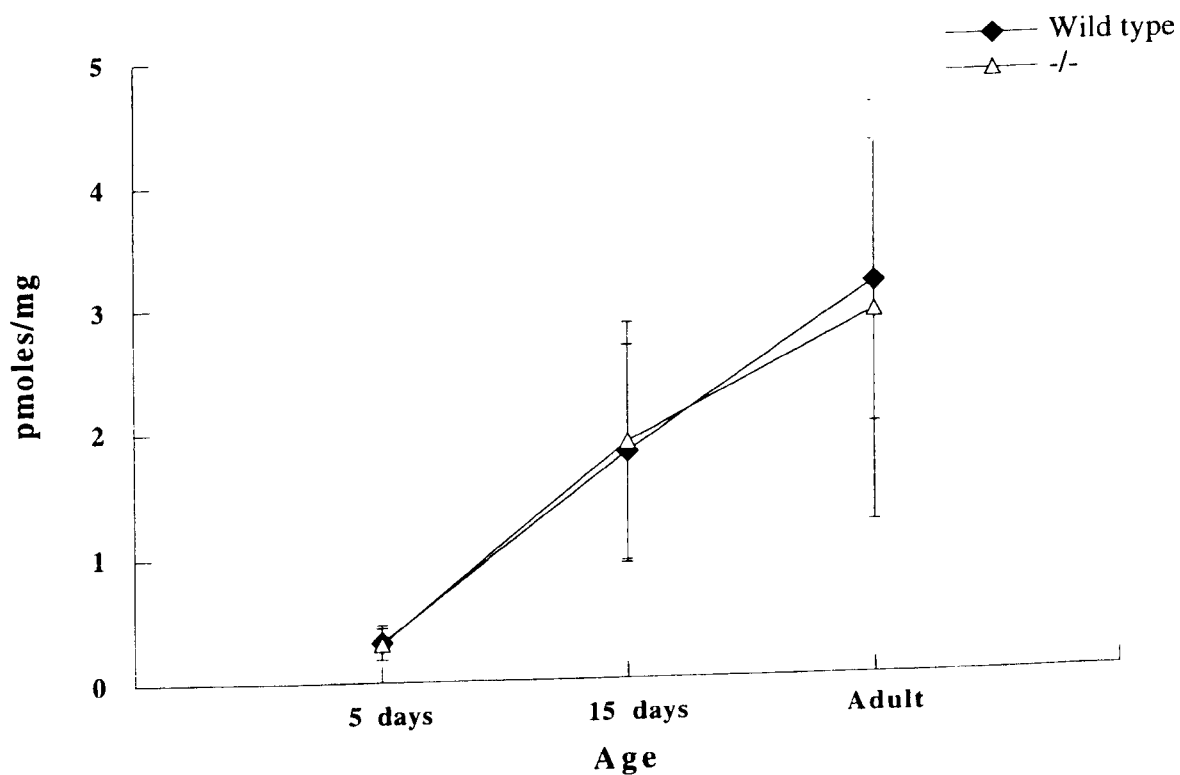
Figure 5.10. [³H]ryanodine binding during development of total hindlimb muscles in +/+ and -/- mice. Data represent the mean of six experiments in duplicate. For each stage, the mean ± S.D. is represented.

Chapter 6

General discussion

6.1. Developmental pattern of expression of RyR3

The expression of the RyR3 isoform in mammalian skeletal muscle (Conti et al. 1996) opens the possibility of involvement of this Ca^{2+} channel in the e-c coupling process regulating skeletal muscle contraction.

We performed an accurate analysis of RyR3 expression in mouse skeletal muscle from the late phase of foetal development throughout neonatal and adult stages.

RyR3 protein is expressed at 18 days of foetal development, and at difference with RyR1, reaches the highest level of expression between 2-3 weeks after birth. Then it decreases and disappears in all adult muscles with the exception of the diaphragm and the soleus, confirming the previous results (Conti et al., 1996).

The relevance of RyR3 expression in the neonatal phase of skeletal muscle development can be understood in the light of the importance of the neonatal phase for the development of skeletal muscles.

The neonatal stages represent a crucial period for skeletal muscle development. By the first 3-4 weeks after birth, skeletal muscles undergo a series of morphological and biochemical changes that allow them to reach a complete structural and functional maturity. This process involves both the contractile components of muscle fibers and the constituents of the Ca^{2+}-release units. One of the best known examples of changes in isoform profile of contractile proteins is the switching from the embryonic to the adult myosin heavy chain (MHC) isoforms: in the rat hindlimb muscles foetal fibers express the embryonic and neonatal isoforms of MHC; during the first weeks of neonatal development they switch to four major isoforms, the MHC β/slow isoform and the three adult fast MHA (MHC-2A, 2B. and 2X), normally repressed during earlier developmental stages (Schiaffino and Reggiani, 1996). The transcripts of these

four different isoforms are differentially distributed in different fibers and muscles.

The development of the Ca^{2+}-release unit and transverse tubule network has been well characterized in chicken skeletal muscle fibers (Takekura et al., 1994). The correct assembly of the main components of the membrane system, that is the feet (RyRs), the tetrads (DHPRs) and the internal protein associated with the junctional surface of the SR (calsequestrin), occurs in different sequential steps. First, in parallel with early myo-fibrillogenesis, the Ca^{2+}-release unit completed with feet, tetrads and internal proteins assembles at the periphery of the muscle fibers, generating the "peripheral coupling". The t-tubules are not present yet. The second step includes the appearance of a complex T-tubule network, which is not transversally oriented yet, but runs longitudinally. The final stage of maturation of these two-membrane systems involves the rearrangement of T-tubules and triads from a longitudinal to a transversal orientation, and localization of triads at the A-I junction or Z line. The coordinated maturation of these two-membrane systems occurs in the neonatal phase of development, that is up to 4 weeks in chick (3 weeks in rat and mouse) (Franzini-Armstrong, 1996).

The highest level of expression of RyR3 isoform coincides with the structural and functional maturation of the skeletal muscles, even though it is not clear why neonatal muscles requires high levels of RyR3 compared to adult.

6.2. Impairment of contractile activity in skeletal muscles from neonatal knockout mice.

The involvement of RyR3 in e-c coupling mechanism during the neonatal phase of muscle development is confirmed by the knockout of the murine RyR3 gene.

The analysis of the contractile activity of the skeletal muscle from RyR3$^{-/-}$ mice reveals an impairment during the first weeks after birth. In agreement with the preferential expression of this isoform in the post-natal period of development, skeletal muscles are about 35% less efficient in translating the electrical stimulation into force generation. Such impairment disappears in the adult diaphragm, still expressing RyR3. The strong reduction in the force of contraction in RyR3$^{-/-}$ muscles represents the first evidence of RyR3 involvement in the e-c coupling machinery for skeletal muscle contraction. The impairment in the skeletal muscle contraction activity is even evident when muscles from neonatal RyR3 knockout mice are treated with high doses of caffeine (30mM), a well-known activator of Ca^{2+}-release through RyRs: the contracture was reduced to about 20% compared to control mice. The significant reduction in the response to caffeine is also in agreement with the results obtained with RyR1 knockout mice (Takeshima et al., 1994), in which skeletal muscles lacking RyR1 isoform still respond to high doses of caffeine (mM range), feature attributed to the presence of RyR3 isoform.

The impairment in the force generation in neonatal RyR3$^{-/-}$ skeletal muscles both after electrical stimulation and caffeine stimulation strongly suggests the involvement of RyR3 in a secondary component of Ca^{2+}-release in the e-c coupling process. According to this hypothesis, RyR3 would work through a Ca^{2+}-induced Ca^{2+}-release mechanism contributing to the amplification of the signal: the depolarization of the plasma membrane elicits activation of RyR1, via mechanical coupling with DHPR; subsequently, Ca^{2+}-release through RyR1 stimulates RyR3 via CICR, determining an amplification of the signal (Fig. 6.1).

Our results strongly support a current model of e-c coupling machinery in skeletal muscle contraction originally proposed on the basis of morphological studies on non-mammalian vertebrate skeletal muscles (Block et al., 1988), but

then further supported by biochemical studies, physiological analysis, and finally, our data. According to this model, two functionally different populations of RyRs co-exist in skeletal muscle, and may be involved in the regulation of skeletal muscle contraction. Electron microscopy analysis revealed an ordered array of RyRs and DHPRs, with only one in every two Ca^{2+}-release channels on the SR facing the voltage sensor on the t-tubule (Block et al., 1988). This structural organization has been observed in muscles of non-mammalian and mammalian vertebrate containing only one RyR isoform (O'Brien et al., 1993; Franzini-Armstrong and Kish, 1995), suggesting that this alternating array may be a general motif in vertebrate skeletal muscles but that two different RyR isoforms are not always required. Physiological studies of Ca^{2+}-release from the SR revealed the existence of two components, a fast activating and inactivating component of large amplitude, and a smaller more steady component (Fleischer and Inui, 1989; Rios et al., 1992; Meissner, 1994; Schneider, 1994): initial voltage-dependent Ca^{2+}-release by the latter component would activate the former, representing the CICR component. RyR1 isoform is involved in the transduction of the signal from the plasma membrane to the SR, probably via a mechanical coupling with the DHPR. The importance of RyR1 in skeletal muscle contraction mechanism has been confirmed by the lack of e-c coupling in RyR1 knockout mice (Takeshima et al., 1994; Nakai et al., 1996), and by cn/cn mutant, a natural chicken mutant not expressing RyR1/α, in which the e-c coupling is abolished (Ivanenko et al., 1995). This specialized function can not be performed by RyR3, because the e-c coupling mechanism can not be restored
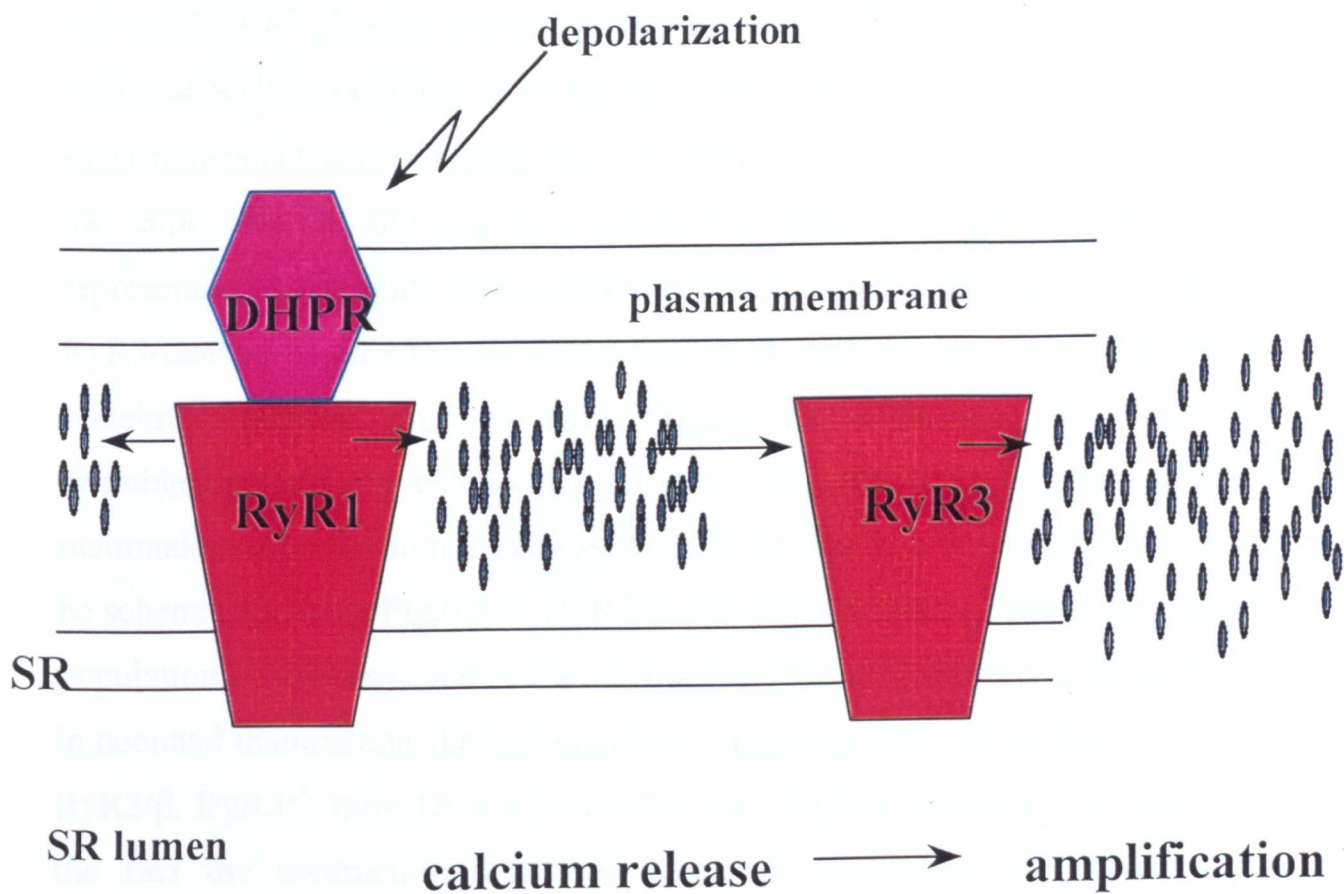
Figure 6.1 Two-channel model of e-c coupling. The depolarization
of the plasma membrane triggers RyR1 actvation via mechanical
coupling with the voltage sensor DHPR. Calcium released by RyR1
stimulates calcium release by RyR3 via CICR, determining an amplification
of the signal.

in the knockout mice for RyR1, and it is absent in the natural chicken mutant despite of the absence of RyR3/β. Thus, RyR1 is the best candidate to cover the role of the Ca^{2+} channel facing the voltage sensor. The arrangement of the two different RyR populations with respect to the DHPRs is shown in Fig.6.2. In most non-mammalian skeletal muscles, RyR1/α and RyR3/β are expressed in the same amount, and can be organized as shown in Fig.6.2 A: RyR1/α is represented by the white bulbs, each coupled to a tetrad; the black bulbs are the RyR3/isoform in an alternate disposition with RyR1/α. Some non-mammalian vertebrate skeletal muscles only express the RyR1/α isoform, like the swimbladder and the extraocular muscles (extra-fast muscles), and most of mammalian muscles do not express RyR3/β. In this case the arrangement could be schematized as in Fig.6.2 B: RyR1/α isoform contributes both to the coupled population of receptors and to the uncoupled. Fig.6.2 C represents the situation in neonatal mammalian skeletal muscles, containing RyR1/α and lower level of RyR3/β. RyR3$^{-/-}$ mice have a functional e-c coupling machinery, according to the fact the contraction following electrical stimulation is controlled by RyR1/α. However, the strong impairment in the response to both electrical and caffeine-mediated stimulation suggests an involvement of RyR3/β in the e-c coupling machinery. Therefore, in the neonatal stages of muscle development RyR3/β uncoupled Ca^{2+} channels provide the amplificatory component of e-c coupling apparatus, based on the CICR mechanism. We can speculate that the presence of a more sensitive system for a CICR-mediated amplification might be of particular relevance in neonatal muscles in view of the incomplete development of the triad structure (Luff and Atwood, 1971; Flucher and Franzini-Armstrong, 1996). This view is also supported by the fact that during neonatal development a sequential use of CICR and DCCR occurs (see above "Introduction").
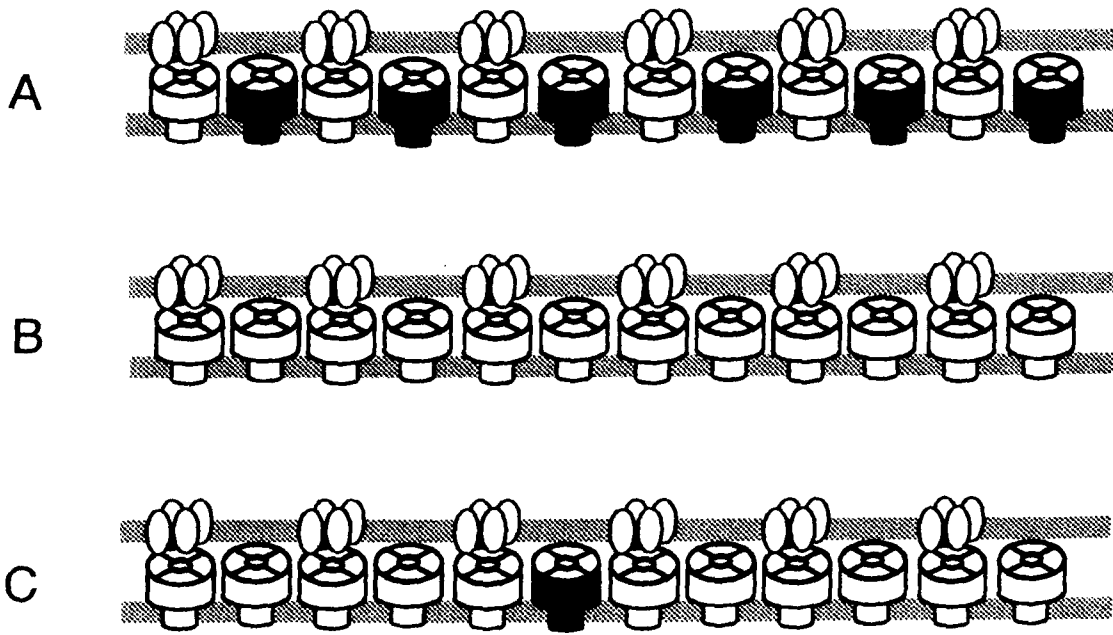
Fig.6.2 Schematic representation of the relative positions of RyRs and DHPRs (tetrads) at triads of skeletal muscles. The DHPRs are on the upper line that represents the t-tubule, RyRs are on the bottom line, that is the SR membrane. The white and black bulbs represent RyR1/α and RyR3/β, respectively. **A)** Skeletal muscle containing equimolar amounts of the two isoforms. **B)** Skeletal muscle containing only RyR1/α. **C)** Skeletal muscle containing predominantly RyR1/α and, at lower amount, RyR3/β.

The data available about the amount of RyR3 in neonatal mammalian skeletal muscles explain the ratio between RyR1 and RyR3 in Fig. 6.2 C, with one RyR3 (in black) among many RyR1 (in white). If this is the relative amount of the two isoforms, what accounts for the strong effect obtained with the lack of such a few receptors in RyR3$^{-/-}$ mice?

The answer to this question represents a challenge for future directions. In general what could accounts for the strong effect on skeletal muscle contraction due to the lack of RyR3 is the amount of the protein, the intrinsic properties of the channels, possible interactions with other proteins.

The data available about the amount of RyR3 in mammalian skeletal muscle suggest that RyR1 is the isoform predominantly expressed, while RyR3 contribution to the total RyRs is very low. In addition to our results on adult and neonatal skeletal muscles (Conti et al., 1996; Tarroni et al., 1997, and this study), biochemical evidences on mammalian adult diaphragm indicate that RyR3 represents the 0.06% of the total RyR amount (Murayama and Ogawa, 1997). Recently, RyR3 isoform immunopurified from bovine diaphragm was shown to represent <5% of total RyRs (Jeyakumar et al., 1998). However, these results are from adult diaphragm, and further analyses are necessary to establish the relative amount of RyR1 and 3 in the neonatal skeletal muscles.

Another interesting aspect concerns the possibility of a differential distribution of RyR3 in diverse muscle fibers. Recently, immunolocalization analysis has been performed at different developmental stages in muscles of wild-type and RyR3 knockout mice, using isoform-specific antibodies (Flucher et al., 1999). This study confirmed the high level of expression of RyR3 during postnatal development, followed by a decrease in all muscle fibers at different rates in different muscles: RyR3-positive fibers could be found in the adult diaphragm, while in EDL RyR3 could not be detected as early as 25 days after birth. Whenever RyR3 was expressed and it co-localized in the triad junction with

RyR1 in same fibers, supporting the idea of a role of RyR3 in e-c coupling together with RyR1, but there were no evidences of any correlation of RyR3 expression with a specific fiber-type. Nevertheless, RyR3 expression in some muscle fibers suggested a functional difference between fibers that contain RyR3 in addition to RyR1 and fibers that do not contain RyR3. Which is this functional difference is not clear yet.

The intrinsic properties of RyR3 could explain RyR3$^{-/-}$ phenotype. The use of RyR3 isoform for the uncoupled release channels is likely to reflect specific regulatory properties of RyR3 that might make it more effective than RyR1 in a CICR mechanism. Such regulatory properties could be specific activation/inactivation kinetics, or a peculiar sensitivity to Ca^{2+} or to other regulators (agonists and antagonists). Recently, taking advantage of the differential distribution of RyR3 in mammalian skeletal muscles and of the RyR3 knockout mice, the single-channel properties of the native mammalian RyR3 channel have been studied using SR vesicles (Sonnleitner et al., 1998). From this study, RyR3 reveals to have a lower sensitivity to inactivation at high Ca^{2+} concentration than RyR1. We can speculate that RyR3 channels are activated by the initial rise of Ca^{2+} concentration provided by the opening of RyR1. The lower sensitivity of RyR3 channels to inactivation at high Ca^{2+} concentration could be important to maintain a sustained Ca^{2+}-release after deactivation of RyR1 (Rios et al., 1992), providing, or, at least, contributing an amplification component for Ca^{2+}-release from SR.

Many other factors could be involved in the regulation of RyR activity. Interaction with other proteins could contribute to a differential regulation of an isoform with respect to the other. As we have seen (see "Introduction"), RyR1 from rabbit skeletal muscles interacts with the small protein called FKBP12 exerting a stabilizing effect on the channel (Brillantes et al., 1994). The

question to be addressed is if the interaction with FKB12 or other molecules can affect RyR3 functional status, stabilizing the channel or changing its behavior in response to modulators.

6.3. Biochemical characterization of knockout RyR3$^{-/-}$ mouse: preliminary results.

The [^{3}H]-ryanodine binding assay on microsomal fractions from RyR3$^{-/-}$ and wild-type mouse skeletal muscle is a useful tool to address what is the amount of RyR3 relative to RyR1 in skeletal muscles.

The saturation curve experiments obtained from RyR3$^{-/-}$ and wild-type muscles reveal a strong difference between diaphragm and hindlimb: while the saturation curve from -/- and +/+ mouse hindlimbs is substantially unchanged, confirming the data from Western experiments, the value of B$_{max}$ from the saturation curve on -/- mouse diaphragm is reduced half compared to the B$_{max}$ from wild-type diaphragm. This picture is also confirmed by the binding analysis during development, where no differences between mutant and wild-type mice were detected, while 50% reduction was present in RyR3$^{-/-}$ compared to RyR$^{+/+}$ at 5 days and 15 days of postnatal development. The discrepancy between the relative amount of RyR3 and RyR1 in diaphragm and the data from Western analysis (Conti et al., 1996; Tarroni et al., 1997; this study), together with the recent immunopurification of RyR3 from bovine diaphragm (Jeyakymar et al., 1998) has still to be defined.

Recent immunostaining experiments using isoform-specific antibodies on diaphragm muscle from newborn and adult mice show that all fibers of newborn mice express RyR3, while in adult diaphragm only a subset of 10 to

15% contains RyR3 (Flucher et al., 1999). The developmental decrease in RyR3 protein observed in adult diaphragm results from the reduced number of RyR3 positive fibers. In this new light, the relative amount of RyR3 in skeletal muscle fibers is higher than previously deduced from biochemical estimates based on total muscle homogenates.

The preliminary results of Ca^{2+} dependence of [^{3}H]-ryanodine binding on diaphragm microsomes from RyR3$^{-/-}$ and wild-type mice reveal a slight but significant difference: in the wild-type maximum activation is obtained at 100μM Ca^{2+} concentration, and binding is still detectable at 10mM Ca^{2+} concentration, a high threshold of inactivation. In the mutants, where only the RyR1 isoform is present, binding is not detectable at 10mM, revealing a higher sensitivity to Ca^{2+} inactivation. Although further experiments are required to confirm the data, they seem to agree with the recent data on single-channel properties on native RyR3 isoform showing a low sensitivity of RyR3 to inactivation at high Ca^{2+} concentration (Sonnleitner et al., 1998).

6.4. RyR3 contribution to Ca^{2+} sparks in embryonic and adult mouse skeletal muscle.

The analysis of the kinetic behavior of Ca^{2+} sparks in a system lacking one of the components of the e-c coupling machinery, either DHPR subunits or RyR isoforms, should provide information on specific arrangements of DHPRs and RyRs required for the e-c coupling.

In a recent study, Ca^{2+} sparks at resting potentials were examined in fast-twitch intercostal muscles from late-gestation wild-type and RyR3 knockout mice, and in fast-twitch muscle cells from the flexor digitorum brevis muscle of wild-type

adult mice (Conklin et al., 1999b). Ca^{2+} sparks in embryonic RyR type3 null myotubes were smaller, briefer and had a faster time to peak than sparks in wild-type muscles of the same age. Sparks in adult cells were significantly smaller than sparks in embryonic RyR type3 null myotubes. The small sparks observed in the absence (RyR type 3 null muscles) or in the presence of very low amount of RyR3 (adult myotubes), suggest a major contribute of RyR3 to the larger and longer-lasting sparks in embryonic myotubes, containing large amount of RyR3.

RyR3 and RyR1 co-localize at junctional triads forming hybrid clusters in which both the isoforms are present (Flucher et al., 1999). In embryonic muscle cells, the pool of RyR1 not controlled by voltage combines with a large pool of RyR3 which is also not controlled by voltage, increasing the density of RyRs that could be activated by Ca^{2+}. Such high density of Ca^{2+}-activated RyR channels could account for the large and long-lasting sparks in embryonic muscle cells. The reason why the large amount of RyR3 would be responsible for the sparks with larger parameters in embryonic myotubes could reside in the ligand gating characteristics of RyR3 channels. In fact a long mean open time has been reported in the mammalian RyR3 channel expressed in HEK293 cells (Chen et al., 1997), and, in addition, mammalian RyR3 is characterized by a low sensitivity to inactivation by Ca^{2+} (Sonnleitner et al., 1998). Therefore, the sub-cellular localization on one side, and the ligand gating features on the other side support the observation that RyR3 enlarges Ca^{2+} sparks.

The contribution of RyR3 to the formation of large sparks is in line with the hypothesis of the requirement for a more sensitive system for a CICR-mediated amplification mechanism of Ca^{2+} release in neonatal skeletal muscle. As already observed, in this phase of development triads are still immature, and a cardiac-like e-c coupling mechanism (CICR) has been using. With the proceeding of

development and the maturation of the triad systems the CICR mechanism is substituted by a DCCR, and RyR3 levels in skeletal muscles strongly decrease. Alternatively, RyR3 could be involved in different processes other than e-c coupling. Some aspects of myogenesis could be influenced by Ca^{2+} sparks. An example is represented by the block of spontaneous Ca^{2+} transients from RyRs in *Xenopus* myocytes, that disrupts the assembly of myosin thick filaments (A band) (Ferrari et al., 1998). In this respect, the separate contribution of RyR1 and RyR3 in Ca^{2+} sparks was investigated using intercostal muscle cells from RyR3 knockout and RyR1 knockout mouse embryos, respectively (Conklin et al., 2000). Both isoforms showed the ability to produce Ca^{2+} sparks. As RyR3 null muscle cells exhibit a normal phenotype and RyR1 null muscle cells are e-c uncoupled, Ca^{2+} sparks seem to result from the activity of small clusters of RyRs regardless of the participation of these RyRs in the e-c coupling process. However, any involvement of RyR3 in muscle developmental process is still to be investigated.

References

Adams, B.A., Tanabe, T., Mikami, S., Numa, S. and Beam, K.G. "Intramembrane charge movement restored in dysgenic skeletal muscle by injection of dihydropyridine receptor cDNAs" *Nature* **1990**, 346, 569-572.

Airey, J.A., Beck, C.F., Murakami, K., Tanksley, S.J., Deerinck, T.J., Ellisman, M.H. and Sutko, J.L. "Identification and localization of two triad junctional foot protein isoforms in mature avian fast twitch skeletal muscle" *J. Biol. Chem.* **1990**, 265 (24), 14187-14194.

Airey, J.Y., Grinsell, M., Jones, L.R., Sutko, J.L. and Witcher, D.R. "Three ryanodine receptor isoforms exist in avian striated muscles" *Biochemistry* **1993**, 32, 5739-5745.

Arai, M., Otsu, K., MacLennan, D.H., and Periasamy, M. "Regulation of sarcoplasmic reticulum gene expression during cardiac and skeletal muscle development" *Am. J. Physiol.* **1992**, 262, C614-C620.

Barone, V., Bertocchini, F., Bottinelli, R., Protasi, F., Allen, P.D., Franzini-Armstrong, C., Reggiani, C. and Sorrentino,V. "Contractile impairment and structural alteration of skeletal muscles from knockout mice lacking type 1 and type 3 ryanodine receptors" *FEBS Lett.* **1998**, 422, 160-164.

Berridge, J.B. "Inositol trisphosphate and calcium signalling" *Nature* **1993**, 361, 315-325.

Berridge, J.B. "Calcium signalling and cell proliferation" *Bioessays* **1995**, 17, 491-500.

Berridge, J.B., Bootman, M.D. and Lipp, P. "Calcium-a life and death signal" *Nature* **1998**, 645-648.

Berridge, J.B., Lipp, P. and Bootman, M. "Calcium signaling" *Current Biology* **1999**, 9, R157-159.

Bertocchini, F., Ovitt, C.E., Conti, A., Barone, V., Schöler, Bottinelli, R., Reggiani, C. and Sorrentino, V. "Requirement for the ryanodine receptor type 3 for efficient contraction in neonatal skeletal muscle" *EMBO J.* **1997**, 16 (23), 6956-6963.

Block, B., Imagawa,T., Campbell, K.P. and Franzini-Armstrong,C. "Structural evidence for direct interaction between the molecular components of the transverse tubule/sarcoplasmic reticulum junction in skeletal muscle" *J.Cell Biol* **1988**, 107, 2587-2600.

Bootman, M.D. and Berridge, M.J. "The elemental principles of calcium signaling" *Cell* **1995**, 83, 675-678.

Bootman, M.D., Berridge, M.J and Lipp, P. "Cooking with calcium: the recipes for composing global signals from elementary events" *Cell* **1997**, 91, 367-373.

Bottinelli, R., Betto, R., Schiaffino, S. and Reggiani, C. "Unloaded shortening velocity and myosin heavy chain and alkali light chain isoform composition in rat skeletal muscle fibres" *J. Physiol.* **1994**, 478, 341-349.

Brandt, N.R., Caswell, A.H., Wen, S.-R. and Talvenheimo, J.A. "Molecular Interactions of the junctional foot protein and dihydropyridine receptor in skeletal muscle triads" *J. Membr. Biol.* **1990**, 113, 237-251.

Brillantes, A.-M.B., Bezprozvannaya, S. and Marks, A.R. "Development and tissue-specific regulation of rabbit skeletal and cardiac muscle calcium channels involved in excitation-contraction coupling" *Circ. Res.* **1994**, 75, 503-510.

Cannell, M.B. Cheng, H. and Lederer, W.J. "The control of calcium release in heart muscle" *Science* **1995**, 268, 1045-1049.

Caswell, A.H. and Brandt, N "Does muscle activation occur by direct mechanical coupling of transverse tubules to sarcoplasmic reticulum?" *Trends Biochem. Sci.* **1989**, 14, 161-165.

Caswell, A.H., Brandt, N.R., Brunschwig, J.P. and Purkerson, S. "Localization and partial characterization of the oligomeric disulfide-linked molecular weight 95,000 protein (triadin) which binds the ryanodine and dihydropyridine receptors in skeletal muscle triadic vesicles" *Biochemistry* **1991**, 30, 7507-7513.

Catterall, W.A. "Excitation-contraction coupling in vertebrate skeletal muscle: a tale of two calcium channels" *Cell* **1991**, 64, 871-874.

Chaudhar, N. and Beam, K.B. "mRNA for cardiac calcium channel is expressed during development of skeletal muscle" *Dev.l Biol.* **1993**, 155, 507-515.

Chen, W.S.R. and MacLennan, D.H. "Identification of calmodulin-, Ca^{2+} and ruthenium red-binding domains in the Ca^{2+} release channel (ryanodine receptor) of rabbit skeletal muscle sarcoplasmic reticulum" *J. Biol.Chem.* **1994**, 269, 22698-22704.

Chen, W.S.R., Li X., Ebisawa, K. and Zhang L. "Functional characterization of the recombinant type 3 Ca^{2+} release channel (ryanodine receptor) expressed in HEK293 cells" *J. Biol. Chem.* **1997**, 272 (39), 24234-24246.

Cheng, H., Lederer, W.J., Cannell, M.B. "Calcium sparks: elementary events underlying excitation-contraction coupling in heart muscle" *Science* **993**, 262, 740-744.

Chomczynski, P. and Sacchi, N., "Single-Step Method of RNA Isolation by Acid Guanidium Thiocyanate-Phenol-Chloroform Extraction" *Analytical Biochemistry* **1987**, 162, 156-159.

Clapham, D.E. "Calcium signalling" *Cell* **1995**, 80, 259-268.

Cognard, C., Rivet-Bastide, M., Constantin, B. and Raymond, G. "Progressive predominance of "skeletal" versus "cardiac" types of excitation-contraction coupling during in vitro skeletal myogenesis" *Pfluegers Arch.* **1992**, 422, 207-209.

Collins, J.H. "Sequence analysis of the ryanodine receptor: possible association with a 12K, FK506-binding immunophilin/protein kinase C inhibitor" *Biochem. Biophys. Res. Commun.* **1991**, 178, 1288-1290.

Conklin, M.W., Powers, P., Gregg, R.G. and Coronado, R. "Ca^{2+} sparks in embryonic muscles selectively deficient in dihydropyridine receptor α_{1s} or β_{1a} subunits" *Biophys. J.* **1999a**,76, 657-669.

Conklin, M.W., Barone, V., Sorrentino, V. and Coronado, R. "Contribution of ryanodine receptor type 3 to Ca^{2+} sparks in embryonic mouse skeletal muscle" *Biophys. J.* **1999b**, 77 (3), 1394-1403.

Conklin, M.W., Ahern, C.A., Vallejo, P., Sorrentino, V., Takeshima, H. and Coronado, R. "Comparison of Ca^{2+} sparks produced independently by two ryanodine receptor isoforms" *Biophys. J.* **2000**, 78 (4), 1777-1785.

Conti, A., Gorza, L. and Sorrentino, V. "Differential distribution of ryanodine receptor type 3 (RyR3) gene product in mammalian skeletal muscles" *Biochem. J.* **1996**, 316, 19-23.

Coronado, R., Morrisette, J., Sukhareva, M. and Vaughan, D.M. "Structure and function of ryanodine receptors" *Am. J. Physiol.* **1994**, 266, C1485-C1504.

Dargie, P.J., Agre, M.C. and Lee, H.C. "Comparison of Ca^{2+} mobilizing activities of cyclic ADP-ribose and inositol trisphosphate" *Cell Regul.* **1990**, 1, 279-290.

Dent, M.A., Raisman, G. and Lai, F.A. *Development* **1996**, 122, 1029-1039.

DiJulio, D.H., Watson, E.L., Pessah, I.N., Jacobson, K.L., Ott, S.M., Buck, E.D. and Singh, J.C. "Ryanodine receptor type III (Ry$_3$R) identification in mouse parotid acini" *J. Biol. Chem.* **1997**, 272 (25) 15687-16696.

Dutro, S., Airey, J.A., Beck, C., Sutko, J.L. and Trumble, W.R. "The junctional foot protein during development of avian embryonic cardiac muscle" *Dev. Biol.* **1993**, 155, 431-441.

Endo, M. "Calcium release from the sarcoplasmic reticulum" *Physiol. Rew.* **1977**, 57, 71-108.

Evans, M.J. and Kaufman, M.H., "Establishment in culture of pluripotential cells from mouse embryos" *Nature.* **1981**, 292, 154-156.

Fabiato, A. "Calcium-induced release of calcium from the sarcoplasmic reticulum" *Am. J. Physiol.* **1983**, 245, C1-C14.

Fabiato, A. "Simulated calcium current can both cause calcium loading in and trigger calcium release from the sarcoplasmic reticulum of a skinned canine cardiac Purkinje cell" *J. Gen. Physiol.* **1985**, 85, 291-320.

Fan, H., Brandt, N.R. and Caswell, A.H. "Disulfide bonds, *N*-glycosylation and transmembrane topology of skeletal muscle triadin" *Biochemistry* **1995**, 34, 14902-14908.

Ferrari, M.B., Ribbeck, K., Hagler, D.J. and Spitzer, N.C. "A calcium signaling cascade essential for myosin thick filament assembly in *Xenopus* myocytes" *J. Cell Biol.* **1998**, 141, 1349-1356.

Fleischer, S. and Inui, M. "Biochemistry and biophysics of excitation-contraction coupling" *Ann. Rev. Biophys. Chem.* **1989**, 18, 333-364.

Flucher, B.E., Takekura, H. and Franzini-Armstrong, C. "Development of the excitation-contraction coupling apparatus in skeletal muscle: association of sarcoplasmic reticulum and transverse tubules with myofibrils" *Dev. Biol.* **1993**, 160, 135-147.

Flucher, B.E., Conti, A., Takeshima, H. and Sorrentino, V. "Type3 and type1 ryanodine receptors are localized in triads of the same mammalian skeletal muscle fibers" *J. Cell Biol.* **1999**, 146 (3), 621-630.

Flucher, B.E. "Structural analysis of muscle development: transverse tubules, sarcoplasmic reticulum , and the triad" *Dev. Biol.* **1992**, 154, 245-260.

Flucher, B.E. and Franzini-Armstrong,C. " Formation of junctions involved in excitation-contraction coupling in skeletal and cardiac muscle" *Proc.Natl.Acad.Sci.* **1996**, 93, 8101-8106

Franzini-Armstrong, C. "Studies of the triad. I. Structure of the junction in frog twitch fibers" *J.Cell Biol.* **1970**, 47, 488-499.

Franzini-Armstrong, C. "Simultaneous maturation of transverse tubules and sarcoplasmic reticulum during muscle differentiation in the mouse" *Dev. Biol.* **1991**, 146, 353-363.

Franzini-Armstrong, C. and Jorgensen, A.O., " Structure and development of E-C coupling units in skeletal muscle" *Ann. Rev. Physiol.* **1994**, 56, 509-534.

Franzini-Armstrong, C. and Kish, J.M. "Alternate disposition of tetrads in peripheral couplings of skeletal muscle" *J. Muscle Res. Cell Motil.* **1995**, 16, 319-324.

Franzini-Armstrong, C. and Protasi, F. "Ryanodine receptors of striated muscles: a complex channel capable of multiple interactions " *Physiol. Rev.* **1997**, 77 (3), 699-729.

Furuichi, T., Furutama, D., Hakamata, Y., Nakai, J., Takeshima, H. and Mikoshiba, K. "Multiple types of ryanodine receptor/ Ca^{2+} release channel are differentially expressed in rabbit brain" *J. Neurosci.* **1994**, 14, 4794-4805.

Futatsugi, A., Kuwajima, G. and Mikoshiba, K. "Tissue-specific and developmentally regulated alternative splicing in mouse skeletal ryanodine receptor mRNA" *Biochem. J.* **1995**, 305, 373-378.

Galione, A., Lee, H.C. and Busa, W. "Ca^{2+}-induced Ca^{2+}-release in sea urchin egg homogenates: modulation by cyclic ADP-ribose" *Science* **1991**, 253, 1143-1146.

Galione, A. "Cyclic-ADP-ribose: a new way to control calcium" *Science* **1993**, 259, 325-326.

Galione, A. and Summerhill, R. "Regulation of ryanodine receptors by cyclic ADP-ribose" In: *Ryanodine Receptors*, CRC Press, Boca Raton, FL **1995**, 51-70.

Giannini, G., Clementi, E., Ceci, R., Marziali, G. and Sorrentino, V. "Expression of a ryanodine receptor- Ca^{2+} channel that is regulated by TGF-β" *Science* **1992**, 91-94.

Giannini, G., Conti, A., Mammarella, S., Scrobogna, M. and Sorrentino, V. "The ryanodine receptor/calcium channel genes are widely and differentially expressed in murine brain and peripheral tissues" *J.Cell Biol.* **1995**, 128, 893-904.

Guo, W. and Campbell, K.P. "Association of triadin with the ryanodine receptor and calsequestrin in the lumen of the sarcoplasmic reticulum" *J. Biol. Chem.* **1995**, 270, 9027-9030.

Guo, W., Jorgensen, A.O. and Campbell, K.P. "Triadin, a linker for calsequestrin and the ryanodine receptor". In: *Organellar Ion Channels and Transporters. Society of General Physiologists, 49th Annual Symposium* New York: Rockfeller Univ. Press **1996**, 19-28.

Hakamata, Y., Nakai, J., Takeshima, H. and Imoto, K. "Primary structure and distribution of a novel ryanodine receptor/calcium release channel from rabbit brain" *FEBS Lett.* **1992**, 312, 229-235.

Inui, M., Saito, A. and Fleischer, S. "Purification of the RyR and identity with the feet structures of junctional terminal cisternae of SR from fast skeletal muscle" *J. Biol. Chem.* **1987**, 262, 1740-1747.

Ivanenko, A., McKemy, D.D., Kenyon, J.L., Airey, J.A. and Sutko, J.L. "Embryonic chicken skeletal muscle cells fail to develop normal excitation-contraction coupling in the absence of the α ryanodine receptor" *J. Biol. Chem.* **1995**, 270 (9), 4220-4223.

Jacquemond, V., Csernoch, L., Klein, M.G. and Schneider, M.F. "Voltage-gated and calcium-gated calcium release during depolarization of skeletal muscle fibers" *Biophys. J.* **1991**, 60, 867-873.

Jayaraman, T., Brillantes, A.-M., Timerman, A., Fleischer, S., Erdjument-Bromage, H., Tempst, P. and Marks, A. "FK506BP associated with the calcium release channel (RyR)" *J. Biol. Chem.* **1992**, 9474-9477.

Jeyakumar, L.H., Copello, J.A., O'Malley, A.M., Wu, G.M., Grassucci, R., Wagenknecht, T. and Fleischer, S. "Purification and characterization of ryanodine receptor 3 from mammalian tissue" **1998**, *J. Biol. Chem.* 273 (26), 16011-16020.

Kelly, A.M. and Rubinstein, N.A. "The diversity of muscle fiber types and its origin during development" in *MIOLOGY* , New York: McGraw-Hill, **1994**, 119-133.

Kim, K.C. Caswell, H., Talvenheimo, J.A. and Brandt, N.R. "Isolation of terminal cisterna protein which may link the dihydropyridine receptor to the junctional foot protein in skeletal muscle" *Biochemistry* **1990**, 29, 9281-9289.

Klein, M.G., Cheng, H., Santana, L.F., Jiang, Y.-H., Lederer, W.J. and Schneider, M.F. "Two mechanisms of quantized calcium release in skeletal muscle" *Nature* **1996**, 379, 455-458.

Kyselovic, J., Leddy, J.J., Ray, A., Wigle, J. and Tuana, B.S. "Temporal differences in the induction of dihydropyridine receptor subunits and ryanodine receptors during skeletal muscle development" *J. Biol. Chem.* **1994**, 269, 21770-21777.

Laemmli, U.K., "Cleavage of structural proteins during the assembly of the head of bacteriophage T4" *Nature* **1970**, 227, 680-685.

Lai, F.A., Erickson, H.P., Rousseau, E., Liu, Q.-Y. and Meissner, G. "Purification and reconstitution of the Ca^{2+} release channel from skeletal muscle" *Nature* **1988**, 331, 315-319.

Lai, F.A., Liu, Q.-L., Xu, L., El-Hashem, A., Kramarcy, N.R., Sealock, R. and Meissner, G. "Amphibian ryanodine receptor isoforms are related to those of mammalian skeletal or cardiac muscle" *Am. J. Physiol.* **1992**, 263, C365-C372.

Lam, E., Martin, M.M., Timerman, A.P., Sabers, C., Fleischer, S., Lukas, T., Abraham, R.T., O'Keefe, S.J., O'Neill, E.A. and Wiiederrecht, G.J. "A novel FK506 binding protein can mediate the immunosuppressive effects of FK506 and is associated with the cardiac ryanodine receptor" *J. Biol.Chem.* **1995**, 270, 26511-26522.

Lee, H.C. "Cyclic ADP-Ribose: a mediator of a calcium signaling pathway" In: *Ryanodine Receptors*, CRC Press, Boca Raton, FL **1995**, 31-50.

Lee, H.C. "Mechanisms of calcium signaling by cyclic ADP-ribose and NAADP" *Pysiol. Rev.* **1997**, 77 (4), 1133-1164.

Lesh, R.E., Nixon, G.F., Fleischer, S., Airey, J.A., Somlyo, A.P., and Somlyo, A.V. "Localization of ryanodine receptors in smooth muscle" *Circ. Res.* **1998**, 82 (2), 178-185.

Lu, X., Xu, L. and Meissner, G. "Phosphorylation of dihydropyridine receptor II-III loop peptide regulates skeletal muscle calcium release channel function" *J. Biol. Chem.* **1995**, 270, 18459-18464.

Luff, A.R. and Atwood, H.L. "Changes in the sarcoplasmic reticulum and transverse tubular system of fast and slow skeletal muscles of the mouse during postnatal development" *J. Cell Biol.* **1971**, 51, 369-383.

MacLennan, D.H. and Phillips, M.S. "The role of the skeletal muscle ryanodine receptor (RYR1) gene in malignant Hypertermia and central core disease" *Soc. Gen. Physiol. Ser.* **1995**, 50, 89-100.

Mansour, S.L., Thomas, K.R. and Capecchi, M.R. "Disruption of the proto-oncogene int-2 in mouse embryo-derived stem cells: a general strategy for targeting mutations to non-selectable genes" *Nature* **1988**, 336, 348-352.

Marks, A.R., Tempst, P., Hwang, K.S., Taubman, M.B., Inui, M., Chadwick, C., Fleischer, S. and Nadal-Ginard, B. "Molecular cloning and characterization of the ryanodine receptor/junctional channel complex cDNA from skeletal muscle sarcoplasmic reticulum" *Proc. Natl Acad. Sci. USA* **1989**, 86, 8683-8687.

Martonosi, A.N., "Regulation of calcium by the sarcoplasmic reticulum" In: *MIOLOGY* New York: McGraw-Hill **1994**, 553-572.

Marty, I., Robert, M., Villaz, M., De Jong, K., Lai, Y., Catterall, W.A. and Ronjat, M. "Biochemical evidence for a complex involving dihydropyridine receptor and ryanodine receptor in triad junctions of skeletal muscle" *Proc. Natl Acad. Sci. USA* **1994**, 91, 2270-2274.

Marziali, G., Rossi, D., Giannini, G., Charlesworth, A. and Sorrentino, V. "cDNA cloning reveals a tissue specific expression of alternatively spliced transcripts of the ryanodine receptor type 3 (RyR3) calcium release channel" *FEBS Lett.* **1996**, 394, 76-82.

McPherson, P.S. and Campbell, K.P. "The ryanodine receptor/ Ca^{2+} release channel" *J. Biol. Chem.* **1993**, 268 (19), 13765-13768.

Meissner, G "Adenine nucleotide stimulation of Ca^{2+}-induced Ca^{2+}-release in sarcoplasmic reticulum" *J. Biol. Chem.* **1984**, 159, 1365-1374.

Meissner, G. "Ryanodine receptor/ Ca^{2+} release channels and their regulation by endogenous effectors" *Annu. Rev. Physiol.* **1994**, 56, 485-508.

Meszaros, L.G., Bak, J. and Chu, A. "Cyclic ADP-ribose as an endogenous regulator of the non-skeletal type ryanodine receptor Ca^{2+} channel" *Nature* **1993**, 364, 76-79.

Mikami, A., Imoto, K., Tanabe, T., Niidome, T., Mori, Y., Takeshima, H., Narumiya, S. and Numa, S. "Primary structure and functional expression of the cardiac dihydropyridine-sensitive calcium channel" *Nature* **1989**, 340, 192-195.

Miyakawa, T., Maeda, A., Yamazawa, T., Hirose, K., Kurosaki, T. and Iino, M. "Encoding of Ca^{2+} signals by differential expression of IP_3 receptor subtypes" *EMBO J.* **1999** 18 (5), 1303-1308.

Monkawa, T., Miyawaki, A., Sugiyama, T., Yoneshima, H., Yamamoto-Hino, M., Furuichi, T., Saruta, T., Hasegawa, M. and Mikoshiba, K. "Heterotetrameric complex formation of inositol 1, 4, 5-trisphosphate receptor subunit" *J. Biol. Chem.* **1995**, 270, 14700-14704.

Murayama, T. and Ogawa, Y. "Purification and characterization of two ryanodine-binding protein isoforms from sarcoplasmic reticulum of Bullfrog skeletal muscle" *J. Biochem.* **1992**, 112, 514-522.

Murayama, T. and Ogawa, Y. "Similar Ca^{2+} dependences of [^3H]ryanodine binding to α and β-ryanodine receptors purified from bullfrog skeletal muscle in an isotonic medium" *FEBS Lett.* **1996**, 380, 267-271.

Murayama, T. and Ogawa, Y. "Properties of RyR3 ryanodine receptor isoform in mammalian brain" *J. Biol. Chem.* **1996**, 271 (9), 5079-5084.

Murayama, T. and Ogawa, Y. "Characterization of type 3 ryanodine receptor (RyR3) of sarcoplasmic reticulum from rabbit skeletal muscles" *J. Biol. Chem.* **1997**, 272 (8), 24030-24037.

Murayama, T., Kurebayashi, N. and Ogawa, Y. "Effects of caffeine and Mg^{2+} on the Ca^{2+} activation and inactivation sites of frog ryanodine receptor" abstract (Pos-98) at *Biophysical Society Meeting* **1998**

Nakai, J., Imagawa, T., Hakamata, Y., Shigekawa, M., Yakeshima, H. and Numa, S. "Primary structure and functional expression from cDNA of the cardiac ryanodine receptor/calcium release channel" *FEBS Lett.* **1990**, 271, 169-177.

Nakai, J., Dirksen, R.T., Nguyen, H.T., Pessah, I.N., Beam, K.G. and Allen, P.D. "Enhanced dihydropyridine receptor channel activity in the presence of ryanodine receptor" *Nature* **1996**, 380, 72-75

Nelson, M.T., Cheng, H., Rubart, M., Santana, L.F., Bonev, A.D., Knot, H.J. and Lederer, W.J. "Relaxation of arterial smooth muscle by calcium sparks" *Science* **1995**, 270, 633-637.

Newton, C.L., Mignery, G.A. and Sudhof, T.C. "Co-expression in vertebrate tissues and cell lines of multiple inositol 1, 4, 5-trisphosphate (InsP$_3$) receptors with distinct affinities for InsP$_3$," *J. Biol. Chem.* **1994**, 269, 28613-28619.

Nori, A., Gorza, L. and Volpe, P. "Expression of ryanodine receptors" In: *Ryanodine Receptors* CRC Press, Boca Raton, FL **1995**, 101-117.

O'Brien, J., Meissner, G. and Block, B.A. "The fastest contracting muscles of non mammalian vertebrates express only one isoform of the ryanodine receptor" *Biophys. J.* **1993**, 65, 2418-2427.

O'Brien, J., Valdivia, H.H. and Block, B.A. "Physiological differences between the α and β ryanodine receptors of fish skeletal muscle" *Biophys. J.* **1995**, 68, 471-482.

Ogawa, Y. and Harafuji, H. "Effect of temperature on [^{3}H]ryanodine binding to sarcoplasmic reticulum from bullfrog skeletal muscle" *J. Biochem.* **1990**, 107, 887-893.

Otsu, K., Willard, H.F., Khanna, V.K., Zorzato, F., Freen, N.M. and MacLennan, D.H. "Molecular cloning of cDNA encoding the Ca^{2+} release channel (ryanodine receptor) of rabbit cardiac sarcoplasmic reticulum" *J. Biol. Chem.* **1990**, 265, 13472-13483.

Ottini, L., Marziali, G., Conti, A., Charlesworth A. and Sorrentino, V. "α and β isoforms of ryanodine receptors from chicken skeletal muscle are the homologues of mammalian RyR1 and RyR3" *Biochem. J.* **1996**, 315, 207-216.

Oyamada, H., Murayama, T., Takagi, T., Hon, M., Iwabe, N., Miyata, T., Ogawa, Y. and Endo, M. "Primary structures and distribution of ryanodine-binding protein isoforms of the bullfrog skeletal muscle" *J. Biol. Chem.* **1994**, 269, 17206-17214.

Papaioannou V. and Johnson, R. In *Gene Targeting, A practical approach* **1993**, 107-146, IRL Press, Oxford.

Peng, M., Fan, H., Kirley, T.L., Caswell, A.H. and Schwartz, A. "Structural diversity of triadin in skeletal muscle and evidence of its existence in heart" *FEBS Lett.* **1994**, 348, 17-20.

Percival, A., Williams, A., Kenyon, J., Grinsell, M., Airey, J.A. and Sutko, J.L., "Chicken skeletal muscle ryanodine receptor isoforms: ion channel properties" *Biophys. J.* **1994**, 67, 1834-1850.

Protasi, F., Sun, X.H. and Franzini-Armstrong, C. "Formation and maturation of the calcium release apparatus in developing and adult avian myocardium" *Dev. Biol.* **1996**, 173, 265-278.

Ramirez-Solis, R., Davis, A.C. and Bradley, A. "Gene targeting in embryonic stem cells" *Methods in Enzymology* **1993**, 225, 855-878.

Rios, E. and Pizarro, G. "Voltage sensor and calcium channels of E-C coupling in skeletal muscle" *News Physiol. Sc.* **1988**, 3, 223-227.

Rios, E. and Pizarro, G. "Voltage sensor of excitation-contraction coupling in skeletal muscle" *Physiol. Rew.* **1991**, 71, 849-908.

Rios, E., Pizarro, G. and Stefani, E. "Charge movement and the nature of signal transduction in skeletal muscle excitation-contraction coupling" *Ann.Rev.Physiol.* **1992**, 54, 109-133

Schiaffino, S. and Reggiani, C. "Molecular diversity of myofibrillar proteins: gene regulation and functional significance" *Physiol. Rev.* **1996**, 76 (2), 371-423.

Shirikova, N. and Rios, E. "Small event Ca^{2+} release: a probable precursor of Ca^{2+} sparks in frog skeletal muscle" *J. of Physiol.* **1997**, 502 (1), 3-11.

Shirikova, N., Gonzales, A., Kirsch, W.G., Rios, E., Pizarro, G., Stern, M.D. and Cheng, H. "Calcium sparks: release packets of uncertain origin and fundamental role" *J. Gen. Physiol.* **1999**, 113, 377-384.

Schneider, M.F. and Chandler, W.K. "Voltage dependent charge movement of skeletal muscle: a possible step in excitation-contraction coupling" *Nature* **1973**, 242, 244-246.

Schneider, M.F. "Control of calcium release in functioning skeletal muscle fibers" *Ann.Rev.Physiol.* **1994**, 56, 463-484

Sitsapesan, R., McGarry, S.J. and Williams, A.J. "Cyclic ADP-ribose, the ryanodine receptors and Ca^{2+} release" *TIPS* **1995**, 16, 386-391.

Sonnleitner, A., Conti, A., Bertocchini, F., Schindler, H. and Sorrentino, V. "Functional properties of the ryanodine receptor type 3 (RyR3) Ca^{2+} release channel" *EMBO J.* **1998**, 10 (17), 2790-2798.

Sorrentino, V. and Volpe, P. "Ryanodine receptors: how many, where and why?" *TIPS* **1993**, 14, 98-103.

Sorrentino, V. *Ryanodine Receptors* **1995**, CRC Press, Boca Raton, FL.

Strube, C., Beurg, M., Georgescauld, D., Bournard, R. and Shimahara, T. "Extracellular Ca^{2+}-dependent and independent calcium transient in foetal myotubes" *Pfluegers Arch.* **1994**, 427, 517-523.

Stevens, L.C. In *Teratocarcinomas and embryonic stem cells: a practical approach, CSH conferences on Cell Proliferation* **1983**, Vol 10, 23-26. CSHL Press, Cold Spring, NY.

Suko, J., Maurer-Fogy, I., Plank, B., Bertel, O., Wyskovsky, W. Hohenegger, M. and Hellmann, G. "Phosphorylation of serine 2843 in ryanodine receptor-calcium release channel of skeletal muscle cAMP, cGMP and CAM-dependent protein kinase" *Biochem. Biophys. Acta* **1993**, 1175, 193-206.

Sun, X.H., Protasi, F., Takahashi, M., Takeshima, H., Ferguson, D.G. and Franzini-Armstrong, C. "Molecular architecture of membranes involved in excitation-contraction coupling of cardiac muscle" *J. Cell Biol.* **1995**, 129, 659-671.

Sutko, J.K., Airey, J.A., Murakami, K., Takeda, M., Beck, C., Deerinck, T., and Ellisman, M.H. "Foot protein isoforms are expressed at different times during embryonic chick skeletal muscle development" *J. Cell Biol.* **1991**, 113 (4), 793-803.

Sutko, J.K. and Airey, J.A "Ryanodine receptor Ca^{2+} release channels: does diversity in form equal diversity in function?" *Physiol. Rev.* **1996**, 76 (4), 1027-1067.

Takekura, H., Nishi, M., Noda, T., Takeshima, H. and Franzini-Armstrong, C. "Abnormal junctions between surface membrane and sarcoplasmic reticulum in skeletal muscle with a mutation targeted to the ryanodine receptor" *Proc. Natl Acad. Sci. USA* **1995**, 92, 3381-3385.

Takeshima, H., Nishimura, S., Matsumoto, T., Ishida, H., Kanawa, K., Minamoto, N., Matsuo, H., Ueda, M., Hanaoka, M., Hirose, T. and Numa, S. "Primary structure and expression from complementary DNA of skeletal muscle ryanodine receptor" *Nature* **1989**, 339, 439-445.

Takeshima, H., Iino, M., Takekura, H., Nishi, M., Kuno, J., Minowa, O., Takano, H. and Noda, T. "Excitation-contraction uncoupling and muscular degeneration in mice lacking functional skeletal muscle ryanodine-receptor gene" *Nature* **1994**, 369, 556-559.

Takeshima, H., Nishi, M., Iwabe, N., Miyata, T., Hosoya, T., Masai, I. and Hotta, Y. "Isolation and characterization of a gene for a ryanodine receptor/calcium release channel in *Drosophyla melanogaster*" *FEBS Lett.* **1994**, 337, 81-87.

Takeshima, H., Yamazawa, T., Ikemoto, T., Takekura, H., Nishi, Miyuki, Noda, T. and Iino, M. " Ca^{2+}-induced Ca^{2+}-release in myocytes from dyspedic mice lacking the type-1 ryanodine receptor" *EMBO J.* **1995**, 13 (14), 2999-3006.

Takeshima, H., Komazaki, S., Hirose, K., Nishi, M., Noda, T. and Iino, M. "Embryonic lethality and abnormal cardiac myocytes in mice lacking ryanodine receptor type 2" *EMBO J.* **1998**, 17, 3309-3316.

Tanabe, T., Beam, K.G., Powell, A.J. and Numa, S. "Restoration of excitation-contraction coupling and slow calcium current in dysgenic muscle by dihydropyridine receptor complementary cDNA" *Nature* **1988**, 336, 134-139.

Tanabe, T., Beam, K.G., Adams, B.A., Niidome, T. and Numa, S. "Regions of the skeletal muscle dihydropyridine receptor critical for excitation-contraction coupling" *Nature* **1990a**, 346, 567-569.

Tanabe, T., Mikami, A., Numa, S. and Beam, K.G. "Cardiac-type excitation-contraction coupling in dysgenic skeletal muscle injected with cardiac dihydropyridine receptor cDNA" *Nature* **1990b**, 344, 451-453.

Tarroni, P., Rossi, D., Conti, A. and Sorrentino, V. "Expression of the ryanodine receptor type 3 calcium release channel during development and differentiation of mammalian skeletal muscle cells" *J. Biol. Chem.* **1997**, 272 (32), 19808-19813.

Taylor, C.W. "Inositol trisphosphate receptors: Ca^{2+}-modulated intracellular Ca^{2+} channels" *Biochem. Biophys. Acta* **1998**, 1436, 19-33.

Timerman, A., Jayaraman, T., Wiederrecht, T., Onoue, H., Marks, A. and Fleischer, S. "The ryanodine receptor from canine heart sarcoplasmic reticulum is associated with a novel FK506 binding protein" *Biochem. Biophys. Res. Commun.* **1994**, 198, 701-706.

Yamazawa, T., Takeshima, H., Sakurai, T., Endo, M. and Iino M. "Subtype specificity of the ryanodine receptor for Ca^{2+} signal amplification in excitation-contraction coupling" *EMBO J.* **1996**, 22 (15), 6172-6177.

Yano, M., El-Hayek, R. and Ikemoto, N. "Role of calcium feed-back in excitation-contraction coupling in isolated triads" *J.Biol. Chem.* **1995**, 270, 19936-19942.

Wagenknecht, T. and Radermacher, M. "Three-dimensional architecture of the skeletal muscle ryanodine receptor" *FEBS Lett.* **1995**, 369, 43-46.

Witcher, D.R., Kovacs, R.J., Schulman, H., Cefali, D.C. and Jones, L.R. "Unique phosphorylation site on the cardiac ryanodine receptor regulates calcium channel activity" *J. Biol. Chem.* **1991**, 266, 11144-11152.

Zhang Y., Chen, H.S., Khanna, V.K., De Leon ,S., Phillips, M.S. Schappert ,K., Britt, B.A., Browell, A.K. and MacLennan D.H. "A mutation in the human ryanodine receptor gene associated with central core disease" *Nature Genet.* **1993**, 5, 46-50.

Zorzato, F., Fujii, J., Otsu, K., Phillips, M., Green, N.M., Lai, F.A., Meissner, G. and MacLennan, D.H. "Molecular cloning of cDNA encoding human and rabbit forms of the Ca^{2+} release channel (ryanodine receptor) of skeletal muscle sarcoplasmic reticulum" *J. Biol. Chem.* **1990**, 265, 2244-2256.